METHOD FOR MINIMIZING TECHNETIUM-99 MIGRATION FROM A GEOLOGIC REPOSITORY

By

VIRLYNDA DEMARTINO

A DISSERTATION PRESENTED TO THE GRADUATE SCHOOL
OF THE UNIVERSITY OF FLORIDA IN PARTIAL FULFILLMENT
OF THE REQUIREMENTS FOR THE DEGREE OF
DOCTOR OF PHILOSOPHY

UNIVERSITY OF FLORIDA

2000

Copyright 2000

by

VirLynda DeMartino

TO THE TWO PEOPLE WITH THE GREATEST INFLUENCE ON MY LIFE:

MY DEAREST MOTHER

WITH ETERNAL LOVE AND ADMIRATION

JAMES HORAK

"ALWAYS ACHIEVE YOUR MAXIMUM POTENTIAL."

ACKNOWLEDGMENTS

I first and foremost thank God, for it is only through Him that all things are made possible.

I thank the U.S. Department of Energy for their financial support administered by AWU-NW, NORCUS, and ORAU Programs. I thank my committee cochairmen: S. Anghaie (University of Florida) and W.J. Gray (Pacific Northwest National Laboratory), and my committee members: G. Schoessow, J. Tulenko, and R. Hanrahan. I thank L. Greenwood (PNNL) and C. Wilson (Westinghouse Corporation). I thank W.H. Ellis, my original cochairman, who retired before I received this degree.

Extra special recognition is given to those listed below. These are my loved ones who were always there for me throughout this endeavor. Their love and support kept me going, and they share my joy in receiving this degree.

I thank my husband, who has always given me emotional support. He helped me to realize and utilize my internal strength to face all life's trials and tribulations, never looking for recognition or thanks,

only what was best for me. His confidence in me has strengthened me and given me the confidence to always achieve my maximum potential in all of life's endeavors.

I thank my daughter, who has had to be without her Mommy many hours while I worked on this degree. Her bright smile and loving ways have definitely been the highlight of many gloomy hours!

I thank my mother, who has given undying support throughout my entire life. Her love, encouragement, and reassurance have given me the ambition to keep my dreams and goals alive. Though many miles away, she was always there enduring my hardest times, as well as triumphing in the more glorious times; always keeping me striving for better and higher goals.

I thank my sister, who gave me immeasurable amounts of encouragement and love throughout this adventure.

I thank James A. Horak whose fatherly love led me to choose this discipline by the tender age of nine. His words of "always strive to achieve your maximal potential" kept me striving to complete the Ph.D.

I thank my family, who were always ready to offer their advice when the going got tough. I especially thank my sister for all her prayers and constant visits to the Grotto.

I thank my numerous friends not individually mentioned, who, nonetheless, have been a great support over the years. I thank them especially for their prayers.

TABLE OF CONTENTS

ACKNOWLEDGMENTS iv

LIST OF FIGURES x

LIST OF TABLES xiii

ABSTRACT xiv

CHAPTERS
1 INTRODUCTION 1
1.1 Technetium Background Information 1
1.2 Computational-Analysis Approach 6
1.3 Experimental Approach 10
1.4 Laboratory Closure 11
1.5 Development of This Dissertation 12

2 COMPUTATION ANALYSIS AND RESULTS 13
2.1 Modeling the System 13
2.2 The EQ3/6 Computer Codes 20
2.3 EQ3/6 Simulations 22
2.3.1 Preliminary EQ3/6 Simulations 23
2.3.2 Interpreting the EQ3/6 Figures 30
2.3.3 Simulations Modeling the Experiments . 35
2.4 EQ3/6 and the Experimental Results 41

3 EXPERIMENTAL PREPARATION AND DESCRIPTIONS 45
3.1 Technetium Solutions 45
3.2 Technetium-Detection System 46
3.3 Material Acquisition 47
3.4 Systems Used and Experiment Descriptions . . 48
3.4.1 FT-4C Flow-Through System 54
3.4.1.1 Equipment description 54
3.4.1.2 Equipment readiness experiment 57
3.4.1.3 Experiments' descriptions . . . 59
3.4.2 Bench-Top Flow-Through System 61
3.4.2.1 Equipment description 62
3.4.2.2 Bench-top experiments 62
3.4.3 Beaker System 63
3.4.3.1 Equipment description 64
3.4.3.2 Experiment description 64
3.4.4 Sealed Vessel System 66
3.4.4.1 Equipment description 66
3.4.4.2 Readiness experiments 68

3.4.4.3 Experiment description 69

4 RESULTS AND DISCUSSION 72
4.1 Overview 72
4.2 Blank-run Experiment 75
4.3 Iron Powder Experiments 81
4.3.1 Bench-Top Iron Powder Experiments . . 81
4.3.2 Sealed Vessel Experiments 93
4.3.2.1 Sealed Vessel Experiment at 70°C 94
4.3.2.2 Sealed Vessel Experiment at 24°C 105
4.3.3 FT-4C Iron Powder Experiments 113
4.3.3.1 High-flow Iron Powder Experiment 114
4.3.3.2 Low-flow Iron Powder Experiment 117
4.3.3.3 Iron Powder Experiment at 85°C 118
4.3.4 Iron Powder Summary and Conclusions . 121
4.4 Copper Experiments 125
4.4.1 Bench-Top Copper Powder Experiment . . 126
4.4.2 FT-4C Copper Shot Experiments 136
4.4.2.1 DIW Copper Shot Experiment . . 136
4.4.2.2 Copper Shot Experiment at 24°C 139
4.4.2.3 Copper Shot Experiment at 85°C 143
4.4.3 Copper Summary and Conclusions 144
4.5 Stannous Chloride Experiments 147
4.5.1 Beaker Stannous Chloride Experiment . 148
4.5.2 Bench-Top Stannous Chloride Experiment 152
4.5.3 Stannous Chloride Summary and Conclusions 156
4.6 FT-4C Tin Shot Experiments 159
4.6.1 Tin Shot Experiment at 24°C 160
4.6.2 Tin Shot Experiment at 85°C 160
4.6.3 Tin Summary and Conclusions 164

5 SUMMARY AND CONCLUSIONS 166

6 RECOMMENDATIONS 172

7 EPILOGUE 177

GLOSSARY 179

APPENDICES
A THE EQ3/6 COMPUTER CODES 185

B BETA DETECTION SYSTEM 196

C GAMMA DETECTION SYSTEMS 200

D CHEMICAL ASSAY DATA 209
REFERENCES 214
BIOGRAPHICAL SKETCH 221

LIST OF FIGURES

Figure		page
1	EQ3/6 Copper Simulation Solution Environment . . .	25
2	EQ3/6 Copper Simulation Precipitated Technetium Compounds	26
3	EQ3/6 Copper Simulation Solution Environment and Precipitated Technetium Compounds	27
4	EQ3/6 Stannous Chloride Simulation Solution Environment	28
5	EQ3/6 Stannous Chloride Simulation Precipitated Technetium Compounds	29
6	Fluid-centered Flow-through Open System	31
7	EQ3/6 Simulation Technetium Concentrations and Product Minerals for Iron Reactant	33
8	EQ3/6 Iron Simulations	36
9	EQ3/6 Closed System Simulation Technetium Concentration	39
10	EQ3/6 Closed System Simulation Solution Environment	40
11	Experimental Systems	49
12	Translational Column Assembly Cutaway View	51
13	Detailed Diagram of the FT-4C Flow-Through System.	56
14	FT-4C Readiness Experiment Using Uranium	58
15	Sealed Vessel System Eh Instrumentation Calibration Using Quinnhydrone	70
16	FT-4C Blank-run Experiment	78

17 Bench-top ^{99}Tc Iron Powder Experiment 82

18 Bench-top ^{95m}Tc Iron Powder Experiment Solution Concentrations 84

19 Bench-top ^{95m}Tc Iron Powder Experiment Reaction Column 86

20 Comparison of the Bench-top ^{95m}Tc Iron Powder Experiment and EQ3/6 Simulations 90

21 Sealed Vessel Experiment at 70°C and the EQ3/6 Simulation Technetium Concentrations and Predicted Precipitation of Technetium Compounds 95

22 Sealed Vessel Experiment at 70°C and the EQ3/6 Simulation Solution pH 96

23 Sealed Vessel Experiment at 70°C and the EQ3/6 Simulation Solution Environment 97

24 Sealed Vessel Experiment at 70°C and the EQ3/6 Simulation Solution pH and Eh 98

25 Sealed Vessel Experiment at 24°C and the EQ3/6 Simulation Technetium Concentrations and Predicted Precipitation of Technetium Compounds 107

26 Sealed Vessel Iron Powder Experiment at 24°C and the EQ3/6 Simulation Solution pH 108

27 Sealed Vessel Iron Powder Experiment at 24°C and the EQ3/6 Simulation Solution Environment 109

28 Sealed Vessel Iron Powder Experiment at 24°C and the EQ3/6 Simulation Solution pH and Eh 110

29 FT-4C High-flow Iron Powder Experiment 115

30 FT-4C Low-flow Iron Powder Experiment 119

31 FT-4C Iron Powder Experiment at 85°C 120

32 Bench-top ^{95m}Tc Copper Powder Experiment and the FT-4C Copper Shot Experiments Using J-13 128

33 Comparison of the Bench-Top Copper Powder Experiment and the EQ3/6 Simulation 131

34 Bench-top Copper Powder Experiment and the EQ3/6 Simulation Using Aqueous Copper 134

35 FT-4C DIW Copper Shot Experiment 137

36 FT-4C Copper Shot Experiments at 24°C and 85°C . . 140

37 EQ3/6 Simulation Technetium Concentrations and Product Minerals for Copper Reactant 141

38 Beaker and Bench-top Stannous Chloride Experiments 149

39 Comparison of the Beaker Stannous Chloride Experiment and the EQ3/6 Simulation 151

40 Comparison of the Bench-Top Stannous Chloride Experiment and EQ3/6 Simulation 155

41 FT-4C Tin Shot Experiments at 24°C and 85°C . . . 161

42 Comparison of the Tin Shot Experiments and the EQ3/6 Simulation 162

LIST OF TABLES

Table		page
1	Pressurized Water Reactor Spent-Fuel Radionuclide Inventories at 1,000 Years	4
2	J-13 Well Water Composition	8
3	Properties of Technetium Isotopes of Interest	46
4	Experiments Conducted	52
5	Experiment Location	73
6	Experimental Results	74
7	Chronology of FT-4C Experiments	76

Abstract of Dissertation Presented to the Graduate School of the University of Florida in Partial Fulfillment of the Requirements for the Degree of Doctor of Philosophy

METHOD FOR MINIMIZING TECHNETIUM-99 MIGRATION FROM A GEOLOGIC REPOSITORY

By

VirLynda DeMartino

December 2000

Chairman: Samim Anghaie
Cochairman: Walter J. Gray
Major Department: Nuclear and Radiological Engineering

A method for minimizing technetium-99 (^{99}Tc) migration in groundwater by using reducing agents was investigated. This information could be used to tailor the spent nuclear fuel waste packages or near-field environment at a geologic repository to prevent ^{99}Tc migration should water infiltration occur. The proposed geologic repository at Yucca Mountain will likely remain dry for several hundred years because (1) it will be located in the unsaturated zone above the water table, and (2) it will have significant radioactive decay heat. As time passes, the decay heat generated will lessen. The repository will then cool below the boiling point of water, and then water could contact spent fuel in any breached waste package. At that time, the

soluble radionuclides, such as ^{99}Tc, may possibly dissolve and migrate from the repository into the environment.

This research also could be applied to technetium-soil decontamination by adding the reducing agent to the soil and disposing of the soil as hazardous mixed waste.

A computational analysis (EQ3/6 software package) and an experimental approach were used during this investigation. Both approaches investigated the effect of reducing agents on technetium(VII) solutions. Theoretically, the ^{99}Tc would precipitate as insoluble, lower valent oxides or technetium metal because of the reducing environment, and its migration would be minimized.

Copper, iron, stannous chloride, and tin were used as reducing agents in both approaches. Experimentally, iron reduced the technetium concentration to below detectable limits; copper, tin, and stannous chloride only temporarily reduced the technetium concentration.

The experimental results were consistent with the computer simulations for iron and one of the stannous chloride experiments. The other stannous chloride experiment temporarily reduced the technetium concentration, but not to the values indicated by the codes. Experimentally, copper and tin developed passivation layers, and therefore, the results did not agree with the computer simulations. The computer codes should be updated to take this into account. Based on the results of these

experiments, iron should be considered for reducing the rate of technetium migration under oxidizing conditions; stannous chloride, copper, and tin should not.

CHAPTER 1
INTRODUCTION

1.1 Technetium Background Information

Perrier and Segré first artificially produced element 43 in 1937.[1,2] They chose the name technetium from the Greek word meaning artificial ($\tau\epsilon\chi\nu\eta\tau$os)[2] because they produced it via the reactions $^{94}Mo_{42}$ (d,n) $^{95m}Tc_{43}$ and $^{96}Mo_{42}$ (d,n) $^{97m}Tc_{43}$ using the University of California's cyclotron.[1,2] Since then, technetium isotopes with mass numbers from 90 to 111 have been identified, as well as isomers with mass numbers 90, 91, 93 - 99, and 102.[3] The shortest-lived technetium isotope is ^{111}Tc (0.30 sec half-life), and the longest-lived is ^{98}Tc (4,200,000 year half-life).[3] However, the three technetium isotopes of significant importance today are ^{95m}Tc, ^{99m}Tc, and ^{99}Tc. Technetium-95m and technetium-99m are important in the field of nuclear medicine.[1,2] Technetium-99 (213,000-year half-life) is important because it is a fission product produced in nuclear reactors, with a yield of about 6%.[4,5] Any consideration for disposing of spent nuclear fuel must account for contributions from technetium-99.

The U.S. Department of Energy (DOE) is evaluating Yucca Mountain, Nevada, as a potential repository site for the

disposal of spent nuclear fuel, as a waste form.[6] The possibility of releasing radionuclides from the repository into the accessible environment must be addressed. The scenario by which most of the radionuclides could do so is by dissolution and transport via groundwater.[7] However, the repository will likely remain dry for several hundred years because it will be located in the unsaturated zone above the water table, and it will be kept hot by radioactive decay heat.[8] As time passes, the decay heat will lessen. Eventually, the repository will cool below the boiling point of water, which will allow liquid water to contact the spent fuel in any breached waste package. At that time, the potential for radionuclide release into the environment would exist, and some means of minimizing this release is necessary.

Radionuclides can be divided into three broad categories, based on solubility, for modeling their potential for release from a repository.[7,8] The two considered in this research are low-solubility and high-solubility. The third (gaseous radionuclides) was not considered in this research.[7,8] Solubility constraints will limit the rate of groundwater transport of actinides (rare earth elements with atomic numbers 89 through 103)[9] and other low-solubility radionuclides away from the repository.[7,8] Dissolution kinetics of the spent fuel and any interactions of the dissolved radionuclides with the

near-field repository environment will limit the transport rate of soluble radionuclides.[7,8]

Technetium-99 falls into the high-solubility radionuclide category under the oxidizing conditions expected to exist at the potential Yucca Mountain repository because it is expected to be present as the pertechnetate anion (TcO_4^-). This radionuclide has a very long half-life of 213,000 years. As shown in Table 1, ^{99}Tc comprises 0.75% of the total 1,000-year activity in the spent fuel, or 13 Curies per metric ton of heavy metal (MTHM).[8] Other investigations have determined that because of the solubility of ^{99}Tc, the U.S. Nuclear Regulatory Commission (NRC) release limit of one part in 100,000 per year from the engineered barrier system could be exceeded if the spent fuel is contacted by groundwater.[10,11,12,13,14,15,16] Americium and plutonium account for 98.12% of the total 1,000-year activity, but their release may be limited by low solubility.[8]

Some means of minimizing ^{99}Tc migration at a geologic repository under the scenario of waste-cask breach and groundwater infiltration may be necessary to remain within the NRC's release limits. The method chosen for investigating a means to reduce the rate of ^{99}Tc migration at a geologic repository was based on the redox characteristics of ^{99}Tc applied to standard chemical thermodynamic equations.[17,18,19]

Table 1 Pressurized Water Reactor Spent-Fuel Radionuclide Inventories at 1,000 Years[a,b]

Radionuclide[c]	Half-Life (yr)	Curies per 1,000 MTHM[d]	1,000 Year Activity (% of Total)	Cumulative Activity (%)
^{241}Am	432	894,500	51.33	51.33
^{243}Am	7,380	31,080[e]	1.78[e]	53.11
^{240}Pu	6,569	476,900	27.37	80.48
^{239}Pu	24,130	304,700	17.45	97.96
^{242}Pu	375,800	1,755	0.10	98.07
^{238}Pu	88	967	0.06	98.12
^{99}Tc	213,000	13,030	0.75	98.87
^{59}Ni	80,000	5,150	0.295	
^{63}Ni	100	354	0.020	
^{93}Zr	1,530,000	1,933	0.111	
^{93m}Nb	15	1,836	0.105	
^{94}Nb	20,300	1,240	0.071	
^{14}C	5,730	1,372	0.079[f]	
^{234}U	244,500	1,984	0.114	
^{238}U	2,470,000,000	317	0.016	
^{236}U	23,400,000	271	0.018	
^{237}Np	2,140,000	1,000	0.057	
^{126}Sn	100,000	722	0.044	
^{79}Se	65,000	405	0.023	
^{135}Cs	3,000,000	345	0.020	
^{151}Sm	90	163	0.009	
^{107}Pd	6,500,000	112	0.006	
^{129}I	15,700,000	32	0.0018	

(a) Reprint of Table 2.5 of Reference 8.

(b) Based on ORIGEN-2 data in ORNL/TM-7431 for 33,000 MWd/MTM burnup PWR spent fuel, actinides plus fission products plus activation products.

(c) Radionuclides with 1,000-yr activity less than ^{129}I or half-life less than 1 year were omitted.

(d) MTHM = metric tons of heavy metals

(e) Includes activity of ^{239}Np daughter product.

(f) Carbon-14 activity may vary considerably, depending on as-fabricated nitrogen impurities.

Under oxidizing conditions, technetium is expected to exist in the (+7) valence state as the pertechnetate anion, which is fairly stable and highly soluble.[2,20] The pertechnetate anion will be reduced to lower valance-state compounds (TcO_2, Tc_3O_4, $Tc(OH)_2$, Tc(OH), Tc, etc.) in a reducing environment. Technetium is less soluble and may be more strongly adsorbed on minerals in these reduced states.[2,11,20,21] Thus, if the waste environment can be made into a reducing environment, technetium migration away from the potential repository may be minimized by precipitating it out of solution or adsorbing it onto minerals as a direct result of its reduced state. Therefore, the intended end result of this investigation is to provide information that could be used to make the waste package and/or near-field environment reducing in case of water infiltration. This would reduce the rate of ^{99}Tc migration away from the potential repository.

I used two approaches to conduct this investigation: a computational-analysis approach and an experimental approach. The information gained by these experiments could be used to tailor the waste package and/or near-field environment to minimize technetium migration, and to assess the results of the computer simulations. To my knowledge, no prior experimental work under the scenario laid out in this report has been done to assess the codes.

1.2 Computational-Analysis Approach

The computational-analysis approach was based on information obtained in preliminary research.[22,23] Methods were investigated to change the waste environment from oxidizing to reducing. After conducting literature searches, applying technical theory, setting up chemical-equilibrium equations, constructing porbaix diagrams, and interpreting those diagrams, it was determined that adding reducing agents to the waste environment may precipitate technetium from solution.[22,23,24]

The EQ3/6 software package (herein called the EQ3/6 codes or simply EQ3/6) was used for computer modeling.[25,26,27,28,29] These codes were chosen because they satisfied seven criteria discussed in Section 2.2. One of those criteria is the code's development is supported by the Yucca Mountain Site Characterization Project.[27]

The EQ3/6 software package has many data files, codes, and a data file preprocessor; however, two main codes characterize the geochemical behavior of aqueous systems. The first is EQ3NR in which speciation-solubility calculations are performed to determine the chemical and thermodynamic state of a solution.[26,29] The other, EQ6, is a reaction path code "... which models water/rock interaction or fluid mixing."[29] Essentially, EQ6 indicates the product minerals formed, differences in solution environment variables, concentrations of reactants in solution, gases

produced, and so on, as it incrementally adds the reactant to the system.

The preliminary computational analysis was conducted while pursuing I was my master's degree.[23] These simulations used the EQ3/6 codes to model the scenario of groundwater infiltration into a breached waste cask, followed by ^{99}Tc leaching into an environment containing a reducing agent. This was simulated by entering into the EQ3 input the concentrations of the elements/compounds present in the groundwater and the concentration of ^{99}Tc. The mass of the reducing agent investigated was entered into the EQ6 input. The codes then calculated the effects of the reducing agent (metallic copper, iron, tin, manganese, and vanadium, and the compound stannous chloride) on (1) solution Eh and pH, (2) solid technetium compounds precipitated from the solution, and (3) the concentrations of technetium in J-13 well water. Well J-13 is a high-flowrate well near the potential repository site at Yucca Mountain.[15] The water composition, shown in Table 2, is very similar to that of the vadose and groundwater at Yucca Mountain and is designated a reference groundwater site.[15]

Computer modeling indicated that the soluble TcO_4^- would be reduced to much-less-soluble compounds such as Tc_3O_4, $Tc(OH)_2$, TcOH, or Tc metal. Thus, the radioactive ^{99}Tc would be replaced by innocuous ions such as Fe^{++} and Fe^{3+} in the groundwater. The computer modeling did not indicate

Table 2 J-13 Well Water Composition[11]

Species	Concentration (mg/L)
HCO_3^-	125.3
$SiO_2(aq)$	57.9
Na^+	41.92
SO_4^-	18.92
Ca^{++}	12.5
NO_3^-	9.6
Cl^-	6.9
K^+	5.11
F^-	2.2
Mg^{++}	1.92
Li^+	0.042
Sr^{++}	0.035
Al^{+++}	0.012
Fe^{++}	0.006
pH = 7.6	

that technetium would precipitate as TcO_2. This is addressed in Section 4.3.1.

Should technetium enter into solution, both the theoretical calculations (for constructing the Pourbaix diagrams, see page 6) and computer calculations indicated that the potential for minimizing technetium migration from a geological repository is promising. However, the computer models are limited by current knowledge limitations of

kinetic and chemical thermodynamic information. The possibility also exists that important low-solubility technetium phases were not included in the computer database. These limitations made experimental confirmation of these results necessary.

An experimental investigation was conducted to determine whether placing reducing agents in contact with technetium-spiked solutions would reduce the oxidation state of technetium, precipitate it out of solution, and therefore decrease its concentration in the solution. Measuring technetium concentrations as low as indicated by the codes was impossible. Technetium-95m was used instead of ^{99}Tc because it was the most sensitive radionuclide for measuring technetium concentrations for the given experimental constraints (i.e., up to 2 months run time, budget constraints). The experimental results were given as below detectable limits (BDL) whenever technetium concentrations approached those indicated by the codes. The experiments distinguished between a reducing agent that was able to reduce the technetium concentrations BDL versus those that had little or no lasting effect on technetium concentrations. This was possible even though the technetium concentration could not be measured as low as calculated by the codes. This approach for measuring the relative experimental effectiveness of different reducing agents and of evaluating differences from calculated

technetium concentrations was determined adequate by the Ph.D. committee and myself.

1.3 Experimental Approach

This research was designed to develop, plan, and perform experiments to evaluate the use of reducing agents to impede the rate of technetium migration. This information could then be used to tailor the spent-fuel waste packages and/or near-field environment to mitigate technetium migration should a waste cask breach and groundwater contact occur. In a geologic repository, this may be accomplished by adding a reducing agent to the engineered barrier system. The computer calculations indicated that the reducing agents (entered as the reactants in the simulations) would cause technetium to precipitate in a J-13 solution environment. This led to an associated set of objectives of comparing the experimental and calculational results to assess the results of the EQ3/6 codes.

The experiments consisted of reacting solutions with known technetium concentrations with different reducing agents, such as iron powder. After the technetium-spiked solutions were allowed to react with the reducing agent, effluent samples were collected and analyzed to determine the extent to which the reactant reduced the technetium concentration. Some of the experiments used flow-through

systems that pumped the solution through reaction columns containing the reducing agent. Other experiments allowed the solution to remain in semi-static contact with the reducing agent. The details of the experiments are presented in Section 3.4. Experimental results and conclusions are discussed in Section 4.

1.4 Laboratory Closure

Experimental work in the 325 Building at Pacific Northwest National Laboratory (PNNL) could not be conducted from April 1994 through February 1995 because laboratory activities were shut down for upgrading various safety-related systems. Afterwards, a phased-in restart of the individual laboratories took place. All those who had laboratories in the 325 Building were involved in a massive laboratory clean-up, taking numerous training classes, writing Technical Work Documents, and preparing Start-Work Packages. During this time, work pursuant to my Ph.D. degree was also undertaken. Several samples from one of the experiments were analyzed for iron concentration, a Fortran program was written to manipulate the data output from the EQ3/6 codes, and numerous EQ3/6 simulations were conducted. Pertinent EQ3/6 simulations are discussed in Section 2.3.

1.5 Development of This Dissertation

Section 2 discusses both analysis and results of the computer simulations. Section 3 describes the preparation for the experiments and the actual experiments. Section 4 discusses the results and individual conclusions for each reducing agent. The overall summary and conclusions are presented in Section 5, and Section 6 lists recommendations.

CHAPTER 2
COMPUTATION ANALYSIS AND RESULTS

2.1 Modeling the System

The theoretical basis for choosing a code or set of codes to model the system was based on the equations that define what is chemically and thermodynamically occurring in the system.[a] The system to be modeled was to use reactants to reduce the solution environment and to cause the technetium in solution to precipitate.

For the solution to become reducing, the reactant must be oxidized by losing electrons. For example, oxidation of iron(0) to iron(II) results in the loss of two electrons

$$Fe^{0} \rightleftharpoons Fe^{++} + 2e^{-} \qquad (1)$$

This expression represents only half of the reaction involved. There must be a corresponding reduction in which a reactant gains electrons and is transformed to a lower oxidation state. In the current case, it is anticipated that Tc(VII) will be reduced, for example to Tc(II)

$$Tc^{+7} + 5e^{-} \rightleftharpoons Tc^{+2} \qquad (2)$$

---

[a]The theory behind the equations in this section can be found in References 17-19, or any good chemical thermodynamics book.

These types of reactions are called electrochemical (or redox) reactions because electrons are being transferred. Of course, many other electrochemical reactions can occur because of all the chemical species involved in the J-13 solution.

Chemical ions can undergo other types of chemical reactions without undergoing oxidation or reduction. For example iron(III) combines with water to form iron(III) hydroxide and, on a much longer time scale, will then form hematite according to the reactions

$$Fe^{+++} + 3H_20 \rightleftharpoons Fe(OH)_3 + 3H^+ \quad (3)$$

$$2Fe(OH)_3 \rightleftharpoons Fe_2O_3 + 3H_2O \quad (4)$$

However, the interaction of iron and water is not limited to hematite; other chemical reactions can form different products, such as magnetite, Fe_3O_4. In other words, each chemical species can be oxidized, reduced, and/or combined with other chemical species to form many different compounds. These compounds can be either aqueous, gaseous, or solids.

Therefore, to model the system that uses reactants to reduce the solution environment and cause the technetium in solution to precipitate, numerous equations must be solved. The equations that were required for modeling this system will be discussed. These equations are required for each

chemical species, ion pair, and ion complex possible for the system.

The Nernst Equation, see Equation (5), was used to carry out the calculations for electrochemical reactions, such as those in Equation (1)

$$E_c = E_c^0 - \frac{2.303\ RT}{nF} \log K \qquad (5)$$

where R is the universal gas constant, T is the temperature in Kelvin, n is the number of electrons being transferred, F is Faraday's constant, K is the equilibrium constant, and $E_c°$ is the standard potential for the reaction being considered. At equilibrium, E_c is equal to 0, and the Nernst equation becomes

$$E_c^0 = \frac{2.303\ RT}{nF} \log K \qquad (6)$$

The standard potential, $E_c°$, is obtained by manipulating the following standard-state Gibbs free energy change for a reaction, $\Delta G_r°$

$$\Delta G_r^0 = -2.303\ RT \ln K = -nFE_c^0 \qquad (7)$$

to obtain

$$E_c^0 = \frac{\Delta G_r^0}{-nf} \qquad (8)$$

$\Delta G_r°$ is determined by

$$\Delta G_r^0 = \sum G_{f\,(products)}^0 - \sum G_{f\,(reactants)}^0 \qquad (9)$$

where ΔG_f° is the Gibbs free energy of formation. The ΔG_f° values can be found in chemical thermodynamic tables.[17]

Equation (7) provides a basis for choosing potential reactants for reducing TcO_4^-. The standard potential for a given reaction can be determined by considering the appropriate half-cell potentials. For example, the half-cell reduction potentials for Fe^{++} and TcO_4^- are as follows:

$$Fe^{2+} + 2e^- \rightleftharpoons Fe \qquad E^\circ = -0.44\ V \qquad (10)$$

$$TcO_4^- + 4H^+ + 3e^- \rightleftharpoons TcO_2 + 2H_2O \qquad E^\circ = +0.70\ V \qquad (11)$$

The standard potential for the reduction of TcO_4^- with iron metal is given by

$$2TcO_4^- + 3Fe + 8H^+ \rightleftharpoons 3Fe^{++} + 2TcO_2 + 4H_2O \qquad (12)$$

$$E^\circ = 0.44\ V + 0.70\ V = 1.14\ V$$

Because E° is a positive value for this reaction, the free energy of formation, as given by Equation (7), is negative. Thus, the reduction of TcO_4^- with Fe metal is thermodynamically favorable. Similar reactions can be derived for copper, tin, and stannous chloride, which showed favorable results for reducing TcO_4^-.

The equilibrium constant in Equation (5) is defined as where a is the thermodynamic activity. As will be discussed momentarily, the activity is a parameter that also must be

$$K_{reaction} = \frac{[a_{product\ 1}]\ [a_{product\ 2}]}{[a_{reactant\ 1}]\ [a_{reactant\ 2}]} \cdots \quad (13)$$

determined.

There are additional equations for chemical reactions. For each ion in solution, there is an associated mass balance equation that calculates the total contribution for that ion regardless of the chemical species. For the case of Fe(II), the mass-balance equation in terms of molalities would be as follows:

$$m_{T,Fe^{++}} = m_{Fe^{++}} + m_{Fe(OH)_{2(aq)}^{+}} + m_{Fe(OH)_3^{-}} + m_{FeCO_{3(aq)}^{+}} \cdots \quad (14)$$

The concentrations of ion pairs and complexes are governed by thermodynamic equilibrium. These are represented by mass-action equations for the dissociation of the ion pair/complex. For example, the dissociation of iron carbonate is

$$FeCO_{3(aq)} \rightleftharpoons Fe^{++} + CO_3^{-2} \quad (15)$$

and the mass-action equation for this dissociation is the equation for the equilibrium constant:

$$K_{FeCO_{3(aq)}} = \frac{[a_{Fe^{++}}]\ [a_{CO_3^{-2}}]}{[a_{FeCO_{3(aq)}}]} \quad (16)$$

The thermodynamic activity, a, for each species must be calculated. The thermodynamic activity of species i, a_i, is

related to the molal concentration, m_i, and the activity coefficient, λ_i, by the equation

$$a_i = m_i \lambda_i \tag{17}$$

To solve Equation (17), it is necessary to calculate the activity coefficient, which is determined by the Extended Debye-Hückel equation:

$$\log \lambda_i = \frac{-A_{\lambda,10} (z_i)^2 \sqrt{I}}{1 + \sqrt{I}} \tag{18}$$

where $A_{\lambda,10}$ is the Debye-Hückel parameter in terms of the base ten logarithm, I is the ionic strength, and z_i is the electrical charge for species i. The ionic strength is defined as

$$I = \frac{1}{2} \sum_i m_i z_i^2 \tag{19}$$

where the summation is over all solute species.

To accurately model the thermodynamic state of an aqueous solution, all the above equations must be solved for all the species involved. The concentrations of species initially used to make the solution are known; however, the concentrations of all the other possible chemical species must be determined. This poses a dilemma. To calculate the concentrations of these other species, the mass-action equations must be evaluated. This requires the activity coefficients of all the species. To compute the activity

coefficients of all the species, the concentration of all species must be known, which was the original goal of the calculation. This dilemma is often solved by making an assumption for the activity coefficients and then calculating the others. To accurately solve the problem, iterative techniques are used. In one such technique, the activity coefficients are estimated, and the mass action equations are solved to obtain the concentrations of all species. The activity coefficients are then calculated using the new concentrations. This type of iterative process is continued until the calculated activity coefficients converge.

Put the above dilemma aside for a moment and assume that all the solution variables are calculated. The interactions that can occur between the solution and the added reactant also must be determined. As the reactant is added to the solution, the number of moles of solution changes, the solution composition changes, and the solution may become saturated with new minerals.

Adding the reactant also moves the system from equilibrium because the reactant dissolves into the system. The system is now in a state of disequilibrium and will be thermodynamically driven toward a state of equilibrium. If the aqueous solution is undersaturated with respect to a mineral, the thermodynamic driving force is for the dissolution of the compound(s) containing that mineral. The

system is driven until no more reactant is left, or the solution is saturated.

To determine the state of the system, all the preceding equations must be evaluated in steps for each new species formed. For each species formed, new equations also must be added. If the species is a pure phase (for example, technetium metal), then only one mass-action expression is added for the corresponding solubility equilibrium, and one unknown is added (the number of moles of technetium). If the compound is composed of more than one endmember, then a new equation is added for each endmember, and the number of unknowns is increased by one for each endmember (number of moles of each endmember).

Once again, to accurately model the thermodynamic state of the entire system, all the above equations must be solved for all the species involved. Although all the above equations are algebraic, and again are solved iteratively by similar methods, the solution is complex. Numerical methods using computers are required for solving the thermodynamic state of the system.

2.2 The EQ3/6 Computer Codes

Using computers for the geochemical modeling of an aqueous system is the only feasible means of solving all the equations mentioned in Section 2.1 and other related equations. There is not a globally adequate set of

geochemical modeling codes currently available because none provide for all the physical and chemical phenomena that can occur. Also, not all the thermodynamic data are available for all the species.

The EQ3/6 software package was chosen to conduct the computational-analysis for this research.[25,27-29] The EQ3/6 codes were chosen for modeling the system because (1) they could perform speciation-solubility calculations of the aqueous system, (2) they could perform reaction-path calculations of the system, (3) the supporting databases are extensive, (4) the speciation modeling is not hard-coded,[b] (5) they include balance equations for computing changes in the amount of solvent water, (6) they are capable of handling some of the experimental systems used, and (7) their development has been supported by the Yucca Mountain Site Characterization Project.[26,27,29]

The EQ3/6 Software Package consists of many parts. The EQ3NR and EQ6 codes characterize the geochemical behavior of aqueous systems. There is a data file preprocessor (EQPT) and a software library (EQLIB). There are also five external supporting thermodynamic data files.

EQ3NR is a speciation-solubility code that is useful for "analyzing groundwater chemistry data, calculating

---

[b]Computer codes that have data entered directly into the program are called hard coded. The EQ3/6 codes, however, have subroutines that look to an external file for the data.

solubility limits, determining whether certain reactions are in states of partial equilibrium or disequilibrium."[29] In other words, it calculates the chemical and thermodynamic state of a solution.[26,29] It is required to initialize the EQ6 calculations.

EQ6 is the code that determines what occurs to the system as the reactant is incrementally added.[27] This is called the reaction path of the system. The reaction path calculations for this code include those for gross composition changes that affect the equilibrium of the system. They also include elements of simple disequilibrium, and they can be defined by rate laws for the addition of reactants and/or the formation of product phases. Appendix A discusses the description of the codes in greater detail.

2.3 EQ3/6 Simulations

Numerous EQ3/6 simulations were conducted for all the reducing agents. Some of these simulations were conducted during the preliminary computational-analysis (see Section 1.2). However, the majority of the simulations have been conducted during and after interning at PNNL. A few of the significant simulations are presented here to help understand the results when the experiments are compared with the computer simulations later.

2.3.1 Preliminary EQ3/6 Simulations

Figures 1 through 5 show the solution environment and the numerous technetium products that are indicated to precipitate for the preliminary simulations using copper and stannous chloride reactants, each in J-13 well water with technetium metal. Technetium metal was used in these simulations because the metal will exist at the proposed repository. Numerous technetium compounds were indicated to precipitate due to the very low Eh values obtained as the technetium was oxidized from the (0) valance state to the (VII) valance state.

In the simulations that represent the experiments, TcO_4^- was entered as part of the solution rather than Tc metal entered as a reactant because pertechnetate solutions were used in the experiments. Not all the technetium compounds were indicated to precipitate in these latter simulations because the metal reactants used could only be oxidized to the (III) valance state and therefore, the Eh values were much higher than the previous simulations. The simulation ended once the system was saturated with the reactant and before all the technetium compounds precipitated.[c]

---

[c] When a system is saturated with a reactant, it is in thermodynamic equilibrium, and any additional reactant added will have no effect on the equilibrium of the system.

Figure 1 Curve 1 shows the change in pH (left axis of ordinates) versus the calculated reaction progress, zi, for the simulation of technetium and copper metal in a solution of J-13. Figure 1 Curve 2 shows the Eh (right axis of ordinates) versus zi for the same simulation. EQ3/6 represents reaction progress by zi, where zi represents the integral number of moles of initial reactant that has dissolved. Zi is not necessarily a linear function of time. In these EQ3/6 simulations, the reactant used for the reaction progress was technetium metal. Zi does not represent solution concentrations of technetium since some dissolved technetium was indicated to precipitate as Tc_3O_4, $Tc(OH)_2$, Tc(OH) and Tc, as will be shown in Figure 2.

Figure 2 Curves 1, 2, 3, and 4 show the number of moles of Tc_3O_4, $Tc(OH)_2$, TcOH, and technetium metal that are indicated to precipitate from solution as the reaction progresses, respectively. In these simulations, once a compound was indicated to precipitate, the compound did not dissolve and re-enter into solution, nor did it convert to another compound. Figure 3 is a combination of Figure 1 and Figure 2. The technetium compounds that were indicated to precipitate from solution did so as the solution environment became reducing, i.e., as the solution redox potential, Eh, decreased (Figure 3).

Figure 4 and Figure 5 show similar plots for the stannous chloride, technetium metal, and J-13 well water

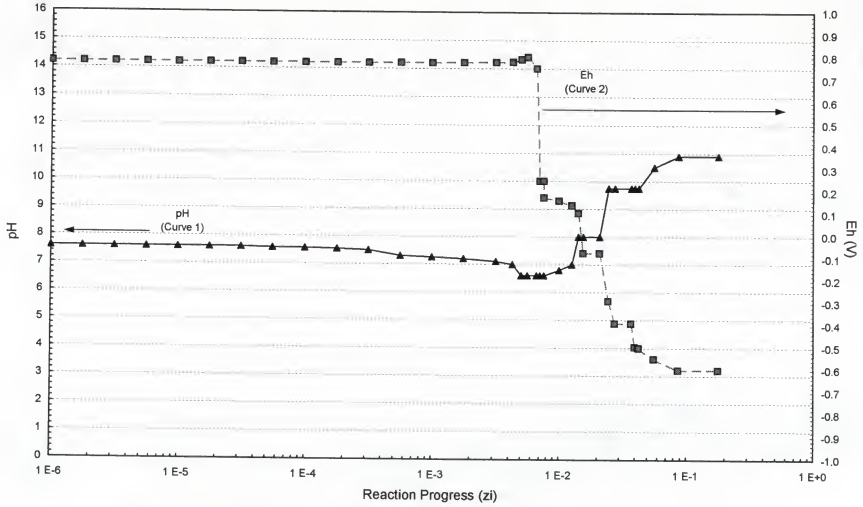

Figure 1 EQ3/6 Copper Simulation Solution Environment. Variations of Solution Environment versus zi. Zi is the measure of the reaction progress and is represented by the integral number of moles of initial technetium metal that has dissolved.

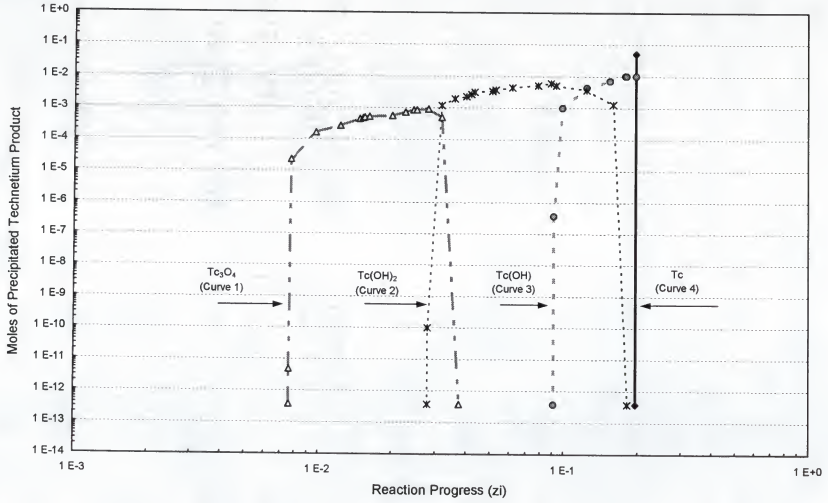

Figure 2 EQ3/6 Copper Simulation Precipitated Technetium Compounds. Calculated precipitation of technetium compounds with increasing zi. Zi is the measure of the reaction progress.

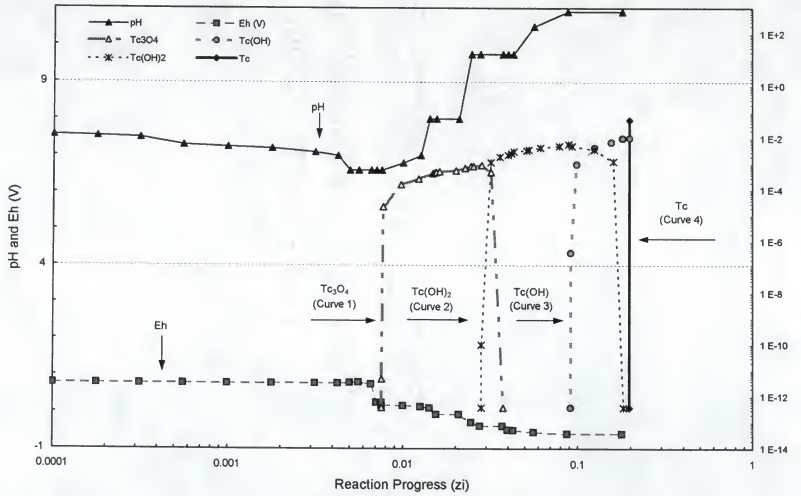

Figure 3 EQ3/6 Copper Simulation Solution Environment and Precipitated Technetium Compounds. Eh, pH, and calculated precipitation of technetium compounds with increasing zi.

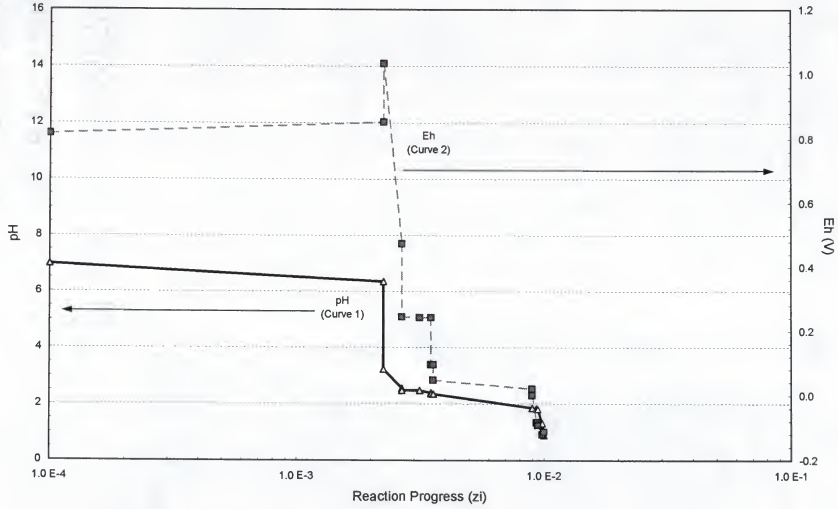

Figure 4 EQ3/6 Stannous Chloride Simulation Solution Environment. Variations of Solution Environment versus zi. Zi is the measure of the reaction progress and is represented by the integral number of moles of initial technetium metal that has dissolved.

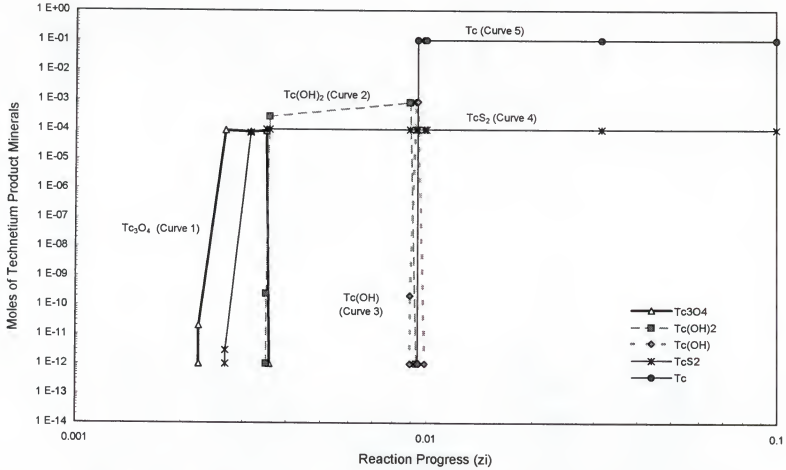

Figure 5 EQ3/6 Stannous Chloride Simulation Precipitated Technetium Compounds Calculated precipitation of technetium compounds with increasing zi. Zi is the measure of the reaction progress and is represented by the integral number of moles of initial technetium metal that has dissolved.

simulation. The reactant used for the reaction progress was technetium metal. Once again, zi does not represent solution concentrations of technetium because some technetium is indicated to precipitate. Figure 4 Curve 1 shows the major difference is that the solution environment became acidic, not alkaline, as in the case for copper (Figure 1 Curve 1).

2.3.2 Interpreting the EQ3/6 Figures

Figure 6 is a symbolic interpretation of the computer simulation results. A discussion of this figure is followed by a detailed explanation of a figure similar to those in the remainder of this dissertation. This section can then be referred to as the graphs become more complicated.

Figure 6 shows the symbolic interpretation for the iron product minerals formed in the simulation that used the reducing-agent iron as a reactant with a solution containing aqueous technetium as pertechnetate (TcO_4^-). This is a representation of a fluid-centered flow-through open system. The changes that occur to the system are from the point of view of the packet of water as it progresses through the reactant. The packet of water that was being followed in the simulation is represented in gray. As the simulation began, the spiked J-13 was highly oxidizing. The iron was oxidized to hematite (Fe_2O_3) and nontronite-Ca ($Ca_{0.165}Fe_2Al_{0.33}S_{13.67}H_2O_{12}$), essentially iron(III) oxides. As

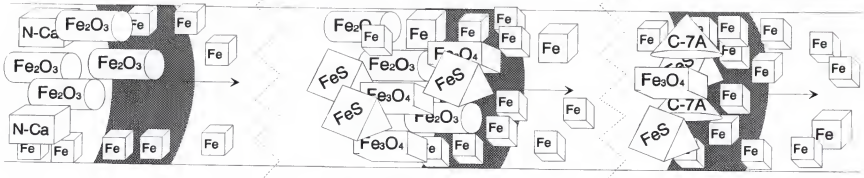

Figure 6 Fluid-centered Flow-through Open System. Packet of water is shown in gray. Region A occurs at the beginning of the simulation when the iron is oxidized mostly to the Fe(III) oxidation state. As the fluid flows through the reactant, it becomes less oxidizing, and the iron reactant is oxidized mostly to the Fe(II) state (Region B). Region C indicates that the solution is least oxidizing, and only Fe(II) compounds are forming. N-Ca refers to nontronite-Ca, and C-7A refers to cronstedite-7A. The chemical formulas are indicated in the text.

the packet moved forward through the iron reactant, the water became less and less oxidizing because the oxygen available to this packet was being used to oxidize the iron and precipitate the compounds. Eventually, it was not oxidizing enough to precipitate hematite or nontronite-Ca. It was able, however, to precipitate the iron(II) oxides pyrite (FeS_2) and cronstedite-7A ($Fe_2Fe_2SiO_5(OH)_4$). The codes then terminated the simulation because the system reached a point where nothing was changing because all the available dissolved oxygen was exhausted.

Figure 7 shows the technetium concentration and solid product minerals that were calculated by the same computer simulation. They are plotted versus the reaction progress (zi). Zi is the measure of the reaction progress and is represented by the integral number of moles of initial reactant that dissolved. In this simulation, the initial reactant was iron metal.

Curve 1 (upper solid line) represents the technetium concentration in parts per billion (ppb). This is the only set of concentrations in this figure. All the other lines represent the number of moles of solid products precipitated.

The first solid iron products indicated to form by the simulation were hematite (represented by Curve 2) and nontronite-Ca (represented by Curve 3). Nontronite-Ca formed until there was a reaction progress of 3.1×10^{-3}.

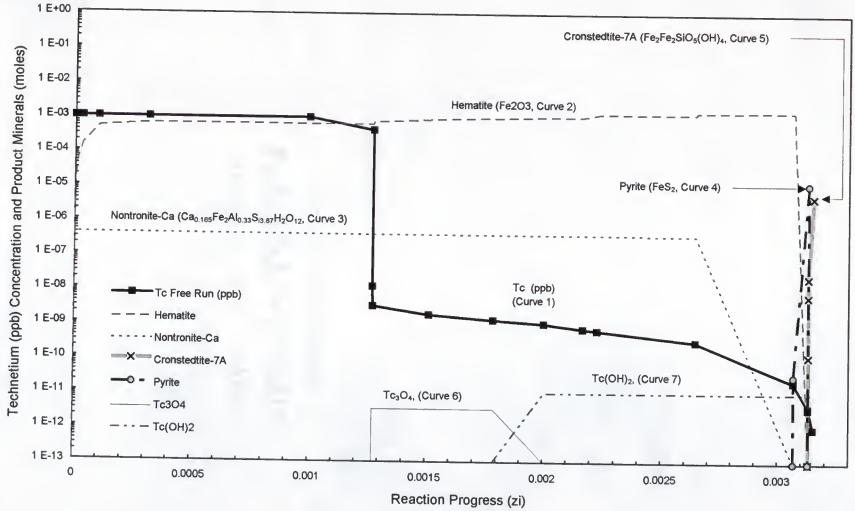

Figure 7 EQ3/6 Simulation Technetium Concentrations and Product Minerals for Iron Reactant. Calculated precipitation of iron and copper compounds with increasing zi. Zi is the measure of the reaction progress and is represented by the integral number of moles of initial reactant that has dissolved.

It was at this point that the solid iron(II) compounds were the thermodynamically favored iron compounds to form. The iron(II) compounds indicated to precipitate were pyrite (represented by Curve 4) and cronstedite-7A (represented by Curve 5). All three iron compounds, hematite, pyrite, and cronstedite-7A, formed until the simulation terminated. The first technetium compound indicated to form at a reaction progress of 1.3×10^{-3} was Tc_3O_4 (represented by Curve 6). The technetium concentration, Curve 1, decreased as expected once Tc_3O_4 (Curve 6) began to precipitate. Actually, the graph shows that the concentration started decreasing at the data point before Tc_3O_4 because the curves are plotted as straight lines between calculated data points. Had a data point existed at a reaction progress of 0.00128, the drop in the technetium concentration would have started at that data point, not at a reaction progress of 0.001. As the reaction progressed further, the iron reduced the technetium to $Tc(OH)_2$ (Curve 7), beginning at a reaction progress of 1.8×10^{-4}, and it continued to form until the simulation terminated.

As the computer simulations are compared to the experiments in later sections of this report, the data will always be plotted versus reaction progress on the upper axis and time on the lower axis. It is important to understand that the two are not related. The reaction progress, although plotted on the same figures as the experiments,

could actually be substantially longer or shorter than the experimental time frame, i.e., months or seconds instead of days.

2.3.3 Simulations Modeling the Experiments

From 1994-1995, during the time of the 325 Building stop-work order, numerous EQ3/6 computer simulations were conducted in an effort to model the experiments more closely than the first simulations (presented in Section 2.3.1), which were conducted by the author in 1989.[23] For instance, rather than using technetium metal as a reactant in the simulation, TcO_4^- entered into the codes at the same concentrations as the experiments with the same quantity of reactants as the experiments. Updated computer simulations for all the reactants have been conducted because the codes have also been modified[29] since 1989. The solution used in the modeling was J-13 well water, Table 2. The composition of J-13 well water was taken directly from the Site Characterization Plan,[15] except that silicon was converted to silicon dioxide. Strontium, which was obtained from work conducted at Lawrence Livermore National Laboratory, was also added.[28]

A simulation, Free Run, used the same initial amount of technetium and iron as those used in one of the iron powder experiments. The technetium and iron concentrations versus reaction progress obtained from this simulation are

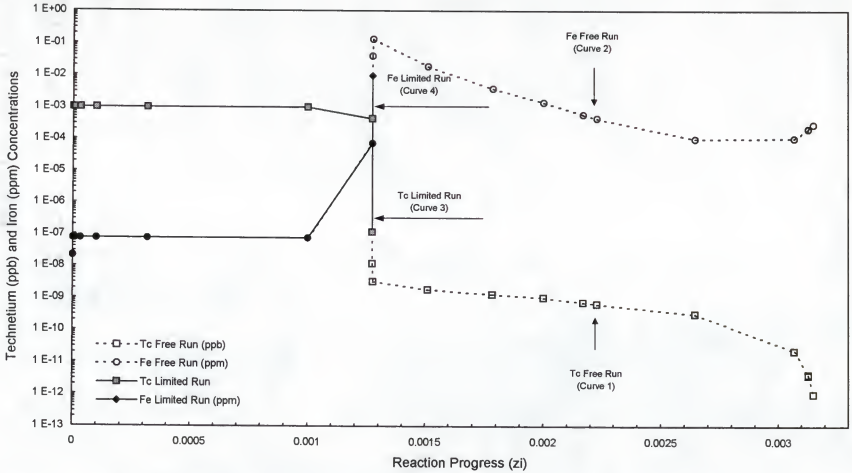

Figure 8 Iron EQ3/6 Simulations. Calculated technetium and iron concentrations with increasing zi. Zi is the measure of the reaction progress and is represented by the integral number of moles of initial reactant that has dissolved. For low reaction progress, Curves 3 and 4 overlap Curves 1 and 2, respectively.

indicated by Figure 8 Curves 1 and 2, respectively. The results obtained from the codes still indicated that iron should reduce the technetium concentration orders of magnitude BDL.

Because the experimental technetium concentrations were not reduced to the values calculated by the codes (as will be discussed in Section 4.3.1), simulations were conducted having various iron and technetium compounds suppressed from forming to determine if there was a solubility controlling compound that prevented the measured technetium concentration from decreasing to the values indicated by the codes. In all of these simulations, the technetium concentrations were orders of magnitude below that which was experimentally observed. No solubility-controlling solid technetium compound was identified because the experimental and calculated results did not agree.

Attempts were also made to model the code input file to be closer to that of the experiments, i.e., a solid-centered flow-through open system, by using back-to-back simulations with an altered EQ6 pickup file (which is also an EQ6 input file). The pickup file was altered to include fresh Tc-spiked solution. By having back-to-back simulations with fresh Tc-spiked solutions, the new technetium solutions would be added to the same initial amount of iron, similar to the experiments. However, none of these simulations accurately modeled the flow-through experiments.

A limiting case simulation, Limited Run, was conducted in which the initial amount of iron entered was just enough to reduce the final technetium concentration to that obtained in the experiments. The technetium and iron concentrations versus reaction progress obtained from this simulation are indicated by Figure 8 Curves 3 and 4, respectively. According to the results of Limited Run, a technetium concentration of 1×10^{-7} ppb, Figure 8 Curve 3, corresponds to an iron concentration of 0.009 ppm, Figure 8 Curve 4. This would be BDL for the iron analysis conducted in this research. However, as will be discussed in Section 4.3.1, the iron concentrations obtained experimentally were higher than calculated by the codes. The reason for these discrepancies are discussed in Section 2.4.

Although EQ3/6 cannot accurately model a solid-centered flow-through open system, it can model a closed-system experiment where the solution remains in contact with the reactant. This is similar to the Sealed Vessel experiments. A computer simulation of a closed system was therefore conducted. The technetium concentrations from the EQ3/6 simulation of the closed system are plotted versus the reaction progress in Figure 9. The pH and Eh from this same EQ3/6 simulation are plotted versus the reaction progress and are indicated by Figure 10 Curves 1 and 2, respectively. The pH corresponds to the left axis of ordinates and the Eh

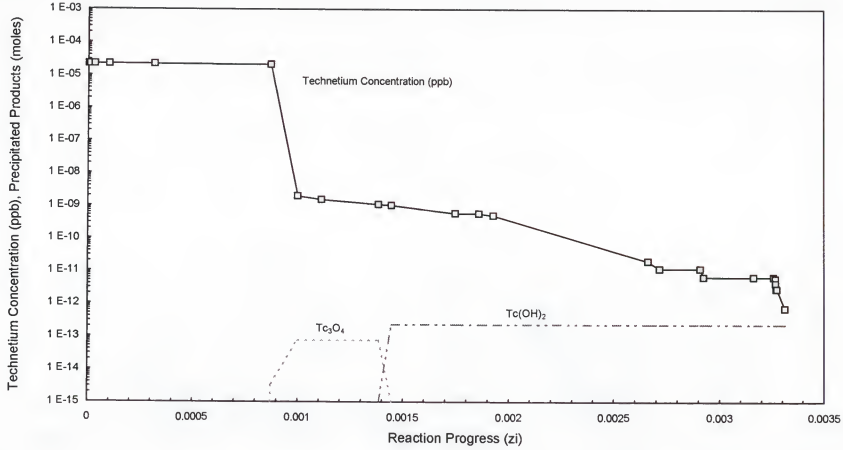

Figure 9 EQ3/6 Simulation of the Representative Closed System. Zi is the measure of the reaction progress and is represented by the integral number of moles of initial reactant that has dissolved.

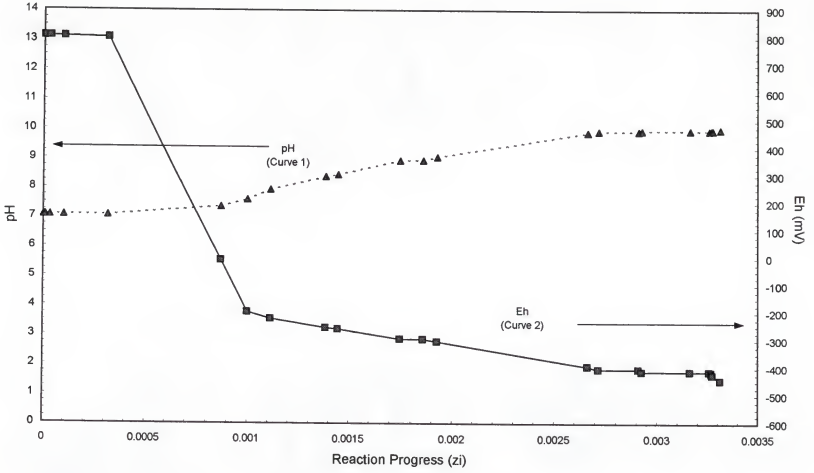

Figure 10 Closed System Iron Powder EQ3/6 Simulation. Note: Zi is the measure of the reaction progress and is represented by the integral number of moles of initial reactant that has dissolved.

to the right axis of ordinates. The technetium concentration dropped 8 orders of magnitude as the solution environment became reducing. As will be discussed in Section 4.3.2.1, these simulations were consistent with the experimental results when iron was the reactant.

2.4 EQ3/6 and the Experimental Results

Reasons for lack of agreement between the measured and calculated activities were sought, such as (1) the solid technetium compound that controls the solubility in the experiment is not listed in the database, (2) the solubility listed in the database is incorrect, (3) there are limitations in the code's modeling capability, or (4) limitations of the experimental setup prevent the system from responding as calculated. An example of the latter is slow reaction kinetics such that the calculated results, which are based on chemical thermodynamics, are never realized within the limited time frame of the experiment.

The reason for the discrepancy between the experimental results and the computer calculations of the fluid-centered flow-through open-system simulations, such as Free Run and Limited Run, was that EQ3/6 cannot accurately model flow-through experiments with continuous fluid recharging (called a solid-centered flow-through open system). As mentioned in Section 2.3.2, the computer simulation models fluid-centered flow-though open systems that differ in that the changes

that occur from a packet of the fluid's reference point are recorded as the packet travels through the reactant. The changes that occur to the fluid at a spacial reference point as new fluid is passed through the same reactant bed are not recorded. Because no other computer codes will satisfy the seven criteria stated in Section 2.2 and model these experiments, back-to-back simulations (mentioned on page 37) were conducted using an altered EQ6 pickup file (which is also an EQ6 input file) in hopes of modeling the flow-through experiments. The pickup file was altered to include fresh Tc-spiked solution. However, none of these simulations accurately modeled the flow-through experiments.

Another suspected reason for the discrepancy between the computer modeling results and the experiments was that the technetium in the experiments was adhering to the reactant and not just being reduced by it. The EQ3/6 codes cannot model sorption. Experimental evidence, which suggests that sorption occurred, is presented in Section 4.3.1.

The results from many of the simulations where the various iron and technetium compounds were suppressed were presented to Dr. Walter Gray.[d] A meeting was then set up

---

[d]Dr. Walter Gray is a Senior Scientist in the Radiochemical Processing Group at PNNL and was the direct onsite advisor for this research.

with Pete McGrail,[e,30] who is very knowledgeable regarding the EQ3/6 computer codes. McGrail also suspected that the technetium was adhering to the iron rather than being reduced by it. He mentioned that the codes do not model adsorption, and therefore, the experimental results will not agree with the results obtained by the codes. McGrail also mentioned that the codes cannot model a solid-centered flow-through open system, even though the code manuals indicate it may be possible.[27] Therefore, the experimental results of flow-through systems may not agree with the results obtained by the codes.

The simulations using copper and tin were also not in agreement with the experiments because copper and tin both appeared to develop passivation layers that prevented them from further reducing the technetium concentration once the layer developed.

Another factor that may have caused disparity between the experimental and calculated results is slow reaction kinetics. The possibility exists that the calculated results were never realized in the limited time frame of the experiments. Evidence suggesting that this occurred in the experiments is presented in Section 4.3.2.2.

Although the EQ3/6 codes cannot accurately model a solid-centered flow-through open system as in the FT-4C and

---

[e]Pete McGrail is a Staff Engineer in the Applied Geology and Geochemistry Group at PNNL.

Bench-top systems, the EQ3/6 codes are continually being updated, and it is planned to add this option as a regular feature into the codes in the future.[27] After adding this feature, the codes should be able to model the experiments.

CHAPTER 3
EXPERIMENTAL PREPARATION AND DESCRIPTIONS

3.1 Technetium Solutions

According to the EQ3/6 computer calculations, the ^{99}Tc concentration in the solution can be decreased to values between 1×10^{-3} ppb and 1×10^{-14} ppb. Technetium-99 is a beta emitter with a detection limit of approximately 1×10^{-1} ppb for the system used at PNNL. Therefore, all the ^{99}Tc concentrations indicated by the codes would be BDL for beta detections. Using a different isotope of technetium (element that has a different mass number for the same number of protons) would be of benefit because they would behave similarly in chemical reactions, but their nuclear characteristics would be different. Technetium-95m was the isotope chosen because it is a gamma emitter, and it has a detection limit of approximately 1×10^{-9} ppb for gamma spectroscopy. The difference in detection limits for these two isotopes is over 8 orders of magnitude. Therefore, if ^{95m}Tc is used, some of the technetium concentrations indicated by the EQ3/6 results would be measurable in the experiments.

Although the codes indicated that the technetium concentration would be BDL for ^{99}Tc, the initial experiments

were conducted with ^{99}Tc to determine if that was indeed the case. Technetium-99 was used first because it is less expensive than ^{95m}Tc and because ^{99}Tc has a long half-life (Table 3). For those cases where lower detection limits were required, as determined by the ^{99}Tc experiments, similar ^{95m}Tc experiments were conducted.

Table 3 Properties of Technetium Isotopes of Interest

	^{95m}Tc	^{99}Tc
Radiation	γ	β^-
Half-Life	60.5 days	213,000 years
Specific Activity	8.48×10^{14} Bq/g	6.03×10^{8} Bq/g
Detection limit	$\sim 1 \times 10^{-9}$ ppb	$\sim 1 \times 10^{-1}$ ppb - 4×10^{-2} ppb

3.2 Technetium-Detection System

Because the two technetium isotopes emit different types of radiation (see Table 3), different detection systems were used to analyze the samples collected from the experiments. Samples containing ^{99}Tc, a beta emitter, were analyzed using a model 2260 XL Packard Instrument Company Tri-Carb Liquid Scintillation Analyzer (LSA). This system was chosen because the efficiency for counting beta particles is very high, up to 100% in ideal situations. The theory of how the LSA functions and sample spectra are described in Appendix B.

Solution samples that contained ^{95m}Tc, primarily a gamma emitter, were analyzed using both high-purity germanium (HPGE) and sodium iodide (NaI[Tl]) well detectors. The NaI(Tl) detector was used almost exclusively. It is highly efficient, it does not need to be cooled with liquid nitrogen, and it was accessible for very long count times. Long counting times were essential because the technetium concentrations could decrease BDL. The reaction column was analyzed using an HPGE/translational column assembly. The theory of how the NaI(Tl) and HPGE function is described in Appendix C.

3.3 Material Acquisition

Four reducing agents that were investigated using the EQ3/6 codes were purchased to experimentally determine a method to reduce the rate of technetium migration at the potential repository. They were also used to compare the experimental data with the results indicated by the EQ3/6 calculations. The reactants obtained were copper shot (1 to 4 mm diameter), copper powder (-50 mesh, i.e., < 0.297 mm), iron powder (-48 mesh, i.e. <0.303 mm), stannous chloride, and tin shot (1 to 4 mm diameter) with purity levels of 99.0%, 99.5%, 99%, 98%, 99.8%, respectively. These impurities are negligible. The only impurity of concern would be iron because, as the experiments in this research show, iron was able to reduce the technetium concentration

to BDL. However the iron impurity was only 0.005%, which was not enough to cause the technetium concentration to drop BDL in the experiments (Section 4). Also, as will be discussed in Section 4.3.4, the reaction kinetics of iron was slow compared to the time-frame of the experiments and the iron impurity did not affect the experiments. The reactant assays are given in Appendix D.

Approximately 1 mCi (3.7×10^7 Bq) of ^{99}Tc was purchased as $NaTcO_4$ in 5.0750 mL of solution (water) from Isotope Productions Laboratory. The data assay from the vender, shown in Appendix D, showed that no radioactive impurities were detected in the ^{99}Tc. Approximately 1 mCi (3.7×10^7 Bq) of ^{95m}Tc was purchased as $NaTcO_4$ in 5-mL of solution (water) from Dupont Pharmaceutical. The data assay from the vender, shown in Appendix D, also showed that no radioactive impurities were detected in the ^{95m}Tc.

3.4 Systems Used and Experiment Descriptions

Four experimental systems were designed, developed, and used to conduct the experiments to determine a method to reduce the rate of technetium migration in a groundwater environment. These four experimental systems were the FT-4C Flow-through System, the Bench-top Flow-through System, a No-flow Beaker System, and a No-flow Sealed Vessel System. These systems fall under two main categories: flow-through systems and no-flow systems. Schematic diagrams of these

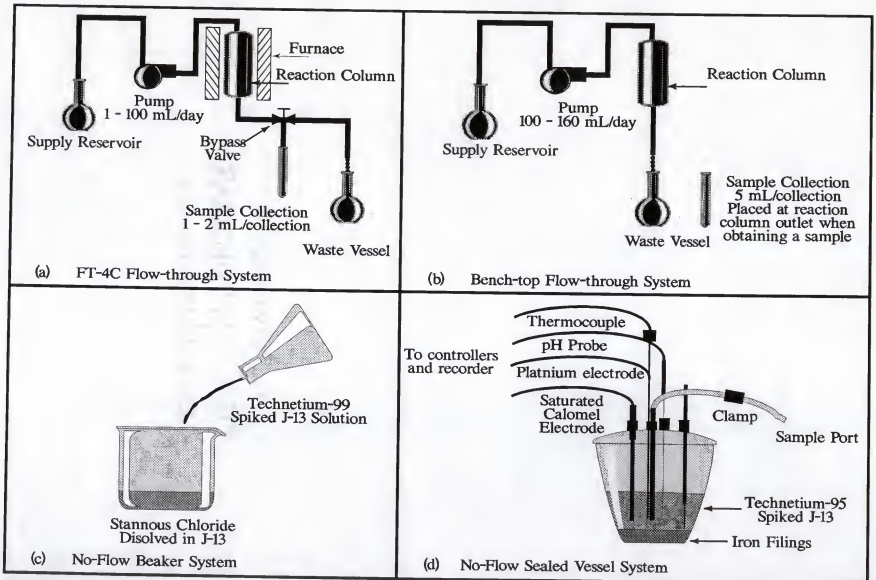

Figure 11 Experimental Systems

systems are pictured in Figure 11. The flow-through systems and experiments conducted with these systems are described in Sections 3.4.1 and 3.4.2. The no-flow systems and experiments conducted with these systems are described in Sections 3.4.3 and 3.4.4.

The Translational Column Assembly (TCA) was also designed. A schematic diagram of the TCA is shown in Figure 12. The TCA held the reaction column (6-mm ID × 30-cm long) from the flow-through experiments in a specially designed leak-proof teflon cylinder. This cylinder was placed in a lead cave with a window. An HPGE detector was located outside the lead cave, in front of the window. The teflon cylinder was passed by the window at 0.25-in. intervals, and the activity along the column was measured. The purpose of designing this TCA was to see where the technetium was depositing along the length of the reaction column. This would enable further understanding of what mechanism was causing the decrease in technetium concentration.

The experiments shown in Table 4 were conducted to determine if copper, iron, stannous chloride, or tin would reduce the rate of technetium migration in a groundwater environment. The scenario chosen to be modeled by these experiments was waste cask breach with groundwater infiltration. This was simulated by allowing technetium-spiked solutions to react with each of the reactants under

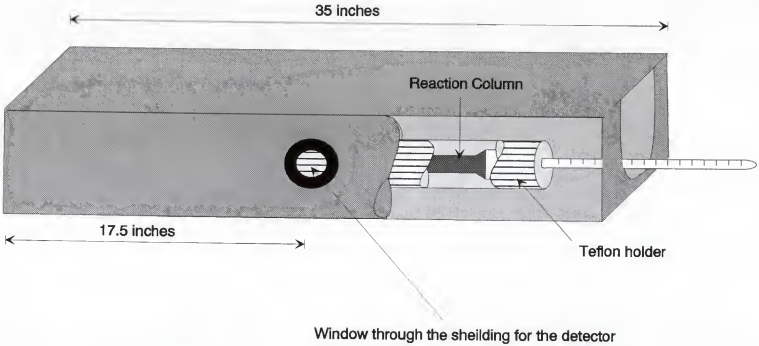

Figure 12 Translational Column Assembly Cutaway View. The teflon holder was 16.5 inches long, and the reaction column was 12 inches long.

Table 4 Experiments Conducted

Experiment	Reactant	Reactant Mass (grams)	Temperature (°C)	Flowrate (mL/day)	Low/High Pressure Set (psi)	Radionuclide	Initial Concentration (ppb)	System Used [1]
Blank Run	-	-	25	50	-	-	-	a
FT-4C Readiness	Fe Powder	~30	25	7.8-78	179/227	^{238}U	1.2×10^{2}	a
High-flow Iron Powder	Fe Powder	29.77	24	0-50-100	195/1013	^{99}Tc	1.5×10^{3}	a
Low-flow Iron Powder	Fe Powder	29.76	24	10-50	194/1013	^{99}Tc	1.5×10^{3}	a
Iron Powder at 85° C	Fe Powder	30.02	85	50	194/1012	^{99}Tc	1.5×10^{3}	a
Bench-top ^{99}Tc Iron Powder	Fe Powder	6.08	24	100	-	^{99}Tc	3.6×10^{1}	b
Bench-top ^{95m}Tc Iron Powder	Fe Powder	32.23	24	100	-	^{95m}Tc	9.4×10^{-4}	b
Sealed Vessel at 70° C	Fe Powder	32.23	70	-	-	^{95m}Tc	2.3×10^{-5}	d
Sealed Vessel at 24° C	Fe Powder	32.23	20/70	-	-	^{95m}Tc	2.3×10^{-5}	d
DIW Copper Shot	Cu Shot	40.95	24	0-25-50	199/216	^{99}Tc	1.2×10^{3}	a
Copper Shot at 24° C	Cu Shot	41.18	24	50-0	206/217	^{99}Tc	1.3×10^{3}	a
Copper Shot at 85° C	Cu Shot	41.89	85	50-0	197/249	^{99}Tc	1.5×10^{3}	a
Bench-top ^{95m}Tc Copper Powder	Cu Powder	31.12	24	100	-	^{95m}Tc	9.4×10^{-4}	b
Tin Shot at 24° C	Sn Shot	35.65	24	50	503/511	^{99}Tc	1.0×10^{3}	a
Tin Shot at 85° C	Sn Shot	36.97	85	50	194/1013	^{99}Tc	1.0×10^{3}	a
Beaker Stannous Chloride	$SnCl_2$	10.00	24	-	-	^{99}Tc	2.6×10^{1}	c
Bench-top Stannous Chloride and Tuff	$SnCl_2$ crushed tuff	1.71/1.71	24	152	-	^{95m}Tc	9.4×10^{-4}	b

(1) Experimental Systems: a. FT-4C b. Bench-top c. Beaker d. Sealed Vessel

different conditions. The initial investigative experiments used ^{99}Tc. Technetium-95m was used in latter experiments where necessary (as explained in Section 3.1).

To interpret this table, the third copper shot experiment (Copper Shot at 85°C) is described. Copper shot (41.89 g) was loaded into the reaction column. The reaction column was placed in the FT-4C, indicated by the "a" in the System Used column. The low pressure was set to 197 psi, and the high pressure was set to 249 psi. The 1.5×10^3 ppb ^{99}Tc-spiked J-13 solution was placed in the supply reservoir. The flowrate was initially set to 50 mL/day, and later the flow was stopped, indicated by 0 mL/day. The pressure was turned on. The temperature controllers were set to have the column heat up to 85°C, and the heat was turned on. The pump was turned on.

The solutions used for these experiments were either distilled, deionized water (DIW), or simulated J-13 well water (J-13). Effluent samples were periodically collected and analyzed to determine the technetium concentration.

Two experiments, at a minimum, were designed for each metal reactant, one at room temperature and one at an elevated temperature. The different temperatures were chosen for two reasons: (1) to determine if reaction kinetics increased because of an increase in temperature and (2) because technetium migration away from a geologic repository, as a result of water infiltration into a

breached waste package, can potentially occur at any temperature below the boiling point of water (95°C at Yucca Mountain). Besides changes in temperature, reaction kinetics were also investigated by changes in flowrates.

3.4.1 FT-4C Flow-Through System

The FT-4C was chosen for the initial investigation of the metal reactants' redox effectiveness on technetium. It has all the necessary mechanics (as explained below) to carry out the experiments: variable flowrate settings, variable temperature setting, capability of safely handling flow-through experiments using radioactive liquids, and capability of taking samples of the column effluent safely.

The equipment description for the FT-4C is presented in Section 3.4.1.1, the FT-4C readiness experiment is presented in Section 3.4.1.2, and the experiments' description using this system is presented in Section 3.4.1.3.

3.4.1.1 Equipment description

The Cortest Systems Incorporated FT-4C Flow-through System, Figure 11a, is a one-of-a-kind high-temperature, high-pressure autoclave designed for investigating liquid/solid reactions at flowrates from 1 mL/day to 100 mL/day.[31] It is shielded to allow use of radioactive liquids or solids, the temperature can be varied from

ambient to 350°C, and the pressure can be varied from 100 psi to 5000 psi.[31]

The FT-4C operates by pumping fluid from the supply reservoir by a two-piston metering pump through a 6-mm-inside-diameter by 30-cm-long horizontal titanium reaction column into the waste-collection vessel. The liner of the column is equipped with a 10-μm frit at the outlet side of the column. The system has three thermocouples that measure the temperature at the front, middle, and rear of the furnace. A bypass valve is located between the outlet of the reaction column and the waste vessel to allow effluent samples to be collected without subjecting the rest of the system to ambient conditions.

The FT-4C was modified such that all tubing and components downstream from the pump could be flushed with an oxidizing agent without contacting the pump's o-rings. This modification was necessary because the pump's o-rings deteriorated with some of the oxidizing flush solutions used, such as nitric acid. There is a flush trap on the vacuum line for collecting the flush-solution samples, which can then be analyzed to determine the amount of technetium deposition along the system's tubing and components. A more detailed schematic diagram of the system is shown in Figure 13.

The FT-4C was used to conduct the Blank-run, Copper Shot, Tin Shot, and four Iron Powder experiments. Solutions

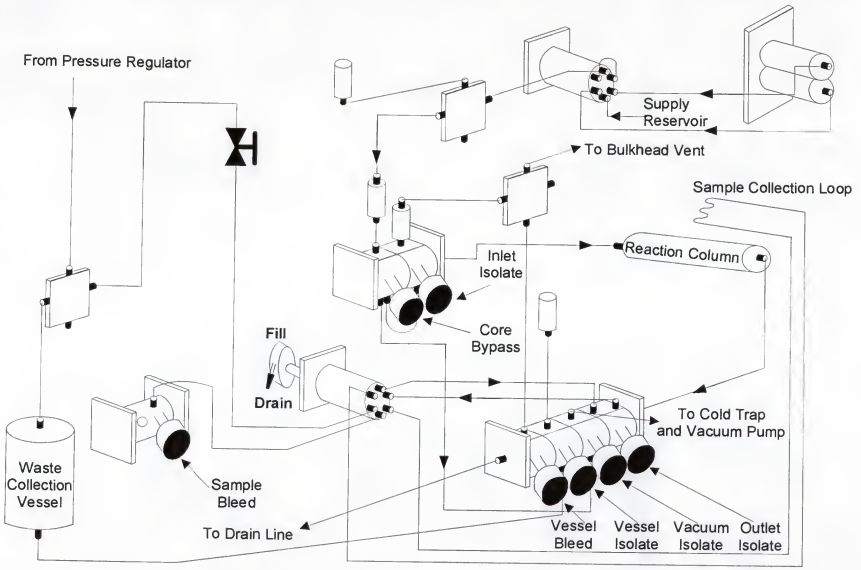

Figure 13 Detailed Schematic Diagram of the Cortest FT-4C Flow-through System. See Figure 11 for a simplified schematic.

with known ^{99}Tc concentrations were pumped through reaction columns in the FT-4C. Effluent samples were collected via the bypass valve after the solution passed through the reaction column. These samples were then analyzed for changes in technetium concentration from the inlet to the outlet of the reaction column. The Blank-run, Copper Shot, Tin Shot, and four Iron Powder experiments conducted using this system are discussed in Section 3.4.1.3. The discussions of the results are presented in Sections 4.2, 4.4, 4.6, and 4.3.3, respectively.

3.4.1.2 Equipment readiness experiment

An equipment readiness experiment was conducted before the technetium experiments using the FT-4C to determine if the system's performance was satisfactory from both safety and operational standpoints for the radioactive experiments. This experiment used uranium as a surrogate for ^{99}Tc since uranium solubility, like technetium, is sensitive to solution redox conditions. By using uranium, the system could be evaluated using a solution that was only slightly radioactive.

A solution containing 100 ng/mL (ppb) of uranium in J-13 was pumped at approximately 50 mL/day through a column containing iron powder at 25°C. The uranium concentration in the column effluent initially dropped more than 95% rather rapidly. It then fell less rapidly to levels below

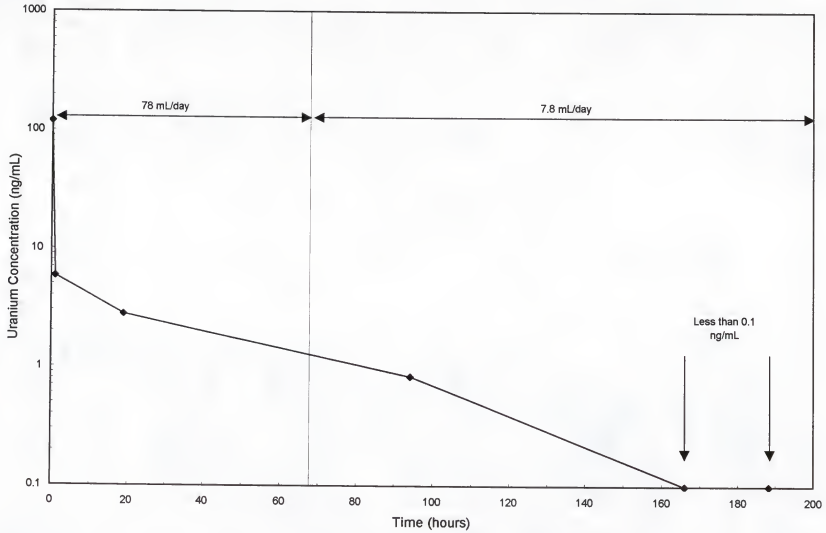

Figure 14 FT-4C Readiness Experiment Using Uranium. A uranium-spiked J-13 well water solution was passed through an iron powder reaction column at 25°C.

the detection limit (≈ 0.1 ng/mL) of the Scintrex UA-3 Uranium Analyzer, as shown in the data in Figure 14. The system's performance was satisfactory from both safety and operational standpoints; it was also judged ready for experiments using technetium since the reaction reduced the uranium concentrations as expected.

3.4.1.3 Experiments' descriptions

Ten of the experiments listed in Table 4 used the FT-4C System (Figure 11a). After the FT-4C Readiness Experiment, three copper shot, two tin shot, three iron powder, and one blank run experiment were conducted.

For all of the technetium-iron powder experiments, the iron powder was washed with ethyl alcohol to remove the fine particulates so that they would not pass through or clog the frit at the downstream end of the reaction column. To accomplish this, the iron powder was placed in a beaker (either 100 mL or 250 mL), and ethyl alcohol was added to sufficiently cover the powder. The mixture was agitated by shaking the beaker. The mixture was allowed to settle for a few seconds before the fine particlulates suspended in solution were decanted off. This was repeated until the solution was not cloudy when agitated. The final solution was then poured out of the beaker, and the iron was allowed to air dry before loading the column.

For each of the experiments, except the Blank-run Experiment, the following were conducted:

- The 6-mm-ID × 30-cm-long titanium reaction column was packed with the reactant being studied.
- The low pressure was set at or above 179 psi. This was the minimum pressure necessary to keep the system functioning smoothly for these experiments. The high pressure at the inlet end of the reaction column was set at or above the values needed to force the liquid through the reactant at the chosen flowrate.
- The technetium-spiked solution was prepared and placed in the supply reservoir. A sample was collected from the supply reservoir.
- The desired flowrate was set.
- The pressure was turned on.
- The temperature controllers were set and turned on for the elevated temperature experiments.
- The pump was turned on.
- Analytical samples were collected periodically.

The Blank-run Experiment determined whether ^{99}Tc was being retained in the plumbing downstream from the reaction column. To do this, non-spiked J-13 solution was passed through the lines downstream from the reaction column only. Samples of this solution were periodically collected to be analyzed for ^{99}Tc. Following the non-spiked J-13 solution, 0.1 M nitric acid was passed through the lines downstream

from the reaction column. J-13 was again flushed through the lines downstream from the reaction column following the nitric acid flush. Samples of this second J-13 flush were collected and analyzed for ^{99}Tc concentration.

The FT-4C was flushed with 0.1 M nitric acid, J-13, and/or deionized water before conducting all experiments. For the first three experiments, the system was flushed with DIW as good laboratory practice. DIW was also pumped through the system when system maintenance was being conducted. After the Blank-run experiment, J-13 and/or nitric acid was used to flush the system. Before the iron powder experiments, the system was flushed with nitric acid and J-13 until the technetium concentration of the samples from the flush solution was less than approximately 1×10^{-1} ppb.

The results obtained from the Blank-run, Copper Shot, Tin Shot, and four Iron Powder experiments that used this system are discussed in Sections 4.2, 4.4, 4.6, and 4.3.3, respectively.

3.4.2 Bench-Top Flow-Through System

Because of some problems with the FT-4C (as will be discussed in Section 4.2), the Bench-top Flow-through System (Figure 11b) was used in some experiments. The system's equipment is discussed in Section 3.4.2.1. The Bench-top System was used to conduct the copper powder, two iron

powder, and the stannous chloride and tuff experiments. The experimental details are shown in Table 4, the experimental descriptions are discussed in Section 3.4.2.2, and the results are presented in Sections 4.4.1, 4.5.2, 4.3.1, respectively.

3.4.2.1 Equipment description

The Bench-top Flow-through System pumped a technetium-spiked solution through a reaction column. Two types of reaction columns were used in this system. One was identical to that of the FT-4C, a 6-mm-ID × 30-cm-long titanium column with a 10-μm frit at the outlet end. The other was a stainless steel reaction column approximately 1-cm-ID × 6-cm-long with a 2-μm frit at the outlet end. The solution was pumped using a Milton Roy metering pump, which is a reciprocating plunger, positive displacement pump capable of flowrates from 50-500 mL/day. The flowrates for the experiments using this system were between 100 mL/day and 160 mL/day. All the tubing for this system was 1/16 inch stainless steel. This system was not equipped with a furnace and was used at ambient conditions.

3.4.2.2 Bench-top experiments

For the Bench-top experiments listed in Table 4, the reaction column was loaded with the reactant being investigated. The copper powder and iron powder were washed

with ethyl alcohol as described in Section 3.4.1.3. The ^{99}Tc Iron Powder Experiment used the 1-cm-ID × 6-cm-long stainless steel reaction column; all the others used the 6-mm-ID × 30-cm-long titanium column.

Except for the Stannous Chloride and Tuff Experiment, the pump was initially connected to the bottom of the vertical reaction column for all the ^{95m}Tc experiments. The solution was pumped from the bottom up through the reaction column until the solution appeared exiting the top of the column. This ensured that it was filled with liquid, and the solution was not channeling through the column. For the remainder of the experiment, the pump was connected to the top of the reaction column to force the solution to flow from the top to the bottom of the column. Then any precipitate formed could be expelled from the column with the flow rather than collecting on the bottom of the column. For the Stannous Chloride and Tuff Experiment, the inlet solution entered the top of the reaction column only. Otherwise, the stannous chloride would have dissolved before changing the direction of the flow from the bottom of the reaction column to the top. Analytic samples were collected periodically from the outlet of the reaction column.

3.4.3 Beaker System

The Beaker No-flow System was used for investigating stannous chloride. A schematic of this system is shown in

Figure 11c. The Beaker No-flow System has the reactant in semi-static contact with the technetium-spiked solution. The equipment is discussed in Section 3.4.3.1, and the experiment is discussed in Section 3.4.3.2.

3.4.3.1 Equipment description

The Beaker No-flow System, Figure 11c, was used at ambient conditions to study the effect of dissolved stannous chloride on ^{99}Tc reduction. To use this system, a technetium solution was added to the beaker, which contained dissolved stannous chloride.

The Beaker System was used because stannous chloride is a soluble salt; i.e., it dissolves when in contact with the solution used in the experiments. By using this system, the dissolved stannous chloride's redox effectiveness could be studied because the dissolved salt would remain in the system rather than being pushed through a reaction column.

3.4.3.2 Experiment description

The Beaker Stannous Chloride Experiment used the beaker setup, Figure 11c. Stannous chloride (10.00 g) was placed in a beaker containing 30 mL of J-13 and stirred vigorously with a magnetic stir-bar for 30 min until the stannous chloride was fully dissolved. Ninety-three mL of a 26 ppb ^{99}Tc-spiked J-13 solution were then mixed into the beaker

containing the dissolved stannous chloride and stirred with the magnetic stir-bar for 15 min.

The first analytical sample collected was from the ^{99}Tc-spiked solution before it was added to the stannous chloride. The second analytical sample was from the stannous chloride/^{99}Tc-spiked J-13 solution. It was collected using a syringe and analyzed for technetium concentration. A third sample was collected 24 hours later, placed in a filter (20 Å pore size) and centrifuged until the solution passed through the filter before analyzing for technetium concentration. To ascertain that the technetium was not absorbed by the filter in the above samples, the filter for the fourth sample was primed. It was primed by passing a portion of the solution through the filter and then discarding the solution. This allowed the filter to be saturated with the sample. After priming the filter, the remainder of the solution from the fourth sample was then centrifuged in this same filter. The centrifuged solution was then analyzed for ^{99}Tc concentration to determine if all the technetium precipitated or if some remained in solution. The centrifuge tube was then washed with 0.1 M nitric acid, and the nitric acid solution from the centrifuge tube was analyzed for technetium concentration.

3.4.4 Sealed Vessel System

The Sealed Vessel System, Figure 11d, was used for the remainder of the experiments with iron powder. This system was designed to obtain more information on the reaction kinetics of iron and on the solution environment of the experiment. This system is described in Section 3.4.4.1, the readiness experiments are described in Section 3.4.4.2, and the experiments conducted using this system are described in Section 3.4.4.3.

3.4.4.1 Equipment description

The Sealed Vessel System used no-flow (steady-state) conditions. It was designed and used to determine if the much longer contact time between the solution and the iron powder, compared to the flow-through systems, would cause the ^{95m}Tc concentration in solution to drop BDL. This system was also used to study the variations in the solution environment (pH and Eh), caused by iron powder. The Sealed Vessel System allowed for comparison of the technetium concentration and the solution environment variables with those obtained from the EQ3/6 simulation results.

The Sealed Vessel System consisted of a sealable vessel inserted into a heating mantle. The cover for the vessel had port holes that held rubber stoppers. The port holes and the vessel cover were all sealed with silicone grease (Dow Corning Compound 111 Valve Lubricant and Sealant

containing Silicon and rated -40°C to 204°C [-40°F to 400°F]) to limit the amount of air infiltrating into the system. A pH probe, a thermocouple, a platinum electrode, a saturated calomel electrode (SCE), and a sample port were inserted through rubber stoppers in the port holes.

The sample port consisted of a stainless steel tube with tygon tubing slipped over it. A clamp on the tygon tubing prevented the solution from leaking and also prevented air from entering the system. The stainless steel tubing was below the solution level, but above the iron powder on the bottom of the vessel. A pipet tip was inserted into the tygon tubing, the clamp was removed, 2 mL of solution was withdrawn, the clamp was replaced, and the solution was discarded. A new pipet tip was inserted, the clamp was removed, and a 5-mL sample was retrieved for technetium-concentration analysis. The tygon tubing was then clamped again. The first 2 mL were discarded because the sample port held 2 mL, and it may have contained solution from the previous sample.

Two iron powder experiments used this system, one at 70°C, and the other at ambient temperature. The experiments are explained in Section 3.4.4.3, and the results are presented in Sections 4.3.2.1 and 4.3.2.2, respectively.

3.4.4.2 Readiness experiments

Three experiments using the Sealed Vessel System determined whether (1) the lack of oxygen limits the amount of aqueous iron such that Eh measurements were unobtainable, (2) meaningful Eh measurements were obtainable, and (3) the system was safe for conducting experiments using radioactive solutions. To measure the system Eh, the iron concentration in solution must be high enough. Eh measurements with iron concentrations of 10^{-6} and 10^{-7} M have been successfully measured using a platinum electrode under anoxic conditions.[33] Because the EQ3/6 simulations calculated some of the iron concentrations to be within this range, meaningful Eh measurements should be obtained. The supply of aqueous iron should not be limited because the Sealed Vessel System was not purged with an inert gas and was not a true anoxic environment. The iron should have reacted with the oxygen in the system resulting in obtainable Eh measurements. The lack of oxygen limiting the supply of aqueous iron to the solution is addressed further when analyzing the results of the technetium experiments using this system (see Section 4.3.2).

The Eh of the system was obtained by using a platinum electrode with an SCE reference electrode, as recommended in the literature.[32,33] The accuracy of the response of this electrode combination was checked using solutions containing quinnhydrone. Figure 15 Curve 1 shows that the measured

potentials were in very close agreement with the theoretical values, Figure 15 Curve 2.[34] It was therefore determined that the Eh measurements were obtained and had thermodynamic significance.

During these readiness experiments, the platinum electrode's surface spontaneously oxidized with atmospheric oxygen. The platinum surface was roughed with very fine emery cloth to remove the oxide layer as recommended in the literature.[32]

After correcting a couple of hardware problems, the system appeared to function correctly and was deemed ready for experiments with technetium from both a safety and operational standpoint.

One limitation could not be addressed before performing the Sealed Vessel experiments using technetium. Guppy and Atkinson[35] have found that solid technetium compounds that precipitate or are retained on iron would prevent the iron from further redox reactions. This limitation was considered when analyzing the results of the Sealed Vessel experiments (see Section 4.3.2).

3.4.4.3 Experiment description

Two experiments were conducted using the Sealed Vessel System, Figure 11d. The sealable vessel was first placed in the heating mantle. The pH probe, SCE, and sample port were placed into the sealable vessel's top. The platinum

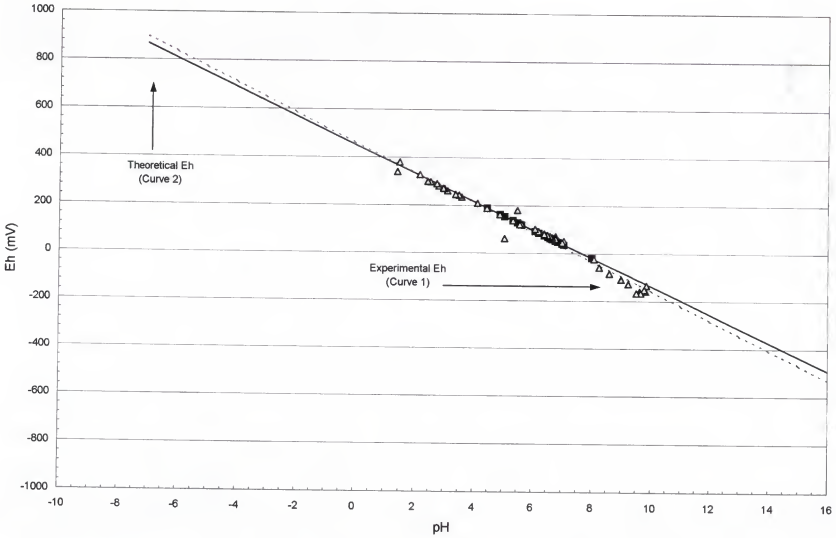

Figure 15 Sealed Vessel System Eh Instrumentation Calibration Using Quinnhydrone

electrode was wiped with a #600 emery cloth and put into the vessel's top. Both of the Sealed Vessel experiments had a 2.1×10^{-5} ppb ^{95m}Tc-spiked J-13 solution placed in the sealable vessel to which 32 g of iron powder were added. The vessel cover was placed on the vessel. The stoppers, pH probe, thermocouple, platinum electrode, SCE, and sample port were all sealed with silicone grease. The vessel cover was then sealed with silicone grease. For the Sealed Vessel Experiment at 70°C, the temperature controller was set to maintain a temperature of 70°C and then turned on. The stopper containing the thermocouple was loosened to relieve pressure while the system was heated, and then it was sealed in place again. Samples were periodically collected via the sample port.

Thirty-five g of sodium chloride crystals were added to the system 39 days into the Sealed Vessel Experiment at 24°C. At this time, the temperature controller was set and turned on to raise the temperature to 70°C. The sodium chloride was added in an attempt to increase the corrosion rate of iron. Eleven days later, another 30 g of sodium chloride crystals were added to the system.

For a discussion of the results obtained for the Sealed Vessel Experiments at 70°C and 24°C, see Sections 4.3.2.1 and 4.3.2.2.

CHAPTER 4
RESULTS AND DISCUSSION

4.1 Overview

The results of the experiments presented in Section 3.4 are arranged by the reactant used rather than by the system used to allow for continuity in the discussion of each reactant. Table 5 indicates the sections where the preparation, description, and discussion for the experiments are located.

The results of the experiments are shown in Figures 16-42. These figures show the times at which flowrates were changed, when applicable, when the technetium concentration went BDL, and when the NaCl was added to the Sealed Vessel Experiment at 24°C. Some figures show comparisons with the results obtained from the EQ3/6 simulations. It may be necessary to review Section 2.3.2 for interpretation of the figures that include the EQ3/6 simulations.

The experimental results are also summarized in Table 6. The table is grouped by reactant and shows the initial, final, highest, and lowest technetium concentrations as well as the time these concentrations were obtained and the total time the experiments were conducted.

Table 5 Experiment Location

Experiments	Progression	Iron	Copper	Tin	Stannous Chloride
		Section Number[1]			
FT-4C	Preparation	3.4.1.1	3.4.1.1	3.4.1.1	
	Description	3.4.1.3	3.4.1.3	3.4.1.3	
	Discussion	4.3.3	4.4.2	4.6	
Bench-top	Preparation	3.4.2.1	3.4.2.1		3.4.2.1
	Description	3.4.2.2	3.4.2.2		3.4.2.2
	Discussion	4.3.1	4.4.1		4.5.2
Beaker System	Preparation				3.4.3.1
	Description				3.4.3.2
	Discussion				4.5.1
Sealed Vessel	Preparation	3.4.4.1			
	Description	3.4.4.3			
	Discussion	4.3.2			

[1] No section number indicates this system was not used to investigate this reactant

Table 6 Experimental Results

Experiment	System used [1]	Initial Tc Concentration (ppb)	Highest Tc Concentration (ppb)	Time of Highest Concentration	Final Tc Concentration (ppb)	Lowest Tc Concentration (ppb)	Time of Lowest Concentration	Total Time (days)
Blank Run J-13	a	0	1.4×10^{1}	0.0 h	BDL	BDL	23 days	23
Blank Run Nitric Acid	a	0	7.8	28.0 days	1.7×10^{-1}	7.8×10^{-2}	29 days	30
High-flow Iron Powder	a	1.5×10^{3}	1.5×10^{3}	0.0 h	1.0	1.5×10^{-1}	4.2 days	5
Low-flow Iron Powder	a	9.8×10^{2}	9.8×10^{2}	0.0 h	1.2×10^{-1}	1.2×10^{-1}	23 days	23
Iron Powder at 85° C	a	1.5×10^{3}	1.5×10^{3}	0.0 h	5.8	5.3×10^{-1}	3.1 days	11.8
^{99}Tc Iron Powder	a	3.6×10^{1}	3.6×10^{1}	0.0 h	BDL	BDL	1.0 days	8
^{95m}Tc Iron Powder	a	9.4×10^{-4}	9.4×10^{-4}	0.0 h	3.2×10^{-5}	1.2×10^{-7}	9.0 days	40
Iron Powder at 70° C	a	2.3×10^{-5}	2.3×10^{-5}	0.0 h	BDL	BDL	7.0 min	15
Iron Powder at 24° C	a	2.3×10^{-5}	2.3×10^{-5}	0.0 h	BDL	BDL	40 days	56
DIW Copper Shot	a	1.2×10^{3}	3.1×10^{3}	3.1 days	1.0×10^{3}	6.0×10^{0}	1.2 h	8
DIW Copper Shot, ≥ 1mL	a	1.2×10^{3}	1.4×10^{3}	1.8 days	1.2×10^{3}	1.2×10^{3}	0.0 h	8
Copper Shot at 24° C	a	1.3×10^{3}	1.5×10^{3}	1.8 days	1.3×10^{3}	1.1×10^{3}	7.7 days	5
Copper Shot at 85° C	a	1.5×10^{3}	2.0×10^{3}	3.3 h	1.4×10^{3}	1.4×10^{3}	3.0 days	3
^{95m}Tc Copper Powder	a	9.4×10^{-4}	1.0×10^{-3}	7.0 days	7.4×10^{-4}	1.5×10^{-6}	3.0 h	7
Tin Shot at 24° C	a	1.5×10^{3}	1.5×10^{3}	0.0 h	9.1×10^{2}	2.3	1.5 h	2.6
Tin Shot at 85° C	a	1.5×10^{3}	1.5×10^{3}	5.1 days	1.0×10^{3}	8.6×10^{2}	3.0 days	11
Stannous Chloride	c	2.6×10^{1}	2.6×10^{1}	0.0 h	BDL	BDL	1.0 days	2
Stannous Chloride and Tuff	b	9.4×10^{-4}	1.2×10^{-3}	7.0 days	1.2×10^{-3}	6.6×10^{-6}	5.4 h	7

(1) ExperimentalSystems: a. FT-4C b. Bench-top c. Beaker d. SealedVessel

It is evident from Table 6 that none of the experiments that used the FT-4C system had the technetium concentration fall to BDL. It was concluded from the Blank-run Experiment (see below) that the FT-4C retained technetium from previous experiments and then released some of the technetium in subsequent runs.

Iron was the only reactant to reduce the ^{99}Tc concentration BDL in the flow-through experiments. In the no-flow experiments, stannous chloride reduced the ^{99}Tc concentration BDL (≈0.4 ppb), and iron reduced the ^{95m}Tc concentration BDL($\approx 1 \times 10^{-7}$ ppb).

Experimental details and discussions are contained in the following sections.

4.2 Blank-run Experiment

To clarify the discussion of this Blank-run Experiment, a chronological listing of the experiments using the FT-4C is shown in Table 7.

It was suspected that the FT-4C, which was shown in Figure 11a, was retaining technetium and releasing it later in the same or subsequent experiments. Experiment 3, the Copper Shot Experiment at 85°C (which will be discussed in Section 4.4.2.3) had an initial increase in technetium concentration. However, the ^{99}Tc concentration analysis for this experiment was not completed until a few days before Experiment 4, the Tin Shot Experiment at 24°C. The flush

Table 7 Chronology of FT-4C Experiments

	Experiment	Reactant	Reactant Mass (g)	Temperature (°C)	Flowrate (ml/day)	Radionuclide	Initial Concentration (ppb)
	Ft-4C Readiness	Iron powder	~30	25	7.8-78	^{238}U	1.2×10^{2}
		DIW (system work)					
1	DIW Copper Shot	Copper shot	40.95	24	0-25-50	^{99}Tc	1.2×10^{3}
		DIW and HNO_3 flushed					
2	Copper Shot at 24° C	Copper shot	41.18	24	50-0	^{99}Tc	1.3×10^{3}
		DIW flush					
		DIW flush (pump work)					
3	Copper Shot at 85° C	Copper shot	41.89	85	50-0	^{99}Tc	1.5×10^{3}
		DIW flushed					
4	Tin Shot at 24° C	Tin shot	35.65	24	50	^{99}Tc	1.0×10^{3}
		HNO_3 downstream vacuum side					
5	Blank Run	J-13 + HNO_3	-	25	50	-	-
6	High-flow Iron Powder	Iron powder	29.77	24	0-50-100	^{99}Tc	1.5×10^{3}
		HNO_3 + J-13					
7	Iron Powder at 85° C	Iron powder	30.02	25	50	^{99}Tc	1.5×10^{3}
		Drained and vacuumed lines downstream of pump					
8	Tin Shot at 85° C	Tin shot	36.97	85	50	^{99}Tc	1.0×10^{3}
		HNO_3 + J-13 acid flush					
9	Low-flow Iron Powder	Iron powder	29.76	24	10-50	^{99}Tc	1.5×10^{3}

solution between Experiments 3 and 4 was not analyzed until after Experiment 4 was started. Therefore, it was not until after the start of this latter experiment that the FT-4C was suspected to retain and release technetium. Rather than terminate the experiment, the Blank-run Experiment was not conducted until after the completion of Experiment 4.

In the Blank-run Experiment, J-13 water was pumped through the system downstream of the reaction column and 10 effluent samples were collected over a period of 23 days. These samples were then analyzed for ^{99}Tc concentration. Since this experiment did not have technetium added to the J-13 solution, no ^{99}Tc should have been detected in the sample effluent. However, as shown in Figure 16 Curve 1, the first effluent sample collected had a ^{99}Tc concentration of 14 ppb. Within the first hour, the ^{99}Tc concentration decreased to 0.7 ppb. The technetium concentration in the effluent samples then fluctuated between 0.02 ppb and 0.3 ppb over the next 23 days. The technetium concentration was BDL after flushing the system with J-13 for 23 days.

Nitric acid (0.1 M) was then flushed through the lines downstream from the reaction column for 5 h to determine if all the technetium had been leached by the J-13 flush. No samples of the nitric acid flush were collected because colleagues suggested that the detection limit would be very high because the fluorescence would be absorbed by the

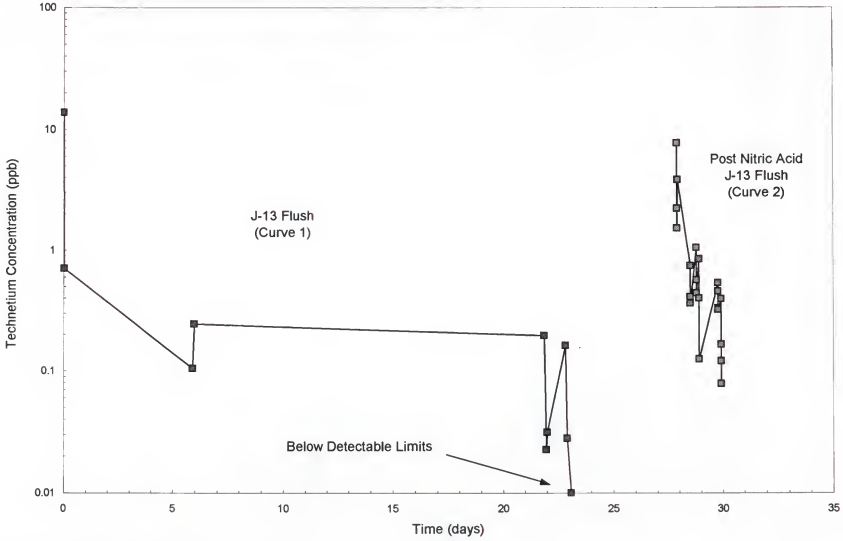

Figure 16 FT-4C Blank-run Experiment

nitric acid.[f] Following the nitric acid flush, J-13 was again flushed through the lines downstream from the reaction column. Over the next 2 days, 23 samples of this second J-13 flush were collected and analyzed for ^{99}Tc concentration. As shown in Figure 16 Curve 2, the first sample of this post nitric acid flush had a technetium concentration of 7.8 ppb, which indicated that not all the technetium was completely removed with the first J-13 flush. The technetium concentration dropped to 0.08 ppb 2 days later.

This experiment confirmed that technetium was indeed being retained within the plumbing downstream from the reaction column in the FT-4C Flow-through System. A technetium concentration below the 0.08 ppb lowest post-nitric acid flush was never reached during any of the experiments using this system. It was presumed that this was due to the demonstrated capacity for the system to retain and then re-release technetium rather than a failure of the reducing agent to lower the technetium concentration.

Because experiments were conducted before realizing that the FT-4C was retaining technetium, the effects of this retention on those experiments had to be considered when analyzing the results. The effects of this retention

---

[f]This turned out not to be true, and later experiments analyzed samples containing nitric acid.

phenomenon will be discussed at length in the applicable sections. They are briefly stated here.

The technetium retention had no significant impact on the DIW Copper Shot Experiment, the Copper Shot Experiment at 24°C, or the Tin Shot Experiment at 24°C (Sections 4.4.2.1, 4.4.2.2, and 4.6, respectively) because the detected technetium concentrations were much greater than 14 ppb (the highest technetium concentration detected in the Blank-run Experiment). The system was also flushed before each experiment either as good laboratory practice or for extended periods of time as an integral part of system maintenance. However, the technetium retention affected the Copper Shot at 85°C and the iron powder experiments even though the system was flushed with DIW before conducting the Copper Shot Experiment at 85°C and with nitric acid before conducting the iron powder experiments. The minimum technetium concentrations detected in these experiments were close to the minimum detected (0.08 ppb) in the Blank-run experiment following the nitric acid flush. Therefore, the minimum technetium concentration in the copper shot and iron powder experiments may have been an artifact of the technetium retention and release by the system rather than a measure of the reducing capabilities of copper and iron on the technetium. The effect of the technetium being re-released during these experiments is discussed in Sections 4.4.2.3 and 4.3.3, respectively.

Because the FT-4C retained the technetium, the Bench-top System, shown in Figure 11b, was designed and also used for flow-though experiments.

4.3 Iron Powder Experiments

Three different experimental systems were used to investigate iron powder as a reducing agent to lower the concentration of technetium in J-13 water: the FT-4C, the Bench-top Flow-through, and the Sealed Vessel systems, Figure 11a, b, and d, respectively. Section 4.3.1 discusses the results obtained from the Bench-top Iron Powder experiments. Section 4.3.2 discusses the results obtained from the Sealed Vessel experiments. The results from the FT-4C experiments (Section 4.3.3) are included for completeness even though no direct conclusions can be drawn from them because the FT-4C was determined to be inadequate for these experiments. A summary of the iron powder results and conclusions are presented in Section 4.3.4.

4.3.1 Bench-Top Iron Powder Experiments

Two Bench-top experiments were conducted; one used ^{99}Tc, and the other used ^{95m}Tc. In the first experiment, a ^{99}Tc-spiked solution was pumped through a reaction column filled with iron powder at 24°C. As shown in Figure 17, the ^{99}Tc concentrations dropped to near detectable limits

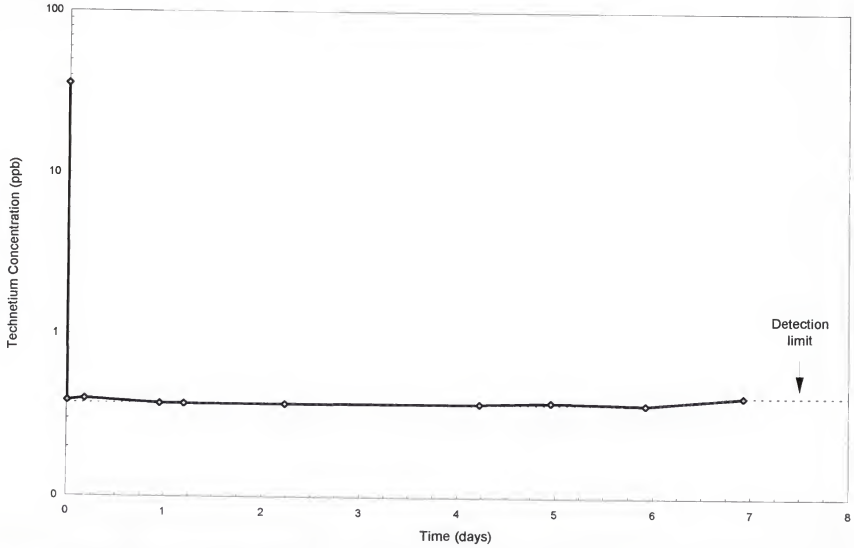

Figure 17 Bench-Top ^{99}Tc Iron Powder Experiment. All measurements after the first sample were near or below detectable limits.

(0.4 ppb) within 25 min and remained at or below detectable limits for the entire 8 days the experiment was conducted.

This was the first experiment conducted using the Bench-top system after the Blank-run Experiment on the FT-4C. The low technetium concentration found in this experiment confirmed that the iron experiments using the FT-4C were affected by the release of ^{99}Tc retained downstream of the pump.

Because the ^{99}Tc concentrations in the first Bench-top experiment were BDL, ^{95m}Tc was used in the next Bench-top experiment to allow for the 8 orders of magnitude improvement in the detection limit. The concentrations of ^{95m}Tc (ppb) and iron (ppm) for this experiment are shown in Figure 18, Curves 1 and 2, respectively. Curve 1 shows that the ^{95m}Tc concentrations in the effluent samples rapidly dropped approximately 4 orders of magnitude to 1×10^{-7} ppb (right at detectable limits) within the first 6 h of the experiment and remained near 1×10^{-7} ppb for the first 13 days of the experiment. Then the concentration steadily increased over the next 22 days to approximately 1×10^{-6} ppb before jumping to about 3×10^{-5} ppb for the last 2 days of the experiment.

The reason for the increase in the technetium concentration after the first 13 days was most likely because the iron was sorbing the technetium and thereby passivating the iron surfaces, as will be discussed in more

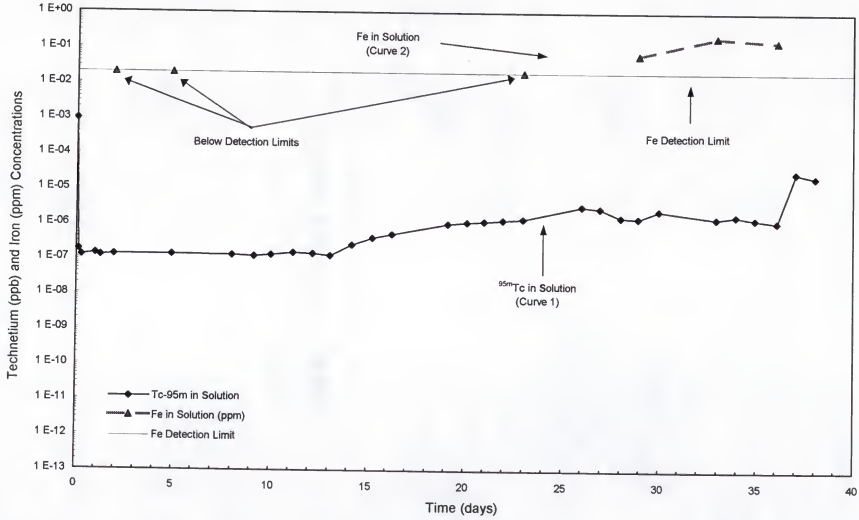

Figure 18 Bench-Top ^{95m}Tc Iron Powder Experiment Solution Concentrations

detail momentarily. The reason for the increase in the technetium concentration on day 37 is uncertain. The only sure means of knowing if the technetium concentration would have remained at this high level would have been to extend the experiment, but the experiment was terminated before the last two samples were analyzed, i.e., before the high technetium concentrations were known.

A few samples were chemically analyzed for iron concentration to allow for comparison with the computer simulations. The results obtained from the experimental iron analyses are shown in Figure 18 Curve 2. The first three samples had iron concentrations BDL (0.02 ppm). The last three samples had measurable iron concentrations that will be discussed later along with the predictions of iron concentrations by the codes.

After the ^{95m}Tc Bench-top Experiment was terminated, the ^{95m}Tc activity along the length of the column was measured using the TCA. The results are shown in Figure 19. The teflon holder was 16.5 in. long, and the reaction column, which was only 12 in. long, was placed inside the teflon holder. As shown in the figure, the ^{95m}Tc activity was concentrated at the inlet end of the reaction column (left hand side in the figure) where it peaked at 1.4×10^{6} Bq. However, there was also measurable activity (3.1×10^{-3} Bq) at the outlet end, which shows that technetium made it all the way to the end of the column. This was in agreement

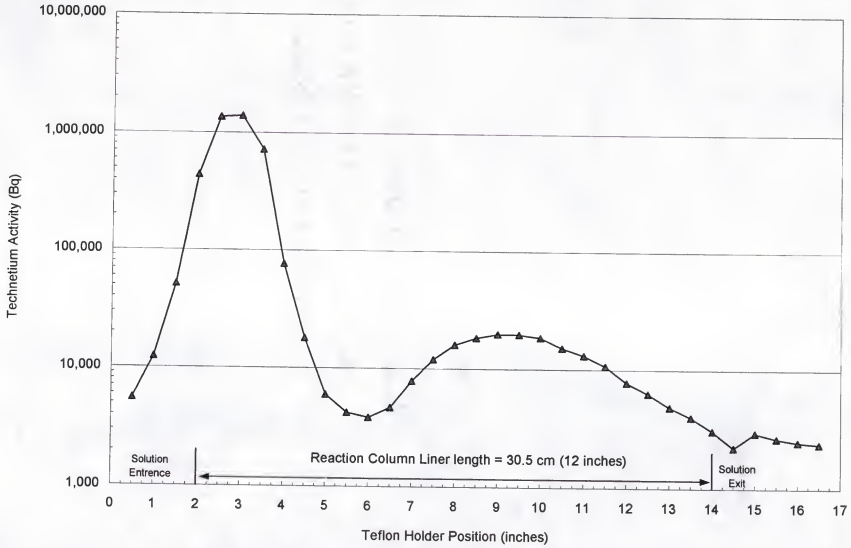

Figure 19 Bench-Top ^{95m}Tc Iron Powder Experiment Reaction Column. Reaction Column analyzed after the experiment.

with the observed increase in technetium concentration in the effluent samples after day 13 (as was shown in Figure 18).

The high activity at the inlet end of the reaction column was caused by the technetium concentrating at the front of the reaction column as it was sorbed onto the active iron surface, as well as reduced and precipitated by the iron. The iron surfaces must have been at least partially passivated by sorption of technetium because the iron became less effective at decreasing the technetium concentration as time passed. This is evident by the increased technetium concentration in the effluent samples after day 13 and because of measurable technetium activity at the outlet end of the reaction column. The precipitation of the technetium between the iron particles would not be expected to passivate the iron. Because the iron surface was passivated, the new incoming technetium had to traverse further down the column before reaching active iron surfaces. Eventually, the end of the column was reached. At that point, technetium activity was present along the entire reaction column, but the activity was greater at the inlet end rather than the outlet end. If the reaction column had been analyzed daily, the first day would have shown technetium activity only near the inlet. Day 2 would have shown the technetium activity a little further down, etc. Eventually, it would have shown that the technetium activity

progressed all the way to the outlet end of the column. However, daily analyses would have required an impractical reconfiguration of the experimental setup to provide for low levels of background radiation.

Also, some technetium was always detected in the effluent samples (just at detectable limits for the first 13 days, then well above detection limits until the end of the experiment) because the slow reaction kinetics of iron prevented all the technetium from being reduced. This was the case even when it could react with the bare iron surface as it traversed down the reaction column. The slow reaction kinetics of iron will be apparent when the Sealed Vessel experiments are discussed in Section 4.3.2.

Results from the two Bench-top Iron Powder experiments agree in the sense that the technetium concentrations dropped rapidly in both cases. In the ^{99}Tc experiment, the concentrations rapidly dropped below the detection limit of about 0.5 ppb and could have been as low as in the repeat experiment with ^{95m}Tc (1×10^{-7} ppb).

The Bench-top ^{95m}Tc Iron Powder Experiment was modeled by the two EQ3/6 simulations, Free Run and Limited Run, that were shown in Figure 8 and explained in more detail in Section 2.3. The initial amounts of iron and technetium entered into the "Free Run" simulation were the same as those used in this Bench-top ^{95m}Tc Iron Powder Experiment. In the other simulation, "Limited Run," the same initial

amount of technetium was entered as was used in the experiment, but the initial amount of iron was limited in the simulation such that the final calculated technetium concentration was equal to the value found in the experiment. Figure 20 shows the combination of Figure 18 and Figure 8 for comparative purposes.

In Figure 20, the technetium and iron concentrations are plotted along the axis of ordinates. Concentrations from the Bench-top ^{95m}Tc Iron Powder Experiment versus time (lower axis of abscissae) are represented by Figure 20 Curves 1 and 2, respectively. Concentrations from the Free Run simulation versus the reaction progress (upper axis of abscissae) are represented by Figure 20 Curves 3 and 4, respectively. And finally, concentrations versus reaction progress from the Limited Run simulation are represented by Figure 20 Curves 5 and 6, respectively.

Comparison of results from the experiment and the EQ3/6 calculations shows that the maximum iron concentrations were approximately the same for the two cases, Figure 20 Curves 2 and 4, respectively. The calculated iron concentration peaks at about 0.2 ppm at a reaction progress of 0.00128. The measured iron concentration reaches this value after 31 days.

Although the measured minimum technetium concentrations were quite low, just at detection limits of 1×10^{-7} ppb (Figure 20 Curve 1), they did not decrease to the calculated

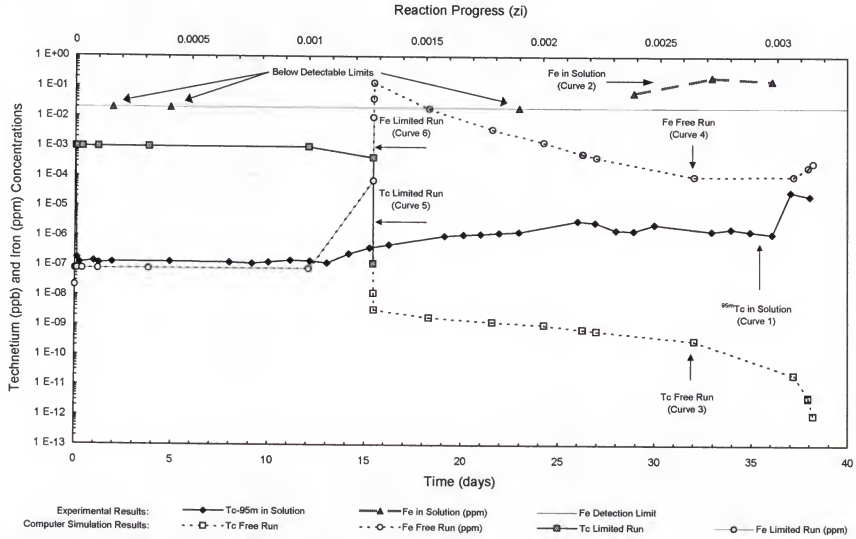

Figure 20 Comparison of the Bench-Top ^{95m}Tc Iron Powder Experiment and EQ3/6 Simulations. Note that at low reaction progress, Curves 5 and 6 overlap Curves 3 and 4, respectively.

concentrations of 1×10^{-9} ppb to 1×10^{-12} ppb, (Figure 20 Curve 3). By the 15th day, the technetium concentrations were well above detectable limits and rising. As previously stated, the rise in technetium concentration in the experiment was most likely caused by the technetium sorbing onto the iron, thereby partially passivating the surface and causing the iron to become less reactive. The codes did not show this rise in technetium concentration because the codes do not model sorption.

The measured technetium concentrations were also orders of magnitude greater than that indicated by the simulation for a given iron concentration in solution. According to the EQ3/6 results, an iron concentration of 0.064 ppm corresponds to a technetium concentration of 9.6×10^{-9} ppb (Figure 20 Curves 4 and 3, respectively), at a reaction progress of 0.0013 (upper axis). However, in the Bench-top ^{95m}Tc Iron Powder Experiment at 29 days (lower axis), the same iron concentration corresponded to a technetium concentration of 1.5×10^{-6} ppb as shown in Figure 20 Curves 2 and 1, respectively.

The analysis of the reaction column (see page 85) also indicates that the technetium was sorbed by the iron, which caused the iron surface to become partially passivated and less effective at decreasing the technetium concentration as time passed. Other researchers have also reported technetium sorption by iron. For instance, Gu and Schulz

reported that the sorption of technetium was "associated with both soil organic matter and iron and aluminum oxides."[36] They attributed this to "nonspecific sorption," which "occurs at the localized positive charges that occur on free hydrous oxides of iron ... which attract anions electrostatically, and the anions are readily exchangeable with those in the soil."

Meyer, Arnold, and Case studied the effect of basalt and basalt plus iron on technetium concentration.[21] Three types of basalt were tested: a virgin basalt, one with iron powder added, and one that was contaminated by iron when the basalt was crushed. In the virgin basalt sample, significant technetium sorption did not occur. The small amount of technetium that was adsorbed on the virgin basalt was mostly present in the (VII) valence state with only a small fraction in lower valence states. Therefore, the technetium concentration was not significantly reduced nor was there significant reduction in the oxidation state of the technetium that was sorbed. However, in the basalt with the iron powder added, all of the technetium was essentially removed from the solution, and all but a few percent of the technetium that was retained by the basalt was in a reduced oxidation state. In the experiment conducted with the basalt that was contaminated with iron during crushing, essentially all of the technetium was removed from solution. Most of it was reported to be present as Tc(VII), which

probably was an artifact of the analytical method used. Meyer et al. noted that the valence state analyses for technetium were not conducted under anoxic conditions. They attributed the Tc(VII) found on the basalt to technetium being easily reoxidized during its extraction.

Meyer et al. also showed that hematite sorbed technetium from solution in anoxic test tube experiments.[21] The amount of technetium that remained in the solution was very small and was present as reduced technetium, but they do not indicate the reduced technetium's oxidation state. Meyer et al. concluded that a surface reaction may have been responsible for removing technetium from solution because the reduction in technetium concentration was very sensitive to the surface conditions. Meyer et al. also noted that if the oxidation state of the technetium could be reduced, then the technetium would be adsorbed on any surface. Again, this suggests that a surface reaction may be ultimately responsible for removing the technetium from solution.

4.3.2 Sealed Vessel Experiments

Although the Bench-top ^{95m}Tc Iron Powder Experiment indicated that the iron would reduce the technetium concentration, this experiment could not be adequately modeled by the codes. Therefore, the Sealed Vessel system was used next because the codes can model a closed system. The term "closed system" refers to no replenishment of the

reactant or solution (iron, j-13 plus technetium, etc.), and the solution volume remains constant. In the experiment, the solution volume was constant except for the removal of the samples, the total volume of which was relatively small. The pH and Eh were measured in the Sealed Vessel System for comparison with those calculated by the codes. To try to gain information on the reaction kinetics between the iron and technetium, experiments at two temperatures were conducted using this system. The Sealed Vessel Experiment at 70°C is presented below, and the Sealed Vessel Experiment at 24°C is presented in Section 4.3.2.2.

4.3.2.1 Sealed Vessel Experiment at 70°C

The Sealed Vessel System was essentially a closed system and was modeled as such by EQ3/6 (see Section 2.3). Because the experiment was started at room temperature and then increased to 70°C, the EQ3/6 simulation had the same temperature change. Figure 21 shows the technetium concentration, Figure 22 shows the system pH, and Figure 23 shows the system Eh. Figure 24 is the combination of Figure 22 and Figure 23. All the figures show both experimental results and computer simulations. In all these figures, the experimental data are plotted versus time (lower axis of abscissa), and the calculated data are plotted versus reaction progress (upper axis of abscissa).

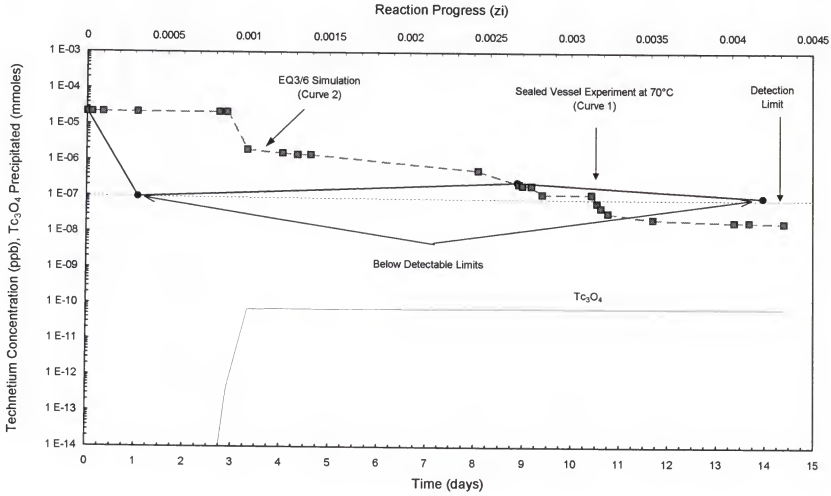

Figure 21 Sealed Vessel Experiment at 70°C, and the EQ3/6 Simulation. Technetium concentration and predicted precipitation of technetium compounds.

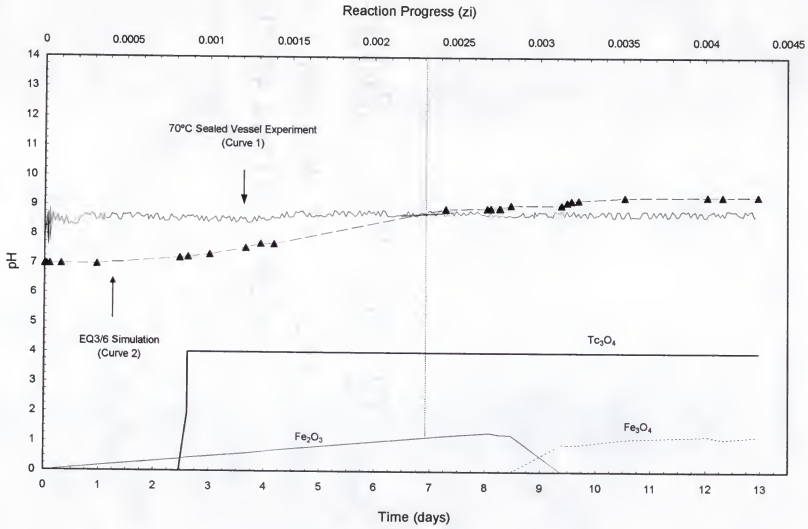

Figure 22 pH of the Sealed Vessel Iron Powder Experiments at 70°C and EQ3/6 Simulation. Precipitated products are relative units.

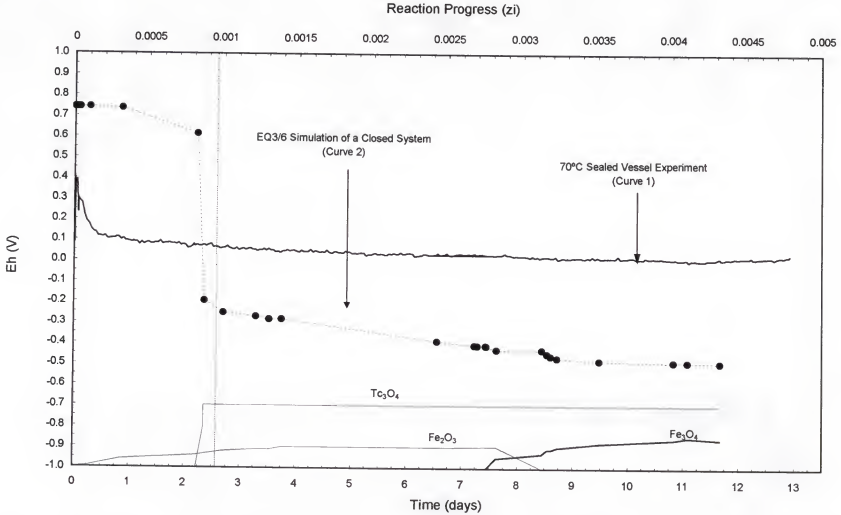

Figure 23 Eh of the Sealed Vessel Iron Powder Experiments 70ºC and EQ3/6 Simulation. Precipitated products are relative units.

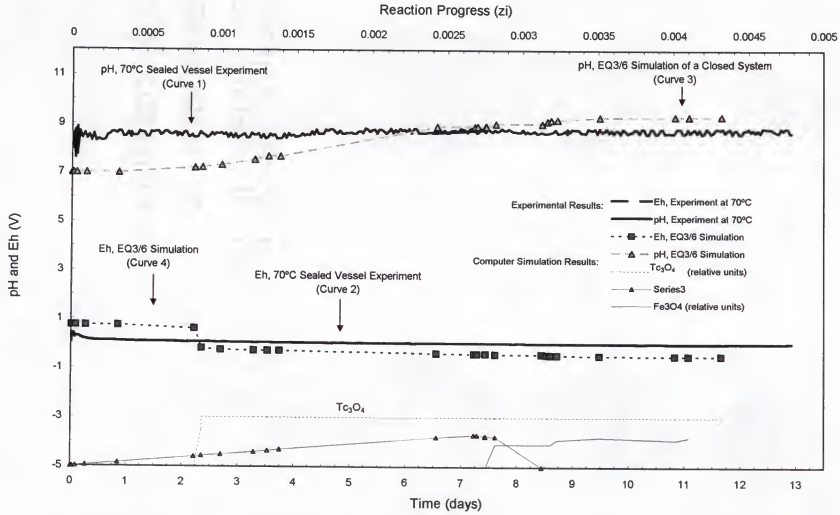

Figure 24 Sealed Vessel Iron Powder Experiment 70ºC, and the EQ3/6 Simulation of a Closed System. Precipitated products are relative units.

Figure 21 Curve 1 shows that after 1 day, the technetium concentration fell to BDL (1×10^{-7} ppb), which is in approximate agreement with the calculated minimum of 2×10^{-8} ppb shown in Curve 2.

Figure 22 Curve 1 shows the measured pH values from this Sealed Vessel Experiment at 70°C. The pH probe was calibrated just before the experiment using pH standards of 4, 7, and 10. After the experiment ended, when the pH probe was again checked with these same standards, it gave readings of 3, 6, and 9. To correct for this systematic error, it was assumed that the pH probe had drifted uniformly over the 14 days of the experiment. Therefore, the 1 pH unit drift was divided by the number of days for the experiment to obtain an average drift per day. The corrected pH was then calculated by multiplying the drift per day times the day of an individual pH measurement, and that amount was added to the corresponding pH measurement. These corrected values, which are plotted in the figure, show the pH of the system to be between 7.9 and 9.5. These values correspond quite well with those predicted by the EQ3/6 codes, which were between 7.0 and 9.2, Figure 22 Curve 2.

Figure 23 Curve 1 shows that the measured Eh decreased markedly the first day but, only slowly thereafter. The Eh never reached the low values indicated by the codes, Figure 23 Curve 2. It is believed that the measured Eh did

not reach the low levels calculated by the codes because oxygen was leaking into the system. The excess oxygen caused the measured Eh values to be much greater than the Eh of the iron redox reactions.

The suspected leakage of oxygen into this experimental system was discussed with Dhanpat Rai[9,37] who has conducted experiments using iron where the Eh values were close to the water-stability boundary where water is reduced to H_2.[38] To achieve the desired low Eh values in those experiments, Rai found it necessary to use a specially designed vessel that was placed in a glovebox purged by an inert gas. Use of an inert-gas glovebox, had it been available, would have minimized oxygen in-leakage in the present experiments where oxygen may have diffused through the rubber stoppers and plastic tubing.[39] Another possible oxygen source may have been the sample line, since it was not greased with silicone.

Although the measured Eh never reached the low values indicated by the codes, the measured Eh and calculated Eh show agreement at a reaction progress of 0.0009 (Figure 24 Curves 2 and 4, respectively). The measured pH of the system matches that of the codes at a reaction progress of 0.0023 (Figure 24 Curves 1 and 3, respectively). Although one would expect the match between the experiment and

---

[9]Dr. Dhanpat Rai is a Scientist and a Technical Group Leader in the Biochemistry Resources department at PNNL.

calculation to occur at the same reaction progress for both pH and Eh, which did not occur because of the oxygen in-leakage, it is worth noting that both these values (0.0009 and 0.0023) correspond to the region where Fe_2O_3 will precipitate. This is shown by the vertical lines in Figure 22 and Figure 23. This is also in the region where Tc_3O_4 begins to precipitate (reaction progress of 0.0009). The Eh/pH in the experiment are in the stability range for the formation of Fe_2O_3 on a Porbaix diagram,[40] thereby indicating that the iron was oxidized and hence, the technetium was reduced in the experiments.

The EQ3/6 calculations indicate that as the iron is oxidized to Fe_2O_3 and Fe_3O_4, the technetium will be reduced to Tc_3O_4 or $Tc(OH)_2$. The intermediate oxidation state, TcO_2 (sometimes referred to as $TcO_2 \cdot 2H_2O$), is never indicated to form in these systems.

The EQ3/6 codes contain data for $TcO_2 \cdot 2H_2O$ rather than TcO_2. Cartledge[41] originally published data on TcO_2, but has since referred to it as $TcO_2 \cdot 2H_2O$ and $Tc(OH)_4$.[42,43,44] More recently, Meyer, Arnold, Case. and O'Kelley have measured the thermodynamic data for $TcO_2 \cdot 2H_2O$ and have found that it agrees well with Cartledge's original research if the compound is assumed to be $TcO_2 \cdot 2H_2O$.[45,46]

Upon examining the vessel at the end of the experiment, the iron on the bottom of the vessel was brownish on top with hints of a red hue. It also had black spots showing

through the brown layer. Under the brownish top layer, the iron was a rich black color. The black and red colors observed were most likely the characteristic colors of an iron(III) oxide (such as hematite, Fe_2O_3).[47] The brown top layer was most likely an iron(III) oxide because the system's solution environment data indicated that the system Eh and pH were in the region where hematite (Fe_2O_3) is the stable phase. Even though brown is also the color of technetium(IV) oxides (such as $TcO_2 \cdot xH_2O$),[48] the formation of this compound was not supported by the codes.

Technetium concentration and pH results from this Sealed Vessel Experiment at 70°C were consistent with the EQ3/6 codes, but the measured Eh was well above the calculated value because of oxygen in-leakage.

In work that may be relevant to the current experiments, the behavior of iron in the presence of silica has been noted by Jantzen[33] in her studies of the leach rates of silica, iron, boron, and sodium from simulated waste glass under both anoxic and oxic conditions. In Jantzen's studies, the simulated waste glass was placed on top of the iron bars inside the vessel.[49]

Jantzen[33] showed that under oxic conditions, iron bars were oxidized, and aqueous iron was produced. As the iron oxidized, the system Eh was driven down into the stability range for iron silicate ($FeSiO_3$). The aqueous iron combined with the aqueous silica. As the iron was oxidized further,

and the silica in solution was scavenged by the aqueous iron, the dissolution of the simulated SRL 165 waste glass was enhanced to produce more silica in solution, and hence, more iron silicate. The Eh range for the formation of iron silicate under oxic conditions was in the stability range for TcO_4^-, which would indicate that technetium would not be reduced to lower valence states and would not precipitate from the solution.

For the anoxic studies conducted by Jantzen,[33] the leachant was deionized water and it was sparged with argon to deoxygenate it. The experiments were conducted in a glove-box continually purged with argon. The lack of oxygen in the system limited the amount of iron that went into solution from the oxidation of the iron bars. However, as in the oxic experiments, there was enhanced silica leach rates from the waste glass. The mobile silica in solution then reacted at the solid-solution interface of the iron bars and formed a protective layer of iron silicate on the iron surface. This used up the limited amount of dissolved oxygen present in the solution. Because there was no influx of oxygen, the reaction ended once the iron surfaces were covered with iron silicate.

As in Jantzen oxic studies,[33] the possibility that iron silicate may have formed in the Sealed Vessel experiments was considered because the vessel was glass, and the J-13 solution does have silica in it. This is important because

the stability region on a pH/Eh diagram for iron silicate is in the same region where technetium would exist as TcO_4^-. Because the TcO_4^- in the Sealed Vessel Experiment was clearly reduced to lower oxidation states and the technetium concentration dropped BDL, the system pH/Eh could not have been in the stability region for iron silicate.

The possibility of protective layers forming in the current experiments, as in the anoxic studies by Jantzen,[33] was also considered. Apparently, the rate of iron oxidation by the oxygen in-leakage in the Sealed Vessel experiments was faster than the formation of a protective layer of iron silicate. If it was not faster, then these protective layers would have prevented the iron metal from reducing the technetium, which in turn would have prevented the technetium concentrations from going BDL.

Guppy and Atkinson[35] have conducted anaerobic experiments in an argon-filled glove-box where magnetite was put into a borosilicate glass bottle with a technetium-spiked solution. In these experiments, there was only a 30% technetium reduction, compared to the 99.8% expected had TcO_2 been the solubility controlling compound. Guppy and Atkinson concluded that, under anaerobic conditions, technetium compounds can precipitate onto, or otherwise coat, the iron with a protective layer and prevent the iron from being further oxidized. This would prevent the iron from buffering the solution.

Although the Sealed Vessel experiments were not like the anaerobic experiments conducted by Guppy and Atkinson because they were not conducted in an argon-filled glove-box, there was restricted oxygen flow. This restricted oxygen flow may actually be more like that expected at a geologic repository. Nonetheless, the possibility of the technetium forming a protective layer needed to be considered.

For the Sealed Vessel experiments, the iron surfaces were not occluded because the technetium concentration decreased and remained BDL the entire length of the experiment (Figure 23). The system Eh also decreased and remained low the entire length of the experiment. Had a protective layer formed on the iron and prevented the iron from buffering the solution, the Eh would not have decreased much because of the influx of oxygen. Also, had the iron not been capable of keeping the system reduced, the influx of oxygen would have re-oxidized the technetium, which would have brought its concentration above detectable limits. This did not occur as can be seen in Figure 23 because the technetium concentrations remained near to or below the detection limit after the first day of the experiment.

4.3.2.2 Sealed Vessel Experiment at 24°C

The Sealed Vessel System at 24°C was previously modeled in Section 2.3. Figure 9 showed the technetium

concentration, and Figure 10 showed the solution environment versus reaction progress. For comparative purposes, the data in these figures have been combined with the data from the Sealed Vessel experiment at 24°C. Figure 25 shows the technetium concentration, Figure 26 shows the system pH, Figure 27 shows the system Eh, and Figure 28 is the combination of Figure 26 and Figure 27. In all of these figures, the experimental data are plotted versus time (lower axis of abscissa), and the calculated data are plotted versus reaction progress (upper axis of abscissa).

The measured technetium concentrations from this experiment are represented by Figure 25 Curve 1. The technetium concentration decreased to 2.5×10^{-6} ppb on day 13. By day 39, the technetium concentration was 1.6×10^{-7} ppb, just above detection limits. The remainder of the samples had technetium concentrations BDL. This portion of the experiment is consistent with the codes because the codes indicated that the technetium concentration should drop BDL after a reaction progress of about 0.0009, Figure 25 Curve 2.

The technetium concentration in this experiment took much longer to drop BDL than in the higher temperature

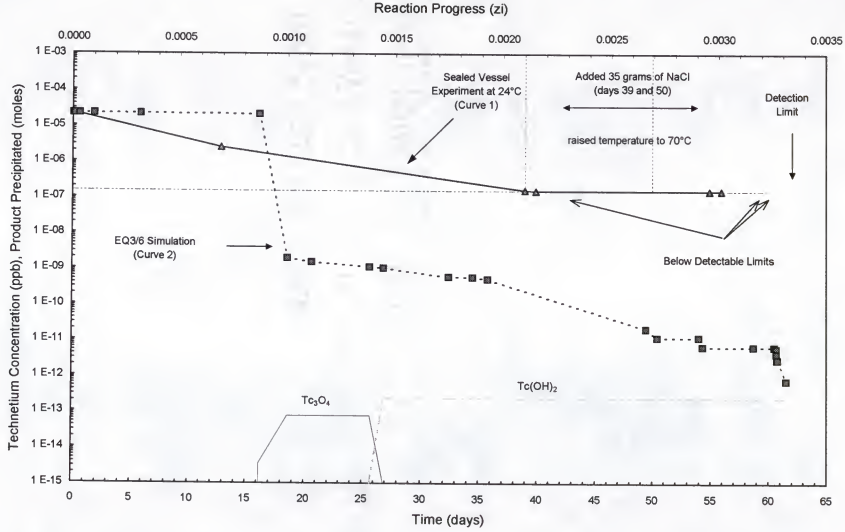

Figure 25 Sealed Vessel Experiment at 24°C and the EQ3/6 Simulation Technetium Concentration and Predicted Precipitation of Technetium Compounds.

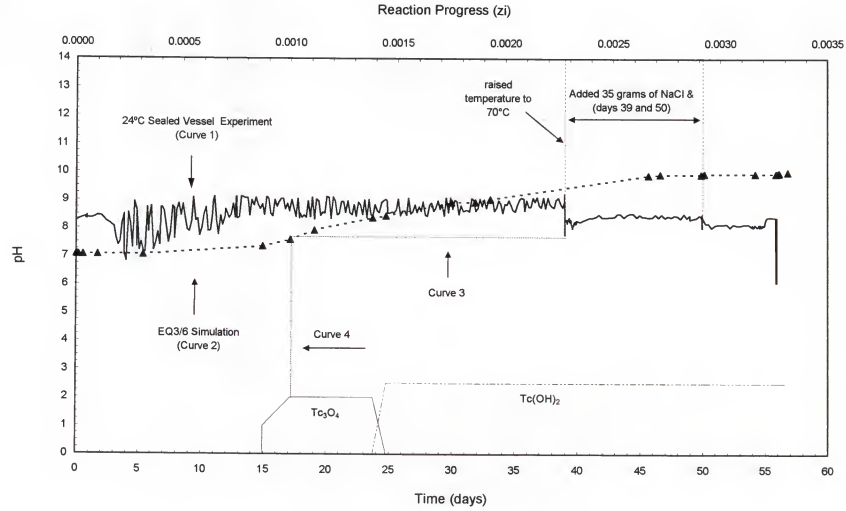

Figure 26 Sealed Vessel Iron Powder Experiment at 24ºC and the EQ3/6 Simulation Solution pH. Precipitated products are relative units.

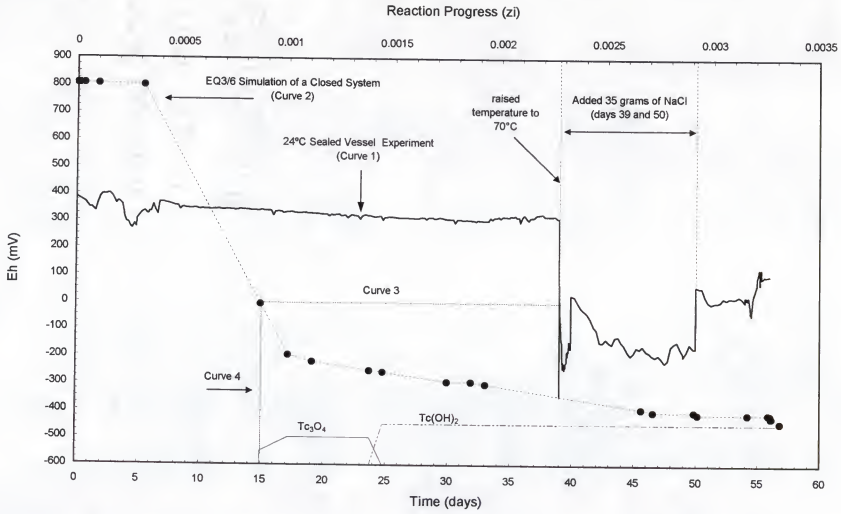

Figure 27 Sealed Vessel Iron Powder Experiment at 24°C and the EQ3/6 Simulation Eh. Precipitated products are relative units.

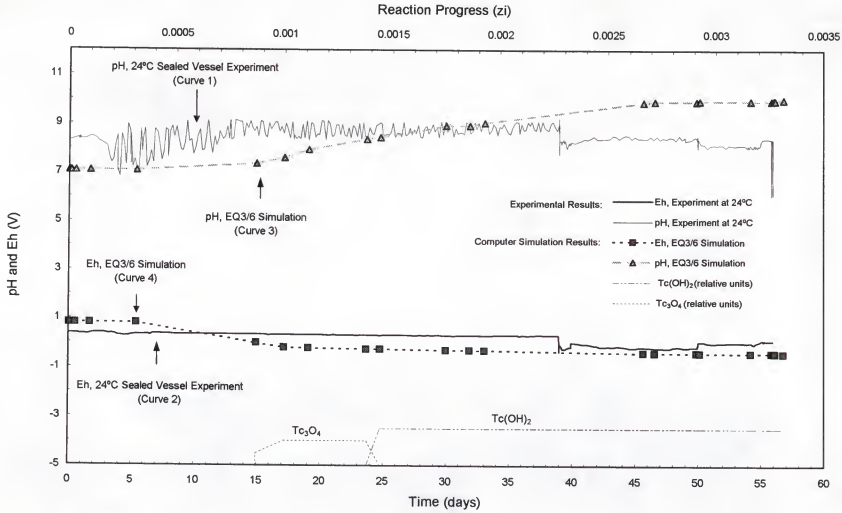

Figure 28 Sealed Vessel Iron Powder Experiment at 24ºC and the EQ3/6 Simulation Solution pH and Eh. Precipitated products are relative units.

experiment. It probably took longer than 13 days[h] for the technetium concentration to drop to BDL because of slower reaction kinetics. Another possible contributing factor was that the technetium took longer to diffuse through the solution to the iron surface on the bottom of the vessel where a reaction could occur. Both the diffusion of technetium and reaction kinetics are slower at lower temperatures.

For the first 39 days, the pH of the system also corresponded well with that predicted by the EQ3/6 codes, Figure 26 Curves 1 and 2, respectively. However, the pH of the system dropped when sodium chloride (NaCl) was added, and the temperature was increased to 70°C (the salt addition and temperature increase will be discussed momentarily). The simulation did not model this temperature increase or salt addition, and therefore, no comparisons between the experimental and calculated pH were made after day 39.

The 0.88 unit drop in pH at day 39 was expected as a direct effect of the 46°C temperature change. This was verified by using the Nernst equation, Equation (5) with either iron metal or Fe^{++} in equilibrium with hematite (Fe_2O_3). Hematite was used because the pH and Eh values

---

[h]The data for 13 days are used because the next data point at 39 days was just above detectable limits. To be conservative with regard to the time required for the technetium concentration to drop BDL, the data for the former point was used.

measured in this experiment are within the region where hematite is stable. The sample collected after the salt addition showed the technetium concentration BDL, as would be expected with the pH/Eh condition of the solution at that point. This is illustrated by the calculations by following Curve 3 from the experimental data over to the calculated data, and then following Curve 4 down to the bottom of the graphs. Both Figure 26 and Figure 27 indicate that the technetium precipitated as Tc_3O_4.

The measured Eh of the system was much greater than expected due to oxygen in-leakage. On day 39, sodium chloride was added to the solution in an attempt to lower the Eh by increasing the corrosion rate of iron. At the same time the temperature was raised to 70°C. This combination caused the Eh of the solution to drop substantially, and it eventually leveled out near -150 mV. This was a lower value than in the Sealed Vessel Experiment at 70°C without NaCl, Figure 23 Curve 1, but it was above the values calculated by the codes, Figure 27 Curve 2. Eleven days later while attempting to lower the Eh more with a second salt addition, additional air was inadvertently admitted into the system. This was quite noticeable by the jump in the Eh at day 50.

The measured Eh probably never reached that predicted by the codes because oxygen leaked into the system for the same reasons as stated in the Sealed Vessel Experiment at

70°C (refer to Section 4.3.2.1). The Eh in this experiment was also substantially higher than in the Sealed Vessel Experiment at 70°C, Figure 23 Curve 1. This was because the oxygen leaking into the system reacted more slowly with the iron at the lower temperature.

The iron in the bottom of the reaction vessel contained the same brownish top layer with hints of red, and it was black underneath the top layer. This was most likely an iron(III) oxide as described for the Sealed Vessel Experiment at 70°C (Section 4.3.2.1).

Just as with the Sealed Vessel Experiment at 70°C, data from this experiment, other than the solution Eh, were consistent with the EQ3/6 codes.

4.3.3 FT-4C Iron Powder Experiments

The FT-4C system was used to conduct three ^{99}Tc Iron Powder experiments. The High-flow and Low-flow experiments were conducted at 24°C, and the third experiment was the Iron Powder at 85°C. In Section 4.2, it was determined that this system was retaining technetium in the system's plumbing and releasing it at a later time. Therefore, no direct conclusions can be drawn from these experiments. They are included for completeness.

4.3.3.1 High-flow Iron Powder Experiment

The High-flow Iron Powder Experiment used the FT-4C to pump a 1500 ppb ^{99}Tc-spiked solution through the iron-filled reaction column at 50 mL/day, and 100 mL/day. Then the flow was stopped such that the solution was in static contact with the iron. Data for this High-flow Iron Powder Experiment are shown in Figure 29. After the initial sharp decrease from the starting ^{99}Tc concentration of 1533 ppb, the concentration gradually decreased further to a minimum of 0.15 ppb. At the end of the third day, the flowrate and pressure were turned off to tighten a loose bolt on the reaction column. Although it only took 10 minutes before the flow was re-started and the system pressurized, this interruption apparently caused the technetium concentration to increase for 1 h before starting to decrease again.

Two and a half hours after tightening the bolt, the flowrate was increased to 100 mL/day for 5 h to determine if the shorter contact time between the iron and the solution would allow the technetium concentration in the effluent to increase again. The technetium concentration did not increase as was expected. Instead, 1 h after the flowrate change, it had actually decreased to about what it was before tightening the bolt. Thus, the change in flowrate appears to have had little effect on the technetium concentration.

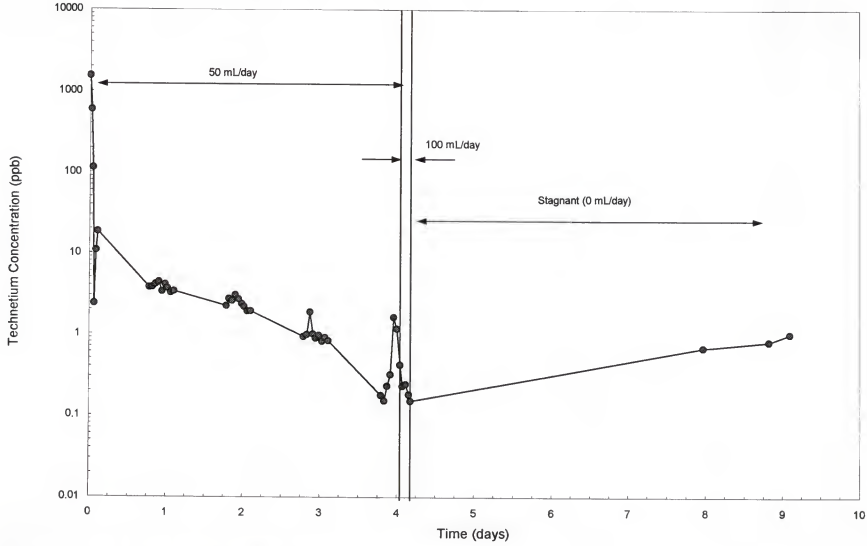

Figure 29 FT-4C High-flow Iron Powder Experiment

Next, the flow was stopped to determine if the technetium concentration would decrease further because of longer contact time with the iron. Although this portion of the experiment was labeled no-flow, there was a very small, insignificant flow as the samples were collected. During this period of no flow, the technetium concentration increased slightly instead of decreasing. In hindsight, this increase appears to be from technetium that was deposited in the system's plumbing during an earlier experiment as described in Section 4.2.

It should be noted that some effluent was observed on the outside of the column when the FT-4C shielded doors were opened to tighten the loose bolt on the reaction column. The liquid that leaked was milky white, and it left a white solid in the reaction column holder. This solid may have contained a precipitate of technetium, or it could have been due to the J-13 evaporating. Although it is possible that this solid was caused by the liquid evaporating, it appears more likely that technetium was precipitating because (1) the reaction column was not heated (which would have increased the rate of evaporation), (2) the solution was milky white, and (3) similar white precipitates were observed in both of the stannous chloride experiments where evaporation did not occur, as will be discussed in Section 4.5.

This precipitate was probably Tc_3O_4 because other compounds, such as TcO_2 (sometimes referred to as $TcO_2 \cdot 2H_2O$ or $Tc(OH)_4$), have been reported to be a brownish precipitate[48] and possibly even a black sludge and brown deposit.[42,43,46] No trace of a black or brown residue was observed. Also, $TcO_2 \cdot 2H_2O$ has a solubility of 4.4 ppb,[41] which is much greater than was observed in the experiment. The codes indicate that Tc_3O_4 will form, not $TcO_2 \cdot 2H_2O$. No data for the color of the precipitates for Tc_3O_4 or $Tc(OH)_2$ exist. However, the solubility limit for $Tc(OH)_2$ is BDL and because technetium was always detected in this experiment, the precipitate would not have been $Tc(OH)_2$. As will be discussed later, a similar white precipitate was also observed in the stannous chloride experiments.

4.3.3.2 Low-flow Iron Powder Experiment

A second iron-powder experiment was conducted. This time the flowrate was lowered after 3 days to determine if allowing longer contact time between the iron and technetium would decrease the technetium concentration to lower values than in the High-flow experiment. During those first few days, the two experiments were conducted at the same flowrate, and the results were similar in that there was a large decrease in technetium concentration (Figure 30). However, the technetium concentration did not change much during the 18-day period at 10 mL/day. Perhaps the minimum

technetium concentration of about 0.2 ppb in both the High-flow and Low-flow experiments was due, in part, to the release of technetium previously retained by the system, as described in Section 4.2.

4.3.3.3 Iron Powder Experiment at 85°C

The next iron powder experiment was an attempt to increase the reaction kinetics by increasing the temperature to 85°C. The flowrate was held constant at 50 mL/day. The results, shown in Figure 31, were similar to those of the two lower temperature iron experiments. That is, the technetium concentration dropped to a minimum of a few tenths of a ppb. Then it slowly increased and by the end of the experiment was 5 ppb.

The minimum technetium concentrations in all three FT-4C experiments were in the same range as the minimum concentrations found in the Blank-run Experiment described in Section 4.2. This suggested that the minimum concentrations in the FT-4C experiments were an artifact of technetium being retained in the plumbing downstream from the reaction column and then re-released. This was not a true indication of the effectiveness of the iron. This was a clear indication that a different system was needed to investigate iron as a reactant to reduce the technetium concentrations. Therefore, all flow-through experiments conducted after these three used the Bench-top system.

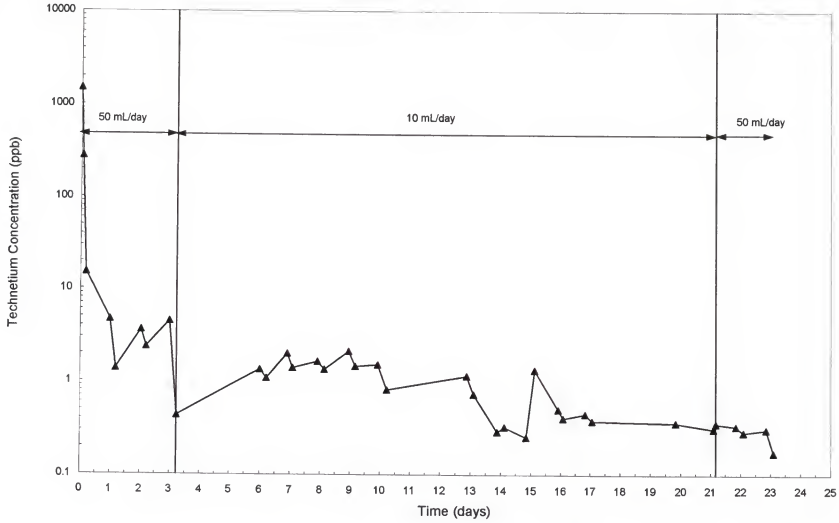

Figure 30 FT-4C Low-flow Iron Powder Experiment

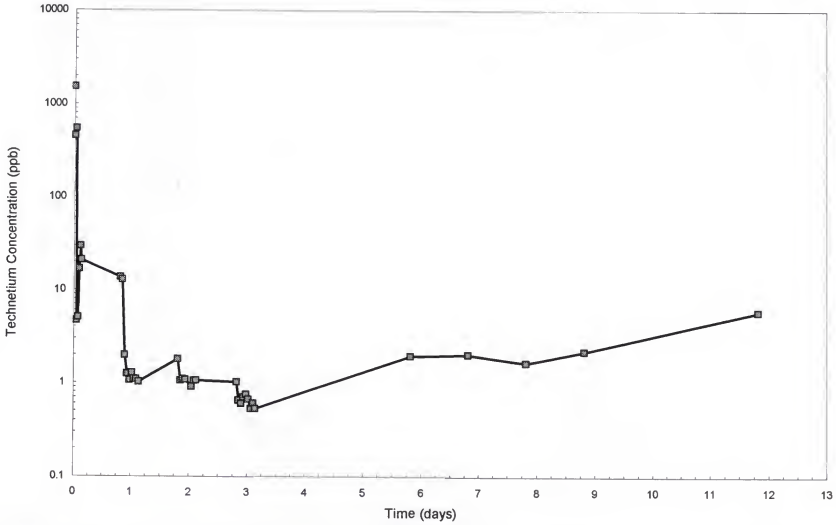

Figure 31 FT-4C Iron Powder Experiment at 85°C

4.3.4 Iron Powder Summary and Conclusions

All the experiments conducted using iron as a reactant had a substantial drop in the technetium concentration. The technetium concentration in the Bench-top ^{99}Tc experiment dropped from a starting concentration of 35.8 ppb to BDL (0.4 ppb). The Bench-top ^{95m}Tc experimental results showed that the technetium concentration dropped from a starting concentration of 9.4×10^{-4} ppb to approximately 1×10^{-7} ppb. The two Sealed Vessel experimental results also showed that the iron reduced the ^{95m}Tc concentration from 2.3×10^{-5} ppb to BDL, i.e., less than 1×10^{-7} ppb.

Before comparing data from the Bench-top experiment to that from the Sealed Vessel experiment, recall that in the Sealed Vessel System (1) the amount of technetium was limited rather than being replenished as in the Bench-top system where the spiked solution was pumped through the iron, (2) the amount of oxygen available to the system was substantially less than in the Bench-top system, (3) the surface area was substantially less because the solution was not pumped through the reaction bed as in the Bench-top experiment, thereby leaving the top layer of the iron as the primary surface area available for the technetium, and (4) the time the technetium was in contact with the iron was days rather than the 1.5 h it took to pump the solution through the reaction column in the Bench-top system.

Now, comparing the results of the Bench-top ^{95m}Tc experiment with the Sealed Vessel Experiment at 24°C, we know (1) it took longer than 13 days in the Sealed Vessel experiment for the iron to decrease the technetium concentration BDL, and (2) the technetium solution was in contact with the iron for only 1.5 h in the Bench-top system, but the technetium concentration was 7% lower (1.8×10^{-7}) than that in the Sealed Vessel experiment sample collected on day 13 (2.5×10^{-6} ppb). Therefore, it is evident that in the Bench-top Experiment, some phenomenon other than just reduction occurred to lower the technetium concentration in the sample effluent so quickly.

As described in Section 4.3.1, the technetium was likely sorbed by the iron, causing the rapid drop in technetium concentration. This can occur more quickly when the solution is pumped through the bed of iron powder than when the iron powder lays at the bottom of a large volume of solution under static conditions. Since the technetium was unlimited in the Bench-top experiment, it did not drop BDL as in the Sealed Vessel experiments, and it eventually started to increase from its minimum concentration of (1×10^{-7}).

The ^{95m}Tc concentrations in the Bench-top Experiment were markedly reduced, but not to the values as low as calculated by the EQ3/6 simulation. This reduction in technetium concentration was due in part to technetium

sorbing on the iron surface (which the codes cannot model), as well as the technetium being reduced by the iron. Once the iron sorbed the technetium, its surface became partially passivated as was indicated by the slight rise in technetium concentration in the latter half of the experiment as well as by the arguments discussed in Section 4.3.1.

Comparing the Sealed Vessel Experiments at 70°C and 24°C shows that the increase in temperature substantially reduced the time it took to decrease the technetium concentration BDL. In the 70°C experiment, the technetium concentration dropped BDL within the first day. However, it took greater than 13 days for this to occur in the lower temperature experiment, most likely because the reaction kinetics of iron are slower at room temperature. A chemical reaction (technetium reduction), rather than technetium sorption, is supported by the visual examination of the iron after the experiment ended. The iron on the bottom of the vessel was brownish on top with hints of a red hue. It also had black spots showing through the brown layer. Under the brownish top layer, the iron was a rich black color. The black and red colors observed are most likely the characteristic colors of an iron(III) oxide (such as hematite, Fe_2O_3).[50] Technetium sorption, as a mechanism of the slower drop in technetium concentration at 24°C, also seems to be ruled out because the associated passivation layer would be expected to form slower at the lower

temperature. Slower formation of a passivation layer would have allowed the technetium concentration to decrease faster, not slower. Because the technetium concentration was measured to decrease more slowly at the lower temperature, technetium sorption must not have been involved. The iron can sorb the technetium until the sorption sites are occluded by being filled. A separate mechanism but with the same effect is the development of a passivation layer. Both mechanisms, occlusion of sorption sites and development of a passivation layer, would limit the amount of technetium concentration reduction and can both occur at the same time.

Diffusion may have been another factor that contributed to the slower decrease in the technetium concentration in the lower temperature experiment. Technetium diffusion through the static solution to reach the iron surface on the bottom of the vessel where the reactions occurred would be expected to be slower at the lower temperature.

The technetium concentration decreased in all three of the FT-4C experiments, but not to the levels calculated by codes. Because the minimum technetium concentrations were within the same range as the Blank-run Experiment, it is likely that the remaining technetium was the result of technetium being retained and then re-released by the system. Therefore, no conclusions can be made regarding

iron's redox effect on technetium for the experiments conducted using the FT-4C.

The technetium concentrations remained at low levels for the duration of all seven of the experiments (two Bench-top, two Sealed Vessel, and three FT-4C experiments). The experiments continued up to 56 days as in the Sealed Vessel Experiment at 24°C. Maintaining low technetium concentrations for geologic time periods in a repository environment would require the continued presence of iron in an active (non-passivated) form. Further work is needed to determine whether iron can be expected to remain active for extended (geologic) time periods.

4.4 Copper Experiments

The four copper experiments listed in Table 4 were conducted. The Bench-top Flow-through System, Figure 11b, was used to pump ^{95m}Tc-spiked J-13 through a reaction column containing copper powder. The details of the Bench-top Copper Powder Experiment are presented in 4.4.1. The other three copper experiments used the FT-4C system, Figure 11a, to pump ^{99}Tc-spiked solutions through reaction columns containing copper shot.

There are some uncertainties associated with the data collected from the FT-4C because the system was retaining technetium in the plumbing downstream from the reaction column and re-releasing it during these experiments

(Section 4.2). However, the data from these experiments are credible because the technetium concentration in the samples were orders of magnitude greater than that detected in the Blank-run Experiment. The details of the three FT-4C copper experiments, are presented in Sections 4.4.2.1 through 4.4.2.3. Despite the uncertainties with the FT-4C, there is no question that the technetium concentrations remained essentially unchanged when the solution was passed through the reaction column.

Because the FT-4C experiments were conducted using copper shot, copper powder was used in the Bench-top experiment to determine whether the larger surface area would reduce the technetium concentration. The Bench-top experiment is discussed in Section 4.4.1, and the FT-4C experiments are discussed in Section 4.4.2.

4.4.1 Bench-Top Copper Powder Experiment

The Bench-top Copper Powder Experiment was conducted after the three FT-4C experiments. It is presented first because of the problems with the data from the FT-4C as described above. However, the trends in the data from all four experiments (three FT-4C and one Bench-top) were consistent, i.e., the technetium concentrations were essentially unchanged except for an initial drop or rise.

The Bench-top Copper Powder Experiment had a ^{95m}Tc-spiked solution pumped through a reaction column loaded with

copper powder. The other details of the experiment are shown in Table 4. This Bench-top experiment used copper powder rather than copper shot because the effect of surface area on technetium retention was being investigated. In addition, this experiment was designed to determine if the initial drop/rise in technetium concentration was reproducible and to determine why it occurred in the experiments, but not in the computer simulations.

The data for this experiment are shown in Figure 32 Curve 1. Curves 2 and 3 in Figure 32 are the results of the FT-4C Copper Shot experiments at 24°C and 85°C, respectively (see Section 4.4.2), and are included for comparative purposes. This experiment was conducted before redoing the computer simulations as mentioned in Section 2.3. Those early computer simulations used both copper and technetium metals as reactants. The technetium metal reactant allowed the simulation to continue even when the system was saturated with copper.[i] Because technetium can exist up to the (VII) valance state, the simulations that used technetium metal as a reactant calculated much lower Eh values than the simulations that only used copper metal as a reactant. The lower Eh values in the simulations containing technetium metal reactant indicated the solution was highly reducing, the technetium precipitated out of solution, and

[i] recall that when a system is saturated with a reactant, it is in thermodynamic equilibrium, and any additional reactant added will have no effect on the equilibrium of the system.

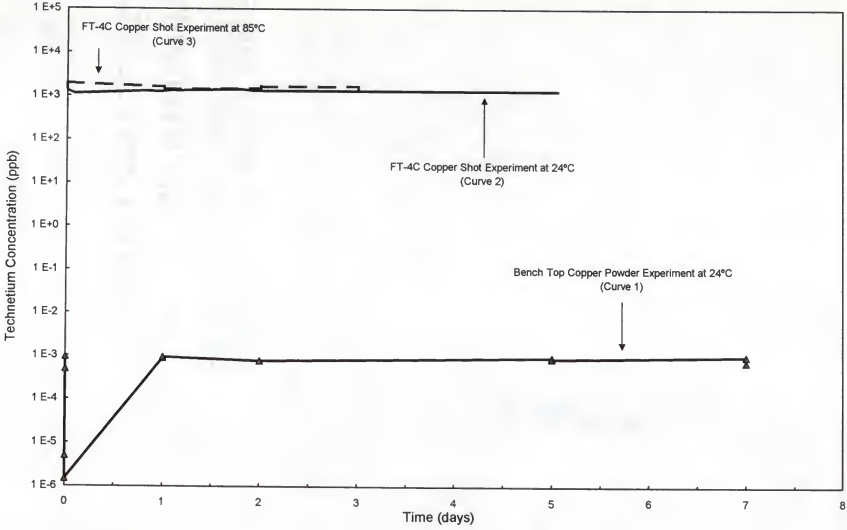

Figure 32 Bench-Top ^{95m}Tc Copper Powder and the FT-4C ^{99}Tc Copper Shot Experiments Using J-13

the technetium concentration dropped below 1×10^{-7} (technetium concentrations are not indicated on those earlier graphs but they were indicated to drop below 1×10^{-7}). Based on those simulations, the starting concentration used in this experiment, 9.4×10^{-4} ppb, would have resulted in a 4 order of magnitude drop in technetium concentration to reach BDL (1×10^{-7} ppb). More recent computer simulations, which used copper metal as a reactant and technetium concentrations similar to those in the experiments, indicated that the technetium concentration would be reduced to 3.4×10^{-4} ppb. In these latter simulations, the simulation ended once the system was saturated with copper metal but before the technetium concentration dropped below 1×10^{-7} ppb. The technetium in these latter simulations was entered as the pertechnetate ion. Because the technetium was in its highest oxidation state (VII), it was not able to drive the Eh of the system lower, and therefore once the copper was in equilibrium with the system, the simulation ended. Had the latter simulations been conducted prior to the experiments, a higher starting technetium concentration would have been used.

Figure 32 Curve 1 shows that the technetium concentration initially dropped from the 9.4×10^{-4} ppb starting value to a minimum of 1.5×10^{-6} ppb within 3 h. Then it returned to essentially the starting concentration.

After the initial drop in technetium concentration and return to the approximate starting value, the concentration decreased to 7.3×10^{-4} ppb, a 21% decrease from the starting concentration. Although this decrease was quite small, it was larger than the total uncertainty of about 3% related to the measurement errors. The initial decrease to 1.5×10^{-6} ppb was possibly caused by sorption. After the sorption sites were saturated, the technetium concentration returned to and remained essentially unchanged from its starting value. This initial decrease could also be the result of the technetium being reduced by the copper, and the rise back to the starting concentration the result of a passivation layer developing. Sorption and passivation layers are two separate mechanisms that give the same effect. They can occur alone or at the same time. The passivation layer that developed in this experiment was most likely cuprite, which is a protective film that forms on the copper and is responsible for not allowing the copper to oxidize further.[40]

The comparison of the Bench-top experimental results with the computer simulation of this experiment is shown in Figure 33. The experimental results are plotted versus time (lower axis), and the computer simulation results are plotted versus reaction progress (upper axis).

The lowest calculated technetium concentration was 3.4×10^{-4} ppb (Figure 33 Curve 2), which is much higher

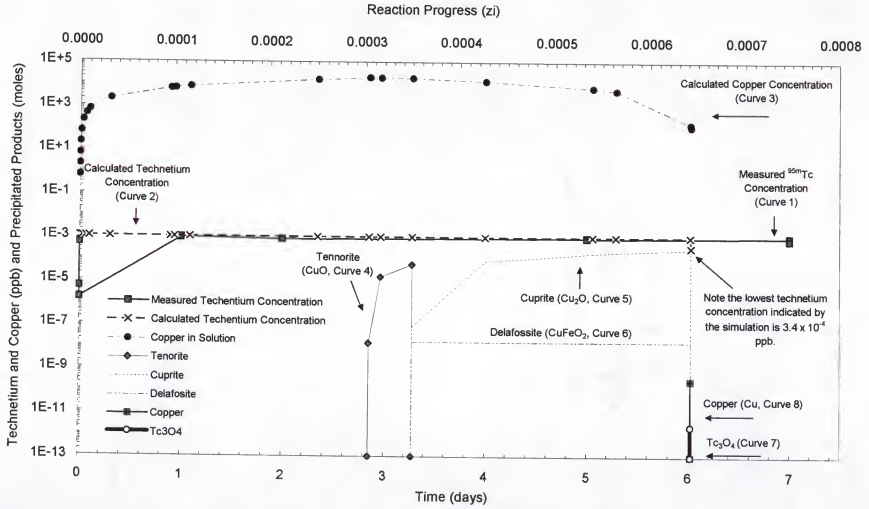

Figure 33 Comparison of the Bench-Top Copper Powder Experiment and the EQ3/6 Simulation. The measured technetium concentrations are plotted versus experimental run time. The calculated technetium and copper concentrations and calculated precipitated product minerals are plotted versus zi.

then the experimental minimum of 1.5×10^{-6} ppb (see note on the figure). The codes followed the individual packet of solution (see Section 2.3.2). As the reaction progressed and the solution environment became less oxidizing because of the oxygen being depleted, the copper metal reactant was first oxidized to Cu(II) as tenorite (CuO, Curve 4). As the oxygen was depleted more, the copper reactant was only oxidized to Cu(I) as cuprite (Cu_2O, Curve 5) and delafossite ($CuFeO_2$, Curve 6). The solution became even less oxidizing as it progressed further through the copper in the simulation. The technetium in the solution was reduced to Tc_3O_4 (Curve 7) at a reaction progress of 0.00065. At this same reaction progress, essentially all the dissolved oxygen was depleted.

The simulation was terminated after all the dissolved oxygen in the packet of solution was exhausted and copper was indicated to be the most stable compound (curve 8). Even though TcO_4^-, and hence oxygen, was available in the simulation, it did not oxidize the copper reactant. The technetium concentration did not decrease below 3.4×10^{-4} ppb because the simulation was terminated once copper metal was indicated to be the most stable copper phase, but before all the technetium precipitated. Experimentally, the technetium concentration did not change much after the initial drop. Based on a recent computer simulation, little change would have been expected because

the lowest calculated technetium concentration was only about 3 times lower then the experimental starting concentration. Therefore, the approximate agreement between the experiment and the simulation (Figure 33) may have been a coincidence of the low experimental starting concentration.

To determine if the simulation containing copper would decrease the technetium concentration BDL or at least as low as the minimum obtained in the experiment, aqueous Cu^{+} was entered as the reactant instead of copper (metal). Copper metal was suppressed from forming. The results of this computer simulation are shown in Figure 34. The initial drop in the measured technetium concentration (Curve 1) corresponds with the same calculated technetium concentration (Curve 2) at a reaction progress of 0.0017 (follow Curve 6 from the experimental minimum to the calculated value). At that reaction progress, cuprite, delafossite, and Tc_3O_4 began to form.

According to the aqueous copper simulation, the technetium concentration should have continued to drop as the copper was oxidized to cuprite and tenorite. This did not occur in the copper metal simulation because there was no more oxygen available to continue to oxidize the copper, and copper metal was indicated to precipitate. Tc_3O_4 was never allowed to completely precipitate in the copper metal simulation because there was no further reaction once all

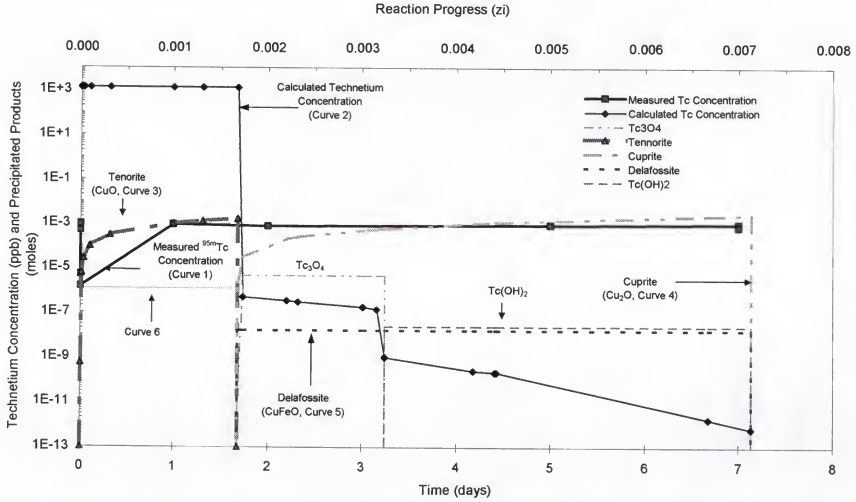

Figure 34 Bench-Top Copper Powder Experiment and the EQ3/6 Simulation Using Aqueous Copper. Measured and calculated technetium concentrations and calculated precipitated products formed.

the oxygen was gone, and the system was thermodynamically driven to precipitate copper metal. The codes did not indicate that there will be a point where the technetium will preferentially precipitate over the copper metal.

The simulation using copper as an aqueous solution did not model the experiment; it was just used to determine the solubility-controlling compound for copper in solution. The technetium concentration did not begin to decrease until cuprite and delafossite (Figure 34 Curves 4 and 5) have began to form and precipitate. The codes do not model passivation layers, but cuprite was most likely the solubility-controlling copper compound in the experiment. Cuprite could form under the current solution environment conditions, it is a protective film,[40] and the reduction of the technetium concentration in the experiment was temporary. Once this protective layer formed in the experiment, no further reduction occurred.

The effect of surface area was also studied by comparing the experiments that used copper shot and copper powder. However, because two variables were changed, the surface area and the initial technetium concentration, comparison is difficult. As will be shown, the FT-4C Copper Shot Experiment at 24°C, Figure 36 Curve 1, reduced the technetium concentration from 1.3×10^3 ppb to 1.1×10^3 ppb, or 200 ppb. As seen in Figure 32 Curve 1, the copper powder reduced the technetium concentration from

1×10^{-3} ppb to 1.5×10^{-6} ppb. Therefore, the copper shot sorbed substantially more technetium than the copper powder. Whether this would be true if the same starting concentrations were used is uncertain. However, in both cases, not all the technetium was removed from solution, regardless of surface area available. Once the passivation layer developed on the copper surface, further reaction of the copper and solution was prevented, and the technetium concentration returned to near the starting values.

4.4.2 FT-4C Copper Shot Experiments

The FT-4C was used to conduct three copper shot experiments. This system was discovered to be retaining technetium and releasing it at some time later. In spite of this problem the data obtained from these experiments are credible because the technetium concentration in the samples was orders of magnitude greater than the 14 ppb of technetium detected in the Blank-run Experiment (Section 4.2).

4.4.2.1 DIW Copper Shot Experiment

The FT-4C system was used to conduct the distilled, deionized water (DIW) Copper Shot Experiment. This was the first experiment conducted, other than the readiness experiments, and DIW was inadvertently used in place of J-13. The technetium concentrations (axis of ordinates)

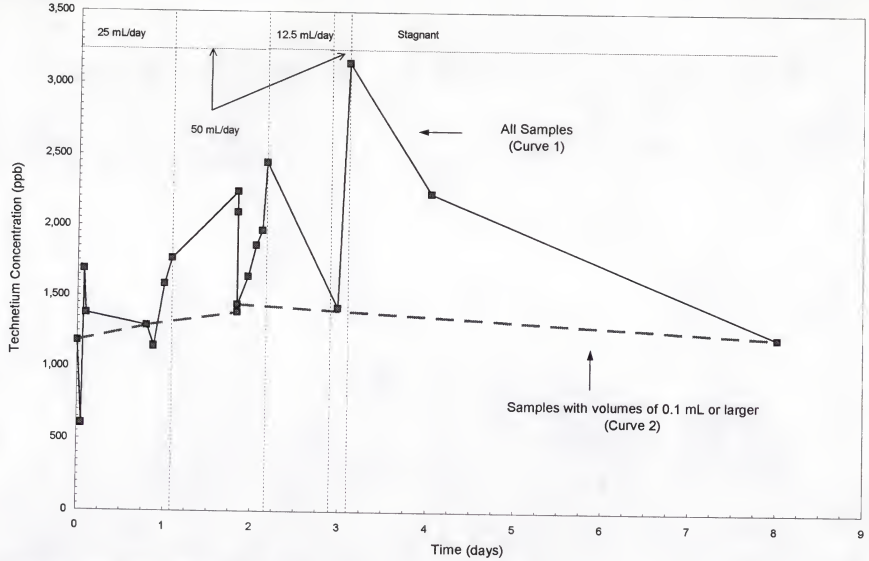

Figure 35 FT-4C DIW Copper Shot Experiment

versus time (axis of abscissae) from the DIW Copper Shot experiment are plotted in Figure 35. The flowrate was changed from 25 mL/day to 50 mL/day, 12.5 mL/day, 50 mL/day, and finally 0 mL/day on days 1.1, 2.2, 2.9, and 3.1, respectively. The flowrate was increased after 1.1 days because the initial flowrate was inadvertently set at half the flow of the expected water flux through the repository.[8,51]. The flowrate was decreased later in the experiment to determine if longer contact time between the copper and technetium would allow the copper to reduce the technetium. The flowrate was increased again to determine if decreasing the contact time between the copper and technetium would cause the technetium concentration to increase. Then the pump was finally turned off on day 3.1 to determine if the longer contact time between the solution and the copper would cause the technetium concentrations to decrease.

The reliability of most of the data collected during this experiment (Figure 35 Curve 1) is questionable. The volume of column effluent used to prepare most of the samples for analysis with the LSA was very small, on the order of 0.009 mL. The uncertainty associated with this volume measurement (> 33%) makes the data questionable. The data are included in this report only for completeness.

Five of the samples from this same experiment had volumes greater than or equal to 0.1 mL. They are plotted

on Figure 35 Curve 2. Uncertainties associated with these samples were considerably less then with the small samples, and the data show the ^{99}Tc concentration essentially did not change during the entire 8 days this experiment was conducted (Figure 35 Curve 2).

4.4.2.2 Copper Shot Experiment at 24°C

The above experiment was repeated using J-13 instead of DIW. Figure 36 Curve 1 shows the technetium concentration versus time obtained from the ^{99}Tc J-13 Copper Shot Experiment at 24°C. These data are consistent with the previous experiment in that the technetium concentration remained essentially the same throughout the experiment. The initial drop in concentration within the first 2 h of the experiment was followed by a return to, and then above, the starting concentration. This may have been caused by a passivation layer developing on the copper surface. The initial drop in technetium concentration could also be the result of the copper sorbing the technetium until the sorption sites were saturated. It was not likely caused by the system first retaining and then re-releasing technetium downstream from the reaction column (refer to the Blank-run Experiment in Section 4.2). The maximum technetium concentration found in the Blank-run Experiment, 14 ppb, is far less than the increase of 132 ppb in the Copper Shot Experiment at 24°C.

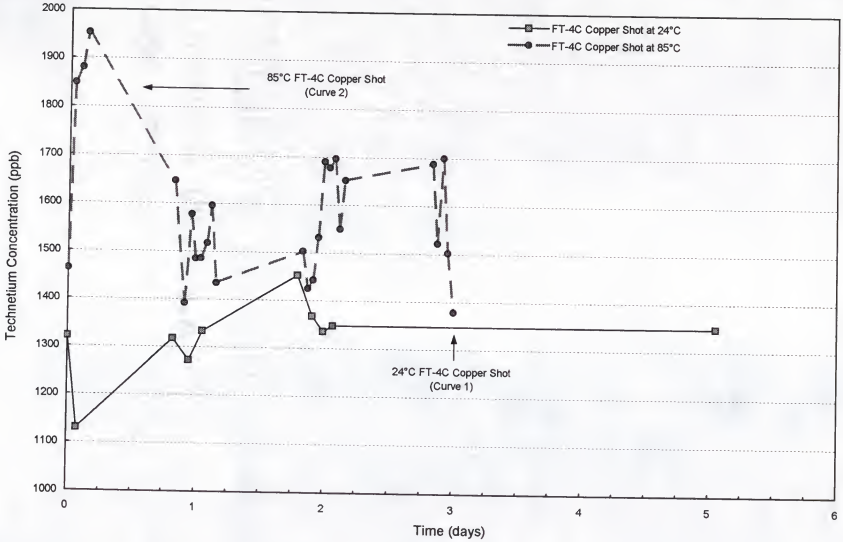

Figure 36 FT-4C J-13 Copper Shot Experiments at 24°C and 85°C

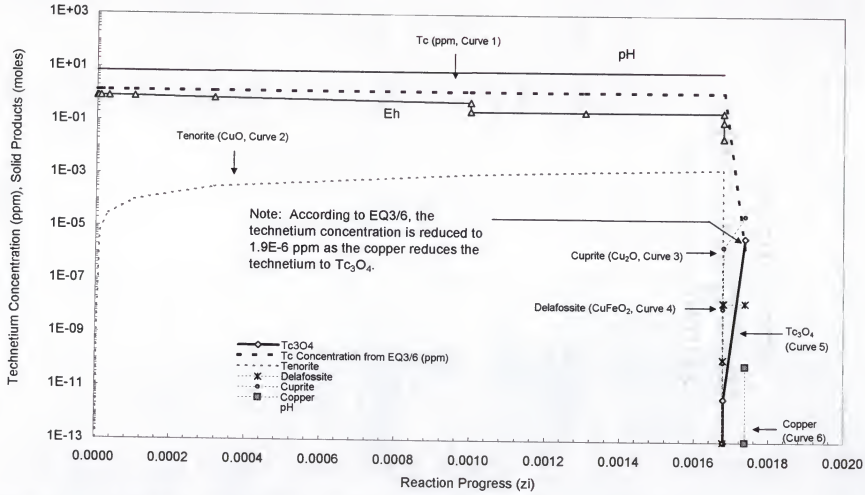

Figure 37 EQ3/6 Simulation of the Copper Shot Experiments. The calculated technetium concentrations and mole of product minerals formed are plotted for copper as a reactant.

Figure 37 shows the technetium concentration and solid product minerals indicated to precipitate by the simulation of this experiment. Curve 1 represents the technetium concentration in parts per million (ppm). This is the only set of concentrations in this figure; all the other lines represent the number of moles of solid products precipitated. The calculated technetium concentration was decreased to 1.9×10^{-6} ppm (1.9×10^{-3} ppb). However, this did not occur in the experiments.

The first solid copper product indicated to form by the simulation was tenorite (Curve 2). Tenorite continues to form until a reaction progress of 1.68×10^{-3} is attained. The solid copper(I) oxides are the most thermodynamically favored copper compounds to form at this same reaction progress. The copper(I) oxides indicated to precipitate are cuprite (Curve 3) and delafossite (Curve 4). The first technetium compound also began to form at this same reaction progress (Tc_3O_4 represented by Curve 5). The technetium concentration, Curve 1, began to decrease as expected once Tc_3O_4 (Curve 5) began to precipitate. Cuprite, delafossite, and Tc_3O_4 continued to form as the reaction progressed. It is at a reaction progress of 1.74×10^{-4} that copper metal, Curve 6, was shown as a the most stable copper product. Nothing further happened to the copper reactant because no more oxygen was available to oxidize the copper, and

copper(0) metal was the most thermodynamically favored compound.

In general, the technetium concentrations did not vary much in this experiment. It was suspected that slow reaction kinetics might be responsible. Therefore, an elevated-temperature copper shot experiment was conducted to determine if indeed slow reaction kinetics was the cause for the discrepancy between the calculation and the experiment.

4.4.2.3 Copper Shot Experiment at 85°C

Figure 36 Curve 2 shows the variation in technetium concentration versus time from the Copper Shot Experiment at 85°C. The technetium concentration initially increased 33% from the initial concentration of 1.5×10^3 ppb. The concentration then decreased and was essentially the same as the initial concentration by time the experiment ended. Despite the scatter in the data, the overall trend in the technetium concentration was such that it appears to not change much. Therefore, raising the temperature did not significantly increase the reaction kinetics. It is unlikely that the copper reduced the technetium to Tc_3O_4. The technetium concentration in the experiments did not drop significantly, as the codes indicated it should (Figure 37).

The reason for the amount of scatter in the concentrations and the initial high peak is unknown, but it is unlikely caused by the release of the technetium retained

in the plumbing downstream of the reaction column (refer to the Blank-run Experiment in Section 4.2). This is because the maximum technetium concentration found in the Blank-run Experiment, 14 ppb, is far less than the increase of 490 ppb in the Copper Shot Experiment at 85°C.

4.4.3 Copper Summary and Conclusions

The results from the four copper experiments were consistent in that the technetium concentrations remained essentially unchanged. Despite the uncertainties with the FT-4C, the results from the three FT-4C copper experiments are considered valid because the effect of the technetium retention by the system is small compared to the starting and ending technetium concentrations of approximately 1300 ppb to 1400 ppb. However, the codes indicated that the technetium concentration should be reduced to 1.9×10^{-3} ppb, which clearly does not agree with the experiments. The technetium concentration decreased approximately 200 ppb and then returned to the starting concentration of 1300 ppb in the Copper Shot Experiment at 24°C. The ending technetium concentrations were also essentially the same as the starting values (1200 ppb and 1400 ppb, respectively) in the DIW Copper Shot and the Copper Shot at 85°C experiments, although there was much scatter. None of the experiments had the technetium concentration drop to the values indicated by the codes.

This disparity between the calculated and experimental results is most likely because a passivation layer, such as a copper oxide, developed on the metal's surface. This prevented any further reduction in technetium concentration beyond the initial drop, allowed the technetium concentrations in the effluent to return to their initial values, and may have allowed some of the technetium initially precipitated to redissolve.

The passivation layer that formed was most likely Cu_2O. This was indicated by a greenish hue, indicative of Cu_2O, that was on the copper surface after the experiment. As cuprite was forming, the copper was less capable of reducing the incoming oxidizing solution until eventually the passivation layer covered the entire surface, and the metal was prevented from further oxidation. Once the passivation layer formed, some of the technetium that was originally retained by the copper dissolved in the fresh incoming solution because technetium is very soluble in an oxidizing environment.

Other possibilities for the disparity between the calculated and experimental results include technetium plate-out on the copper (which is a variation of the above explanation) and slow reaction kinetics; i.e., the time it would take for the reactant to react with the solution is much longer than the time in which the two were in contact with each other. Slow reaction kinetics is considered

unlikely because 1) a reaction occurred that allowed the technetium concentration to be reduced temporarily but quickly, 2) an increase in temperature did not cause the technetium concentration to drop BDL or even cause it to continue to drop, and 3) the general trend in the experiments at 24°C and 85°C was similar.

The ending technetium concentration in the Copper Powder Experiment was similar to that of the starting values. This was expected from the latter simulations, but, at the time of the experiment, the earlier simulations indicated that the technetium concentration should be reduced to BDL. Because the experiment starting concentration was close to the calculated ending concentration, there was no disparity between the experimental and calculated results.

Comparing the surface area of the Copper Shot and Copper Powder experiments indicates that the protective passivation layer developed at essentially the same rate, regardless of the smaller surface area of the copper shot. This apparent similarity in rate may be a coincidence though, because there were two variables changed, the surface area and the initial technetium concentration. For the Copper Shot Experiment, it took 2 h for the technetium concentration to drop to a minimum of 1.13×10^{3} ppb and then begin to rise again. In the Copper Powder Experiment, it took 3 h to drop to a minimum of 1.5×10^{-6} ppb. The

difference in the flowrates from a maximum of 50 mL/day in the copper shot experiments to 160 mL/day in the copper powder experiment did not affect the time for the passivation layer to develop, even though there was less time for the solution to react with the copper with the higher flowrate.

Comparing the efficacy of technetium reduction as a function of surface area between the Copper Shot and Copper Powder experiments is difficult because two variables were changed, the surface area and the initial technetium concentration. The FT-4C Copper Shot Experiment at 24°C reduced the technetium concentration by 200 ppb, which is considerably more than the reduction from 1×10^{-3} ppb to 1.5×10^{-6} ppb in the copper powder experiment. However, in both cases, not all the technetium was removed from solution, regardless of surface area available. Once the passivation layer developed on the copper surface, further reaction of the copper and solution was prevented, halting further reduction in the technetium concentration.

The results of these experiments do not show promise for copper reducing the rate of technetium migration in a geologic repository.

4.5 Stannous Chloride Experiments

Two stannous chloride experiments were conducted. The Beaker No-flow System, Figure 11c, was used at ambient

conditions to study the effect of dissolved stannous chloride on ^{99}Tc concentration reduction. This system was used because stannous chloride is a soluble salt. By using the Beaker System, the dissolved stannous chloride's redox effectiveness could be studied because the dissolved salt would remain in the system.

A second stannous chloride experiment used the Bench-top Flow-through System shown in Figure 11b. This Bench-top Stannous Chloride and Tuff Experiment was conducted to determine if the tuff would retain the precipitated technetium. The results from the Beaker and Bench-top experiments are discussed in Sections 4.5.1 and 4.5.2, respectively.

4.5.1 Beaker Stannous Chloride Experiment

The Beaker Stannous Chloride Experiment had the ^{99}Tc-spiked solution added to a beaker containing dissolved stannous chloride. The technetium concentration decreased immediately from the starting concentration of 26 ppb to BDL (0.3 ppb) in the Beaker Stannous Chloride Experiment, Figure 38 Curve 1. Also, a white precipitate formed almost immediately after the technetium-spiked solution was mixed into the beaker containing the dissolved stannous chloride.

A total of four samples was collected. The first was the starting ^{99}Tc-spiked solution, the other three were from the beaker. The first sample had a technetium concentration

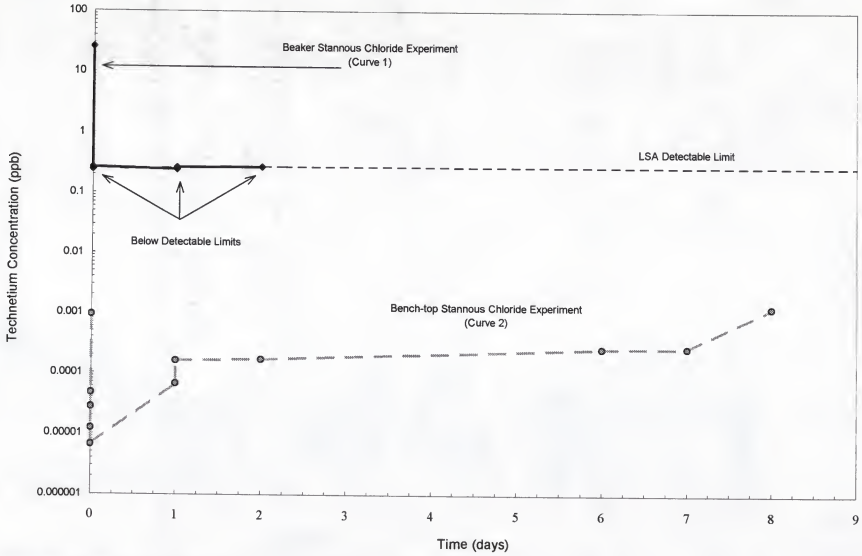

Figure 38 Beaker and Bench-top Stannous Chloride Experiments

of 26 ppb. The second and third samples had technetium concentrations that were BDL. The third sample was filtered (20 Å pore size) to remove any precipitate before being analyzed for technetium concentration. The filter for the fourth sample was primed as per the procedure in Section 3.4.3.2 to ensure that the technetium was not absorbed by the filter in the third sample. The remainder of the solution from the fourth sample was filtered and analyzed after priming the filter. Once again, the technetium concentration was BDL.

Technetium has been observed to sorb onto glass.[42] To determine if any technetium may have passed through the filter but sorbed onto the glass centrifuge tube, the tube was emptied and flushed with 0.1 M HNO_3. The nitric acid flush was analyzed for ^{99}Tc retention. Again, the ^{99}Tc concentration was BDL.

The white precipitate that formed when the technetium solution was added to the stannous chloride solution was most likely Tc_3O_4. This is supported by the EQ3/6 simulation of this experiment as shown in Figure 39. The model indicates that the technetium concentration (Curve 2) falls BDL at a reaction progress of 0.0019. This corresponds to the same point, as Tc_3O_4 (Curve 3) begins to precipitate. In the experiment, the technetium concentration was BDL with the first sample collected, at which time the white precipitate had formed. Although the

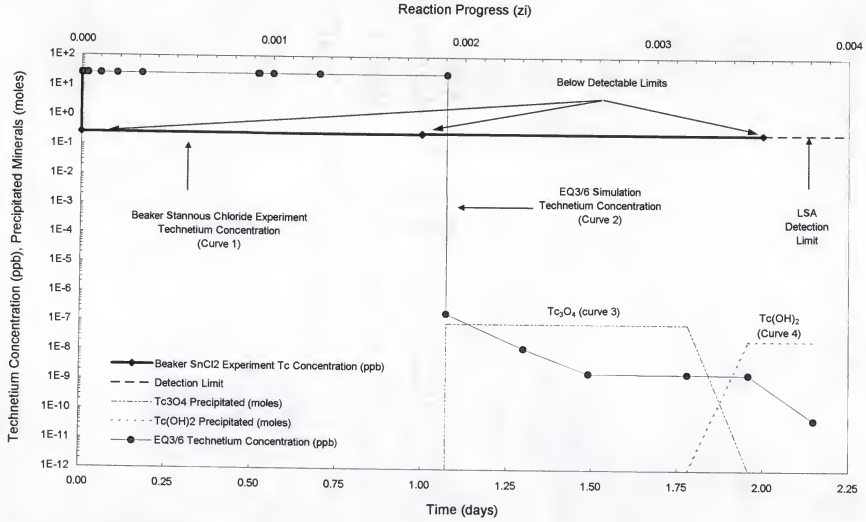

Figure 39 Comparison of the Beaker Stannous Chloride Experiment and the EQ3/6 Simulation. Technetium concentrations and predicted product minerals precipitated versus zi.

codes also indicate that the compound could be $Tc(OH)_2$ (Curve 4), it does not appear to be this compound. A similar white precipitate was observed in the iron experiments, and the codes did not indicate that $Tc(OH)_2$[j] would form in those simulations. Another technetium compound that is known to exist, TcO_2 (sometimes referred to as $TcO_2 \cdot 2H_2O$ or $Tc(OH)_4$), has been reported to be brown[48] or a black sludge.[42] This was not the compound, however, since the precipitate was clearly white with no signs of black or brown. The experiment is consistent with the results indicated by the codes. Because the detection limit for ^{99}Tc is high, the only possible conclusion is that the stannous chloride reduced the technetium concentration from 26 ppb to BDL (0.3 ppb).

4.5.2 Bench-Top Stannous Chloride Experiment

The Bench-top Stannous Chloride Experiment used a reaction column loaded with 1.71 g each of stannous chloride and crushed tuff. It was conducted to determine if tuff in the reaction column would retain the precipitated technetium. Because the Beaker Stannous Chloride Experiment had a ^{99}Tc concentration BDL, ^{95m}Tc was used because of its 8 orders of magnitude lower detection limit (Section 3.1).

---

[j]There is no recorded data on the color of this compound.

A 9.4×10^{-4} ppb ^{95m}Tc-spiked solution was pumped at a flowrate of 152 mL/day through the column at 24°C.

The results from this Bench-top Stannous Chloride Experiment are shown in Figure 38 Curve 2. As shown in Curve 2, the technetium concentration in the effluent decreased from the starting concentration of 9.4×10^{-4} ppb to 6.5×10^{-6} ppb within the first 6 h of the experiment. These values are above the detectable limits for ^{95m}Tc for this experiment (detection limit was 7.6×10^{-8} ppb). This initial decrease in technetium concentration was followed by an increase with an ending concentration of 1.3×10^{-3} ppb after 8 days, which is slightly over the starting value.

The first sample collected contained a white precipitate. The total technetium activity of this entire 7.7-g sample was 57 Bq before it was filtered (0.45-μm openings), and 9.83 Bq after it was filtered. Very little precipitate (0.38 g) remained in the original sample vial and was therefore not filtered. This is being referred to as the residue. The residue was analyzed and had a ^{95m}Tc activity of 4.91 Bq. If it is assumed that the residue was all precipitate, then:

$$(1 - \frac{9.8\ Bq}{57\ Bq}) \times 100 = 83\%$$

indicating that 83% of the technetium that was detected in the first sample was in the form of a precipitate. Only 17% was still in solution.

The precipitate observed in the first sample was most likely Tc_3O_4, caused by the reduction of TcO_4^- with stannous chloride. This is supported by the comparison with the computer simulation, which shows that the measured technetium concentration decreased below the concentration at which EQ3/6 predicts that Tc_3O_4 should start to precipitate (Figure 40). This is represented by following Curve 5, which (1) connects the point where the measured technetium concentration was minimum (Curve 1), (2) equals that of the calculated technetium concentration (Curve 2); and (3) follows Curve 6 vertically down to the point where it intersects the moles of Tc_3O_4 precipitated (Curve 3). The technetium concentration decreases substantially just as the Tc_3O_4 begins to precipitate.

Although the technetium concentration never went BDL in the experiment, it dropped over 2 orders of magnitude. It is highly unlikely that the technetium was reduced to any form with lower oxidation states than Tc_3O_4 because the concentration never went BDL, as it should if lower oxidation states were obtained. It is most likely that the technetium concentration did not drop BDL because the stannous chloride dissolved too quickly to reduce all the Tc_3O_4. It is likely that the solubility-controlling

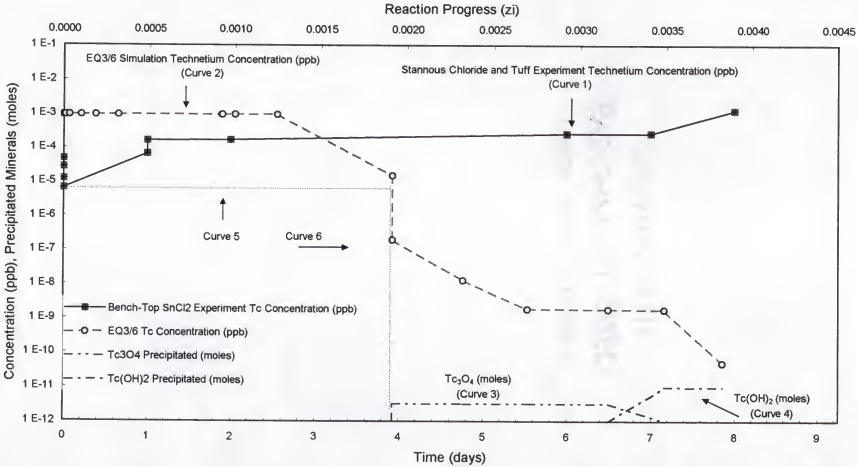

Figure 40 Comparison of the Bench-top Stannous Chloride Experiment and the EQ3/6 Simulation. Technetium concentrations and predicted precipitated product minerals versus zi.

compound was Tc_3O_4 because the precipitate was white, similar to those observed in the iron experiment and the Beaker Stannous Chloride Experiment. The technetium concentration was well above the 1.8×10^{-9} ppb (reaction progress of 0.0032) concentration where the codes predict $Tc(OH)_2$ will precipitate.

The computer simulations in Figure 39 and Figure 40 look different because the curves are plotted as straight lines between calculated data points. These points were calculated at different values of reaction progress in the two different simulations. The main information to be obtained from these figures is that the codes indicated that the technetium concentration should drop substantially BDL, and the first technetium compound to precipitate was Tc_3O_4.

4.5.3 Stannous Chloride Summary and Conclusions

The ^{99}Tc concentration in the Beaker Experiment dropped to BDL (0.3 ppb) and stayed there for the duration of the experiment (2 days). Using ^{95m}Tc to improve the detection limit, concentrations in the effluent samples from the Bench-top Experiment dropped to a minimum of 6.5×10^{-6} ppb. This concentration was well above detectable limits for ^{95m}Tc, but it was still 5 orders of magnitude greater than the calculated results from the computer codes. Following the minimum, the technetium concentration immediately (within 1 day) increased back toward the starting

concentration and eventually exceeded it slightly by the time the experiment was terminated on day 8.

The technetium concentration decreased and then returned to that of the entering solution because the stannous chloride dissolved and was expelled from the column. Initially, the stannous chloride dissolved when the ^{95m}Tc-spiked J-13 solution encountered the stannous chloride in the reaction column. The solution became reducing, causing the technetium in the solution to precipitate. As the solution continued to enter the reaction column, the concentration of the dissolved stannous chloride decreased, and eventually the stannous chloride concentration was not high enough to yield a reducing solution environment. Any technetium that precipitated and/or was retained by the tuff then dissolved because the solution environment was now oxidizing because of the oxidizing solution entering the column. This then caused the technetium concentration in the effluent samples to be greater than that of the starting concentration.

Comparing the results of the experiments with those indicated by the codes shows that since the stannous chloride concentration was constant in the Beaker Experiment, the ^{99}Tc concentration remained BDL as expected. However, the flow-through experimental results were not in agreement with the results indicated by the codes because the stannous chloride dissolved and exited the column.

Stannous chloride does not show promise for reducing the rate of technetium migration at a geologic repository based on the results of the Bench-top Stannous Chloride Experiment. These results show that stannous chloride reduced the technetium concentration only for the limited time that it remained in the column before it dissolved and was expelled from the column. The white precipitate that exited the reaction column also indicates that even though the stannous chloride temporarily reduced the technetium concentration, the precipitate was transported through the crushed tuff in the column. It is unsure how fast this mobile precipitate would travel because it could get stuck in the corners of fragmented tuff, or it may preferentially travel along the fault lines of the repository. This has significant ramifications because it may not be enough to only chemically reduce the technetium; the technetium must also be immobilized. Otherwise, the mobile technetium precipitate, albeit chemically reduced, could be oxidized once it encountered an oxidizing environment. Once it is oxidized and redissolved, it would likely have greater mobility than it would as a finely divided precipitate.

Using stannous chloride as a reducing agent also poses the possible disadvantage of increasing the degradation of the spent fuel waste package because of the acidic environment it may create. The advantage of using stannous chloride, namely its faster reaction kinetics, does not

outweigh the disadvantage that the stannous chloride rapidly dissolves. Nor does it outweigh the disadvantage that the precipitate that formed was mobile in the crushed tuff of this experiment. Because of its high solubility, all the stannous chloride in a waste package could potentially be exhausted during the first groundwater infiltration. Should there be more than one occurrence, there would not be a reactant available to reduce the incoming groundwater and inhibit technetium migration away from the repository.

4.6 FT-4C Tin Shot Experiments

Two experiments pumped ^{99}Tc-spiked J-13 through reaction columns containing tin shot. One was at room temperature, 24°C, and the other was at an elevated temperature, 85°C. Both of the Tin Shot experiments used the FT-4C, Figure 11a. It is known that the FT-4C system had problems with technetium being retained in the plumbing and later being released in the same or subsequent experiment, as discussed in the Blank-run Experiment, Section 4.2. However, the concentrations of technetium in the Tin Shot experiments were substantially higher than was found in the Blank-run Experiment. Therefore, this retention phenomena had no significant impact on the tin data, and the results from these experiments are credible.

4.6.1 Tin Shot Experiment at 24°C

The technetium concentrations versus time from the FT-4C ^{99}Tc Tin Shot Experiment at 24°C are represented by Figure 41 Curve 1. The technetium concentration in this experiment had a maximum drop from the starting concentration to approximately 2 ppb within the first 3 h of the experiment. This drop lasted less than 4 h, and the technetium concentration then increased to 972 ppb (3% below the starting concentration), which is within the range of uncertainty (4.9%). The technetium concentration then fluctuated within 14% of the starting concentration, having a final technetium concentration of 900 ppb, 9% below the starting concentration.

Figure 42 shows the comparison of the tin shot experiments and the EQ3/6 simulation of these experiments. The codes predicted that the technetium concentration would drop to 1×10^{-12} ppb as Tc_3O_4 and $Tc(OH)_2$ would precipitate out. The experiments never had the technetium drop BDL (as it would have if it dropped to the levels indicated by the codes).

4.6.2 Tin Shot Experiment at 85°C

The technetium concentration versus time from the FT-4C ^{99}Tc Tin Shot Experiment at 85°C is represented by Figure 41 Curve 2. This experiment also had an initial drop in technetium concentration. However, it was only an 8.5% drop

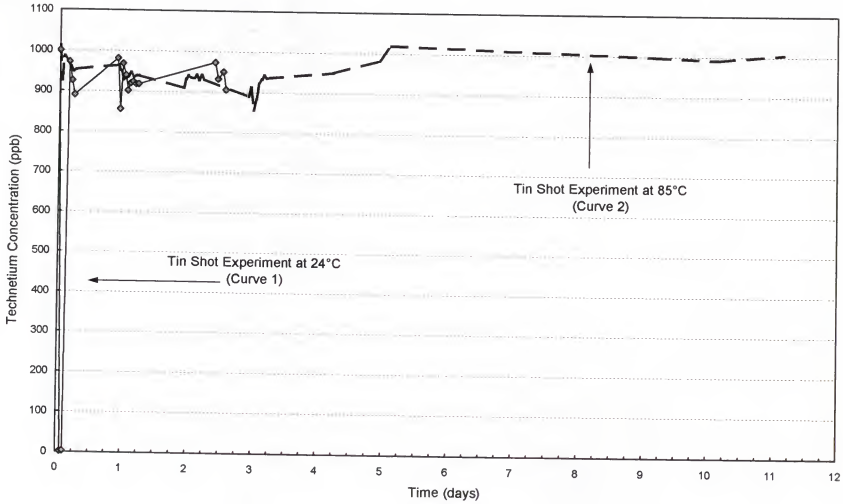

Figure 41 FT-4C Tin Shot Experiments at 24°C and 85°C

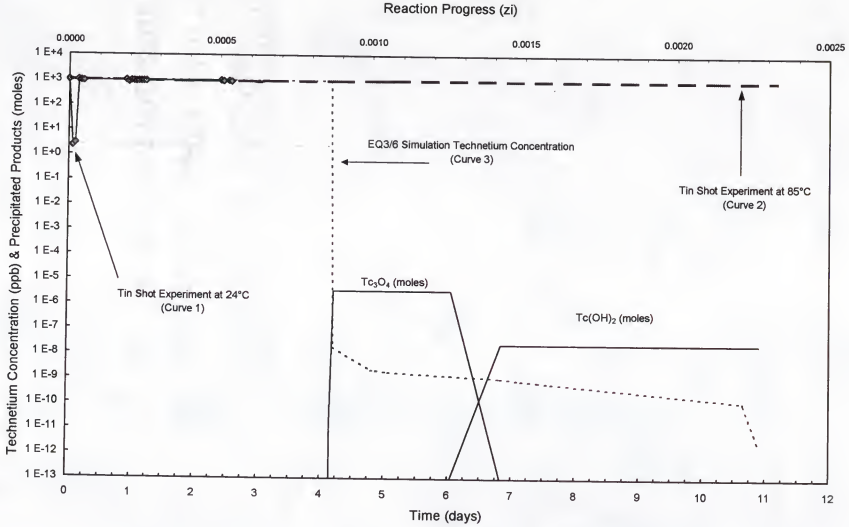

Figure 42 Comparison of the FT-4C Tin Shot Experiments and the EQ3/6 Simulation

from 1011 ppb to 925 ppb. The technetium concentration then increased 3% to 985 ppb. It continued to fluctuate within 12% of the starting concentration, reaching a minimum of 856 ppb 3 days after the start of the experiment. The technetium concentration then increased, and 5 days after the experiment started, it was 1020 ppb, which is within the uncertainty limits (5%) of the starting concentration. The technetium concentration essentially remained equal to the starting concentration for the remainder of the experiment.

Because the reaction kinetics are faster at higher temperatures, it is possible that this experiment did not quite agree with that of the 24°C experiment. The initial drop in technetium concentration was much less dramatic in this experiment than that of the Tin Shot Experiment at 24°C, which is an example of the effect of faster reaction kinetics at higher temperatures. It is possible that the technetium concentration dropped as much as in the experiment at 24°C, but the drop may have been missed by the time the first sample was collected (50 min after the start of the experiment) because of the faster reaction kinetics.

The tin shot experiments did not agree with the EQ3/6 simulation as the experiments never had the technetium drop BDL (Figure 42). The tin shot had essentially no effect on reducing the concentration of technetium in solution.

The ^{99}Tc concentration in the tin experiments was approximately 1000 ppb compared with a maximum of 14 ppb in

the Blank-run Experiment, Section 4.2. Therefore, the discrepancy between the results from the experiments and the computer simulation is not due to the system retaining technetium (in the plumbing downstream from the reaction column).

4.6.3 Tin Summary and Conclusions

Similar to the results for copper, it is believed that a passivation layer formed on the tin that prevented the tin from reducing the technetium concentration after the initial drop. This is supported by the fact that tin forms an insoluble film of SnO in waters with a pH of 7.4 and 8.6 (J-13 is within this range).[40] The passivation layer that developed on the tin in the experiments (1) prevented further reduction of the solution environment, (2) allowed the solution that entered the reaction column to remain in its original oxidizing state, and (3) allowed the oxidizing solution to dissolve any technetium that was previously reduced. Evidence for the third statement is that the technetium concentration would be expected to increase above the starting concentration after the initial drop, which it did.

The EQ3/6 simulations indicated that cassiterite (SnO_2) would form and precipitate, but not romarchite (SnO). According to known tin reactions, the formation of romarchite would be necessary to provide a protective

passivation layer on the tin.[40] Therefore, in an attempt to have romarchite precipitate in the EQ3/6 simulations, cassiterite was suppressed. Neither romarchite nor any other compound containing tin was indicated to precipitate. As the reaction path progressed, all the added tin went into solution. Another simulation had romarchite added as the reactant, thus forcing romarchite into the system (cassiterite was suppressed again). The simulation for that run also indicated that all the tin would be in solution with no tin compounds precipitating. Even though the codes do not predict that SnO forms, this may be in error because experimental evidence[40] suggests that it actually does.

The possibility of slow reaction kinetics being responsible for the discrepancy in technetium concentrations between the experiments and the codes is unlikely because the technetium concentration was quickly reduced 3 orders of magnitude in the 24°C experiment. In the 85°C experiment, the drop was not as substantial, but it did drop. Thus, the initial reaction was quite rapid, but formation of the passivation layer prevented further reaction.

The results of these experiments do not show promise for tin reducing the rate of technetium migration in a geologic repository.

CHAPTER 5
SUMMARY AND CONCLUSIONS

The conclusions listed here are based upon computer simulations performed at the University of Florida and during and after interning at PNNL, and on the experiments conducted at PNNL. This work was performed to evaluate different reactants with a potential for reducing the rate of ^{99}Tc migration under the scenario of waste cask breach and groundwater infiltration at a geologic repository. Reducing the rate of technetium migration at a geologic repository is of interest because ^{99}Tc is expected to be present as pertechnetate (TcO_4^-), which is highly soluble under oxidizing conditions. It has a very long half-life of 213,000 years.[2,20] However, technetium is less soluble and may be more strongly adsorbed on minerals when it is reduced to lower valance-state compounds (TcO_2, Tc_3O_4, $Tc(OH)_2$, $Tc(OH)$, Tc, etc.).[2,11,20,21]

Therefore, iron, copper, stannous chloride, and tin were investigated in the hope that they would lower the redox potential of the solution environment and thus precipitate technetium from solution. Because the reduced technetium compounds are much less soluble, they should remain close to where they precipitate.

Experimentally, iron was the only reducing agent investigated in these experiments that shows promise for reducing the rate of technetium migration from a geologic repository. The ^{95m}Tc concentration decreased from a starting concentration of 9.4×10^{-4} ppb in the flow-through experiment to near detection limits (1×10^{-7} ppb). Then it increased, reaching 3×10^{-5} ppb at the experiment's end (38 days). In the static experiments, the ^{95m}Tc concentration was reduced to BDL (1×10^{-7} ppb).

Comparison of the two static experiments (one at 70°C and the other at 24°C) showed that the increase in temperature substantially reduced the time it took to decrease the technetium concentration BDL. In the 70°C experiment, the technetium concentration dropped BDL within the first day, versus more than 13 days required in the 24°C experiment. This was caused by the slow reaction kinetics at the lower temperature.

In each of the iron powder experiments, the technetium concentrations were reduced for the entire time that the experiments were conducted; however, the longest experiment lasted only 56 days. Follow-up studies should be conducted to determine whether iron can be expected to reduce technetium concentrations on a geologic time scale. If so, adding iron into the waste package design for spent nuclear fuel should reduce the rate of technetium migration from a geologic repository should a breached waste package be

contacted by groundwater. The technetium would be less mobile in the reduced and precipitated state.

Comparing the results of this research with those calculated by the EQ3/6 codes indicates that the measured technetium concentrations in the static iron powder experiments were consistent with those indicated by the codes, as both experiments terminated with technetium concentrations BDL. The pH measurements were also in agreement with the codes for these two experiments. However, the measured minimum Eh value (-0.28 mV) was substantially higher than the minimum indicated by the codes (-492 mV) for the 70°C experiment. The measured minimum Eh value (-343 mV) for the 24°C experiment was also substantially higher than the minimum indicated by the codes (-444 mV). This was because the experimental environment was not as anoxic as hoped. Although the experiments were conducted in sealed vessels, there was oxygen in-leakage.

The iron powder flow-through experiments were not modeled correctly by the codes for three reasons. First, the reaction kinetics of iron are slow, and therefore the values calculated by the codes were never realized in the limited time frame that the iron and technetium were in contact with each other (approximately 1.5 h). Second, the EQ3/6 codes cannot accurately model a solid-centered flow-through open system as in the experimental flow-through

systems.[k] Finally, the EQ3/6 codes cannot model sorption. In the Bench-top ^{95m}Tc Iron Powder Experiment, the technetium concentration decreased because it was being sorbed as well as reduced by the iron.

The results from the four copper experiments were consistent in that the technetium concentration remained essentially unchanged. In two of the experiments, there was an initial drop in technetium concentration, after which the concentration returned to the starting values. This occurred because the technetium was first precipitated, and then it redissolved once the Cu_2O passivation layer developed and prevented the metal from further oxidation. These experimental results are in contrast to the calculations which show that the technetium concentration should have dropped to 2×10^{-3} ppb. The fact that the technetium concentration remained essentially unchanged for the copper experiments indicates that copper would not prove promising for reducing the rate of technetium migration at a geologic repository.

When stannous chloride was used in a static experiment, the technetium in solution precipitated instantaneously. This was consistent with the results indicated by the

---

[k]The EQ3/6 codes are continually being updated. It is planned to revise the code so it will be capable of modeling a solid-centered flow-through open system as a regular feature in the future.[27] After adding this feature, the codes would be capable of modeling the experiments.

computer codes. However, in the flow-through experiment, the technetium concentrations returned to, or were higher than, the starting concentration once the stannous chloride dissolved and was expelled from the reaction column. The technetium precipitate was also mobile in the crushed tuff of the flow-through laboratory experiment. Therefore, it might also be mobile in a repository environment. It is unsure how fast this mobile precipitate would travel because it could get stuck in the corners of fragmented tuff, or it could preferentially travel along the fault lines of the repository. Even if the technetium precipitate moved quite slowly, it might eventually reach an oxidizing environment where it would redissolve and then migrate along with the water.

The tin shot experiments at 85°C and 24°C were consistent in that the technetium concentration remained essentially unchanged in both experiments. There was an initial drop in the technetium concentration, after which it returned to near the starting values. This was most likely because of the formation of a protective passivation layer of SnO on the tin. As a result, the experimental results are not in agreement with those indicated by the codes because the codes cannot model a passivation layer. Although the codes cannot model this type of flow-through experiment, it is also unlikely that a stagnant experiment

would be modeled by the codes correctly. The passivation layer would likely develop in that experiment also.

The possibility that slow reaction kinetics in the tin shot experiments was responsible for the discrepancy in technetium concentrations between the experiments and the codes is unlikely because the technetium concentration was quickly reduced 3 orders of magnitude in the 24°C experiment. In the 85°C experiment, the drop was not as substantial, but it did drop. Thus, the initial reaction was quite rapid, but formation of the passivation layer prevented further reaction.

Iron appears promising for reducing the rate of technetium migration from a geologic repository. Copper, tin, and stannous chloride did not appear promising.

CHAPTER 6
RECOMMENDATIONS

A flow-through experiment with iron showed that the ^{95m}Tc concentration dropped from a starting value of 9.4×10^{-4} ppb to approximately 1×10^{-7} ppb in under 2 h. The technetium concentration remained near this detection limit for 13 days and then began to increase, reaching a maximum concentration of 3×10^{-5} ppb after 30 days. It is believed that the rise in technetium concentration in the latter half of the experiment was caused by the sorption of technetium by the iron, thereby passivating its surface. Future experiments lasting substantially longer times would be beneficial to determine if the technetium concentration would remain at reduced values or continue to increase as passivation of the iron surface became more effective. Analyses of the iron at the end of the experiments would also be beneficial to determine if the technetium was actually being sorbed by the iron.

The two Sealed Vessel experiments showed that the iron reduced the ^{95m}Tc concentration from 2.3×10^{-5} ppb to BDL, i.e., less than 1×10^{-7} ppb. Although these experiments were conducted in a sealed vessel, there was oxygen in-leakage. Therefore, the Eh values were much greater than

indicated by the codes. Experiments using a system similar to the Sealed Vessel System could be performed in an oxygen-free environment. This could be obtained by using a specially designed leak-free system in an inert-gas-purged glovebox. These experiments would alleviate the problem of oxygen infiltration that occurred in the Sealed Vessel experiments. These experiments could then have a known concentration of oxygen added to the system to determine the effect of oxygen on the reduction of technetium. Because the proposed geologic repository at Yucca Mountain would not be in an anoxic environment, understanding the rate of technetium concentration reduction as a function of oxygen concentration would be beneficial. Although the technetium concentration was reduced BDL for the entire 15 and 56 days that the experiments were conducted and would not be expected to increase in longer experiments, the new experiments could be conducted for substantially longer times to ascertain that it would not increase. Analyses could also be conducted on the precipitates and the iron after the experiments are terminated to determine the oxidation states of the reduced technetium and oxidized iron.

To take advantage of the 8 orders of magnitude difference in detection levels, a static experiment using ^{95m}Tc instead of ^{99}Tc is recommended to gain further information on the reducing capabilities of stannous

chloride on technetium. In the static experiment using ^{99}Tc, the concentration was BDL as the spiked solution was added to a dissolved stannous chloride solution. Using ^{95m}Tc instead of ^{99}Tc would allow the lowest technetium concentration to be determined and possibly determine the solubility-controlling technetium compound. The precipitate that formed as the spiked solution was added to the stannous chloride solution can be analyzed to determine its chemical form. In similar flow-through experiments, the reaction column could also be analyzed to determine if any of the technetium gets caught on the corners of the fragmented tuff, or if it travels with the fluid flow. A similar experiment using uncrushed tuff could be conducted to determine the mobility of the precipitate in this medium.

The copper powder experiment used a technetium concentration of 9.4×10^{-4} ppb, which was close to the minimum indicated by the codes, 3.4×10^{-4} ppb. Thus the technetium concentration remained essentially unchanged, except for a temporary initial drop. An experiment should be conducted using a starting technetium concentration much greater than the minimum predicted by the codes. Then it could be determined if the technetium concentration would drop to the predicted values or remain essentially unchanged as it did in the experiment described here.

To obtain these much greater starting concentrations, these new experiments may be conducted with a combination of

^{99}Tc and ^{95m}Tc. They may also be conducted with another tracer material that should chemically behave as technetium, e.g., rhenium (Re). Rhenium has radioactive and non-radioactive isotopes. Experiments using large concentrations of rhenium can be conducted using the non-radioactive isotope. The radioactive isotope could then be used for experiments with trace concentrations. Therefore, samples from experiments that use high concentrations of the non-radioactive isotopes can be analyzed chemically. Samples from experiments that use trace amounts of the radioactive isotopes can be analyzed radiochemically as in the technetium experiments. Rhenium-183 is a gamma emitter with a relatively short half-life of 70 days,[52] and low detection limits similar to ^{95m}Tc can be obtained (see Table 3).

The disadvantages versus advantages would need to be researched before conducting any experiments. Using ^{183}Re may have a disadvantage because of the complex redox reactions associated with this isotope. The advantage of using large concentrations without radioactivity may outweigh those disadvantages due to the rules, regulations, and costs of conducting radioactive experiments. The financial feasibility of conducting these experiments also needs to be considered. Conducting chemical analyses may cost significantly more than conducting radiochemical analyses, especially if the chemical analyses must be

contracted out. However, one could use high concentrations of the non-radioactive rhenium and spike it with ^{183}Re to follow what occurs radioactively. Obtaining ^{183}Re may also be financially prohibitive. It would also need to be ascertained that rhenium chemically behaves as technetium. Otherwise, the experimental results would be useless for comparison to those of the technetium experiments, or for application to reducing the rate of technetium migration at a geologic repository.

CHAPTER 7
EPILOGUE

During this investigation, the author received inquiries regarding the possibility of using the information gained through this research to prevent the migration of technetium in the ground at sites that contain organic contaminants (especially trichlorethylene, TCE) along with technetium. The inquiring groups had already ascertained that iron would bind the organic contaminants and that the site in question was oxidizing. The information obtained from this dissertation research suggests that the use of iron would reduce the oxidation state of technetium, thus causing it to precipitate. The rate of technetium migration would be expected to also be much less as a solid precipitate than as an anion (TcO_4^-) in solution. Thus it appears that the addition of iron to the contaminated sites would bind both forms of contaminants. The soil and associated contaminants could then be dug up and properly disposed of as hazardous mixed waste.

PNNL is currently studying In Situ Redox Manipulation (ISRM), originally called Redox Manipulation, to cheaply stop the flow of highly toxic chromium toward the nearby Columbia River.[53] ISRM involves creating an iron(II) zone

by injecting a chemical reagent (containing sodium dithionite and potassium carbonate/bicarbonate pH buffers) into the aquifer through a groundwater well. This chemical causes the naturally occurring iron(III) in the aquifer sediments to be reduced to iron(II). The reduced iron is then capable of reducing the contaminants in the ground that are redox-sensitive. Technetium is among the list of redox sensitive contaminants that PNNL wants to remove from its site. This is very similar to the concept of placing iron in a geologic repository to reduce the oxidation state of technetium and hence reduce its concentration should a breach occur in a waste package and be infiltrated with groundwater. The difference is that PNNL uses the iron present in the soil rather than adding it to the waste environment. PNNL's technology is being hailed as a means to treat contaminated groundwater throughout the world.

The kinetic and thermodynamic properties of technetium are still being researched. There are many unknowns and uncertainties in these data because of the complex nature of technetium's chemical properties. One such investigation is being conducted at Los Alamos National Laboratory to study technetium attenuation and the role of mineral interactions with technetium. This study will investigate the mechanisms of surface-related sorption of technetium on surfaces containing iron(II).[54]

GLOSSARY

Abscissa	The horizontal coordinate of a point in a plane Cartesian coordinate system obtained by measuring parallel to the x-axis.
Activity	The value that replaces concentration in a thermodynamically correct equilibrium expression. Also, a measure of radioactive decay in units of Bq or Ci.
Activity coefficient	The number by which the concentration must be multiplied to give the activity.
Actinide	Elements that are in the seventh period of the periodic table. Uranium and plutonium are members of the actinide series.
Adsorb	The process by which a substance becomes attached to the surface of another substance.
Anoxic	Without oxygen.
BDL	Below detectable limits.
Chemical equilibrium	The state in which the forward and reverse rates of all reactions are equal so that the concentrations of all species remain constant.
Conduction band	In a crystal, the band contains electrons that are not bound and migrate throughout the crystal.

Debye-Hückel equation	Gives the activity coefficient, γ, as a function of ionic strength, I. The extended Debye-Hückel equation, applicable to ionic strengths to about 0.1 M, is $\log \gamma = [-0.51z^2\sqrt{I}]/[1 + (\alpha\sqrt{I}/305)]$ where z is the ionic charge and α is the effective hydrated radius in picometers.
Decay heat	Heat generated by nuclear decay of isotopes.
Disequilibrium	The state in which the forward and reverse rates of all reactions are not equal so that the concentrations of all species are changing.
Fluid-centered	The view as would be seen by a packet of fluid traveling through a medium.
Florescence	The property of emitting radiation as the result of absorption of radiation from some other source. The emitted radiation persists only as long as the exposure is subjected to the radiation that may be either electrified particles or waves. The fluorescent radiation generally has a longer wave length than that of the absorbed radiation.
Forbidden band	Energy band within a crystal where electrons are normally forbidden.
Geochemical	The chemical and geological properties of a substance.
Half-life	The time required for one half the atoms in a sample of a radioactive element to decay.
Integral number of moles	The total moles added in the incremental steps taken by the EQ3/6 codes.

Interstitial states	Places for electrons in the normally forbidden band made by adding an impurity into the lattice.
Isomer	Nuclei with the same mass number, *A*, and the same number of protons, *Z*, but with different energies.
Isotope	An element having various values of the mass number *A*, for a given number of protons, *Z*. Isotopes behave similarly in chemical reactions, but their nuclear characteristics may be markedly different.
Iterative technique	Technique where an approximation for solving a numerical equation is made on the basis of a previous approximation. This processes is performed repeatedly to successively compute better and better approximations.
Kinetics	The rate of change in a chemical system.
"m" in ^{95m}Tc	Metastable. Nuclei with a given mass number, *A*, and number of protons, *Z*, that exists temporarily in a state having more energy than the ground state, corresponding to that of *A* and *Z*. See "isomer".
Molality	The number of moles of solute per kilogram of solvent.
Ordinate	The vertical coordinate of a point in a plane Cartesian coordinate system obtained by measuring parallel to the y-axis.
Oxic	Containing oxygen.
Oxidation state	A bookkeeping device used to tell how many electrons have been gained or lost by a neutral atom when it forms a compound.

Oxygen fugacity	The activity of oxygen gas. $A = P_{O2}\gamma_{O2}$
Passivating layer	A layer on the compound that makes it inactive or less reactive.
Pentavalent	Having five electrons in the outer shell.
Pertechnetate	The chemical name for TcO_4^-.
pH	Defined as pH = - log A_{H+}, where A_{H+} is the activity of H^+. In most approximate applications, the pH is taken as $-\log[H^+]$.
pHCl	Defined as pHCl = - log A_{HCl}, where A_{HCl} is the activity of HCl.
Phase assemblage	The collection of chemical phases that can occur.
Porbaix diagram	A diagram of Eh versus pH illustrating the possible chemical species formed in a system.
Precipitate	The solid substance that separates from a solution.
Radionuclide	Radioactive nuclide.
Reactant	The species that is consumed in a chemical reaction. It appears on the left side of a chemical equation.
Redox reaction	A chemical reaction involving the transfer of elections from one element to another.
Reducing agent	A substance that donates electrons in a chemical reaction. Also called Reductant.
Reduction	A gain in electrons or a lowering of the oxidation state.

Repository	A site that may be designated for the long-term storage of radioactive spent fuel generated from nuclear reactors that is not at the reactor sites themselves.
SCE	Saturated Calomel Electrode is the common reference electrode based on the half-reaction $Hg_2Cl_2(s) + 2e^- = 2Hg(l) + 2Cl^-$.
Solid-centered	The view as would be seen by a solid as fluid travels through the medium.
Solubility	Is the mass of a substance, a solid or liquid, contained in a solution in equilibrium with an excess of the substance.
Sorb (sorption)	The method by which a chemical species is retained by another without a chemical reaction occurring.
Supersaturated solution	A solution that contains more dissolved solute than would be present at equilibrium.
Thermocouple	An electrical junction across which a temperature-dependent voltage exists. Theremocouples are calibrated to measure temperatures and usually consist of two dissimilar metals in contact with each other.
Thermodynamic	Relating to a system of atoms, molecules, colloidal particles, or larger bodies considered as an isolated group in the study of thermodynamic processes.
Titration	A procedure in which a substance (titrant) is carefully added to another (analyte) until a complete reaction has occurred. The quantity of titrant required for a complete reaction tells how much analyte is present.

Tuff	Rock composed of fine volcanic rock/dust that has been fused together by heat.
Vadose	Water or solution above the groundwater table and located in the tuffaceous rock (see tuff).
Valance band	The band that contains electrons that are bound to specific lattice sites within the crystal.
Valence state	Numerical value equal to the number of electrons in its outer shell.

APPENDIX A
THE EQ3/6 COMPUTER CODES

Computational-analysis was conducted using the EQ3/6 software package.[25,27,28,29] The EQ3/6 codes are actually two codes that characterize the geochemical behavior of aqueous systems, EQ3NR and EQ6; a data file preprocessor, EQPT; a software library, EQLIB; and supporting thermodynamic data files.

This software package was originally developed at Northwestern University in the 1970s "to model seawater-basalt interaction in mid-ocean ridge hydrothermal systems."[29] It has been revised numerous times since then. It is currently the property of Lawrence Livermore National Laboratory (LLNL). The EQ3/6 codes were written in Fortran 77 and were developed to run within the UNIX operating system on workstations and supercomputers.

EQ3NR and EQ6 both require using one of the thermodynamic data files. Currently, there are five of these files that are used with the EQ3/6 codes. These files are all formatted ASCII files called DATA0.* where * is COM, SUP, NEA, HMW, and PIT. However, EQ3NR and EQ6 require using unformatted data files. EQPT is the program used to convert the formatted data files into the required

corresponding unformatted data files called DATA1.* files. Each of the five data files contains the activity-coefficient parameters and standard-state thermodynamic data. These data are needed to determine the activity coefficients. The files correspond to the equations used for modeling the activity coefficients of the aqueous species it contains.

The COM, SUP, and NEA data files can be used in EQ3NR and EQ6 with the Davis equation or the B-dot equation because these files contain data specific to a general extended Debye-Hückel model to determine the activity coefficients. The Davis and B-dot equations are only valid in dilute solutions.

The COM (composite) file is the largest of the files with the information obtained from many sources, including those used by the other four data files. The COM file represents 886 pure minerals, 852 aqueous species, 76 gaseous species, 78 chemical elements, and 12 solid solutions. It has a temperature range of 0 to 300°C. This allows for modeling aqueous solutions with a high degree of compositional complexity, such as those of J-13. The COM file was produced by Lawrence Livermore National Laboratory.

The HMW and PIT data files can be used in EQ3NR and EQ6 when there are solutions containing high concentrations (like brine solutions) needing to be analyzed. These data use specific semi-empirical equations proposed by Pitzer

that have been successful in describing the activity-coefficients in highly concentrated solutions.[27] The HMW and PIT data files do not contain as many chemical components as the others.

EQ3NR is the speciation-solubility code that is used for geochemical modeling. Static calculations based on water-chemistry analysis are used to model the thermodynamic state of an aqueous solution. The user specifies the chemical analysis of the input solution, usually in terms of concentrations of dissolved components. These are simply the initial concentrations used in the equations. The input concentrations are the total concentrations for the species and not individual contributions from simple ions, ion pairs, and aqueous complexes. However, the data may distinguish a dissolved component by oxidation state. For instance, Fe^{++} may have one concentration entered and Fe^{+++} another. The pH of the solution is usually entered; however, the pHCl may be used. The redox potential (Eh) or the oxygen fugacity (pe) may also be used. The redox state may alternately be specified by a redox couple.

A master set of basis species that represent the chemical components of the solution are then determined on a one-to-one basis from the input concentrations. The strict basis is then determined as the minimum number of species and includes one species for each element plus one for oxidation-reduction and charge balance. An auxiliary basis

contains species that are related to the strict basis through various chemical reactions. Sometimes, a strict basis is switched with an auxiliary basis to improve the initial starting values for solving the algebraic equations.

EQ3NR then takes these input concentrations and uses them with mass-balance equations and/or charge-balance equations. The governing equations are the mass-balance equations and charge-balance equations, depending on whether concentrations, or redox couples, etc., were entered in the input and also depending on the output parameters desired. For example, the mass-balance equation is the governing equation for an input of total concentration. For the case of calcium, the mass-balance equation in terms of molalities would be represented by

$$m_{T,Ca^{+2}} = m_{Ca^{+2}} + m_{Ca(OH)_{2(aq)}} + m_{CaCO_{3(aq)}} + m_{CaHCO_3^+} + \cdots \qquad (A.1)$$

The concentrations of ion-pairs and complexes are governed by thermodynamic equilibrium and are represented by a mass-action equation for its dissociation. For example, the dissociation of calcium carbonate and the corresponding mass-action equation would be

$$CaCO_{3(aq)} \rightleftharpoons Ca^{+2} + CO_3^{-2} \qquad (A.2)$$

$$K_{CaCO_{3(aq)}} = \frac{[a_{Ca^{+2}}]\,[a_{CO_3^{-2}}]}{[a_{CaCO_{3(aq)}}]} \qquad (A.3)$$

where K is the equilibrium constant, and a is the thermodynamic activity. The thermodynamic activity is related to the molal concentration, m, and the activity coefficient, λ, by the equation:

$$a_i = m_i \lambda_i \qquad (A.4)$$

Using the input values and supporting library and data files, EQ3NR then uses the standard-state thermodynamic data taken from the data file of all the species involved and the equations that describe the activity coefficients to compute the thermodynamic state of the aqueous solution. For all the species, it calculates the concentrations, activity coefficients, and thermodynamic activities.

Because the above equations need to be solved simultaneously, EQ3/6 solves equations A.1 through A.4, which are intrinsically algebraic, by using a highly effective hybrid Newton-Raphson algorithm. The Newton-Raphson method is a well known iterative technique for solving non-linear systems of algebraic equations. It is "perhaps the most widely used of all root-locating formulas."[55] The code uses a first-order algorithm and may do some basis switching to optimize the starting estimates of the activity coefficients it creates for the Newton-Raphson iteration. The activity coefficients of the aqueous species are then held constant in each iteration. The

hybrid part comes from readjusting the activity coefficients between iterations.

After going through many iterations, the concentration, activity coefficients, and thermodynamic activities of all the species are determined. Using these data, it then calculates a set of saturation indices and thermodynamic affinities of various reactions. The saturation indices are measures of the degree of disequilibrium of the reactions: the larger the number, the larger the degree of disequilibrium. The formula for the saturation indices is

$$SI = \log \frac{Q}{K} \tag{A.5}$$

where Q is the activity product, and K is the equilibrium constant. The thermodynamic affinity of the precipitation reaction is represented by the formula

$$a = 2.303\ RT \log \frac{Q}{K} = -2.303\ RT \log \frac{K}{Q} \tag{A.6}$$

and the two preceding formulas are related by

$$A_{-} = 2.303\ RT\ SI \tag{A.7}$$

where R is the universal gas constant (8.31441 J K^{-1} $mole^{-1}$), and T is the temperature in Kelvin. The thermodynamic state of each aqueous redox couple, the theoretical Eh, pe, oxygen fugacity, and redox affinity (Ah) are also calculated when there are aqueous redox reactions. EQ3NR next calculates a

mass balance for each chemical element corresponding to the strict-basis species. This mass balance is represented in terms of moles. It then computes a charge-balance equation based on the charge equivalents. The mass- and charge-balance relations obtained are also used by EQ6 to determine the number of moles of each strict-basis species as well as the oxygen fugacity of the system. If EQ3NR determines a charge imbalance, it will pass on to, and be maintained by, EQ6.

The EQ3NR output file is a regurgitation of the input plus the output results. The pickup file contains the concentrations, affinity coefficients, and thermodynamic activities based on mass- and charge-balance equations. The pickup file gets added to the bottom of the EQ6 input file, and therefore, EQ3NR is "required to initialize the EQ6 calculations".[29] EQ6 can then be used to model what occurs in (1) titration processes (including fluid mixing), (2) irreversible reactions in a closed system, (3) irreversible reactions in fluid centering flow-through systems, and (4) heating and cooling processes. It can also solve single-point thermodynamic equilibrium problems. This code models both mineral dissolution and growth kinetics. The reaction progress or chemical development is driven by irreversible reactions, and these reactions are usually the dissolution and precipitation of solids and minerals.

Modeling one of the four processes mentioned above using EQ6 requires supplying the thermodynamic model of an aqueous solution, obtained by running EQ3NR, choosing a set of irreversible reactions ("reactants") and/or changing the temperature/pressures of the system, providing parameters to define the rates of these processes, and choosing from among the various model options that are available.

It is important that in EQ3NR, the number of moles of solvent water is constant and corresponds to 1 kg. However, in EQ6, this is a calculated variable. Therefore, the thermodynamic equations in EQ3NR and EQ6 differ, and EQ6 uses a mass-balance equation for oxygen as the added equation for this unknown. The amount of solvent water in EQ6 changes, as well as the pH and oxygen fugacity of the system; therefore, EQ6 indicates that compounds will precipitate when EQ3NR does not.

Because EQ6 indicates that compounds will precipitate, the thermodynamic equations in EQ6 are made in steps, each step presuming a phase assemblage. The first is that obtained from EQ3NR via the pickup file. EQ6 will then check for any phase that is supersaturated. If there are supersaturated phases, one of these phases is added to the assemblage, and a new calculation is made. A number of new unknowns are added, depending on what phase is added. One unknown is added if the phase is a pure mineral. The added equation for this unknown is the mass-action equation for

the pure mineral. However, the number of unknowns will increase by the number of end members present in a solid solution should that be the phase added. The added equations will therefore include a new equation for each end member. If the process is successful for the supersaturated phases, then it is repeated for all unexcused supersaturated phases.

Similar to EQ3NR, the mathematical expressions for the activity coefficients for solid-solution end members are used in the mass-action equations that define the solubility equilibria. Correction of these activity coefficients is done in a Newton-Raphson step.

The process by which a set of irreversible reactions proceeds to thermodynamic equilibrium is represented by the reaction path. Chemically speaking, a system is driven as the irreversible reactions move toward a state of equilibrium. If the aqueous solution is undersaturated with respect to a mineral, the thermodynamic driving force is for the dissolution of the compound containing that mineral. In EQ6, this process is divided into incremental steps of adding the mineral. This creates a series of thermodynamic equilibrium calculations for systems with increased mass-balance totals for each of the elements in the compound being dissolved. The reaction path ends when the solution is saturated or no more reactant is left. Secondary

minerals may also form and precipitate during the course of this path.

Reaction-path calculations may take place in "reaction progress" mode as relative rates, without reference to time, or in "time" mode. Thermodynamic calculations in the reaction progress mode are intrinsically algebraic, and as such are handled algebraically using iteration variables. Choosing time-mode operation is tricky because "the study of kinetics of reactions occurring in aqueous geochemical systems is still in the pioneering stage."[27] General agreement of the functional form of the rate law does not exist. There is also not general agreement in the values of the corresponding constants (rate constants, activation energies, etc.).[27] Rate-law calculations in the time mode are intrinsically differential and as such are handled by linear ordinary differential equations. Therefore, if a time mode is used, the code must integrate ordinary differential equations (the rate laws).

EQ6 has three output files that indicate the reaction path of a system. These output files indicate the product minerals formed, the variations in solution environment variables, concentrations of reactants in solution, gases produced, and so forth. The three files are the output, tab, and pickup files. The output file is usually extremely large and cumbersome to work with; however, it gives the complete details of what occurred during each step in the

run. The tab file puts this information in a tabular format, which is still quite large and not always convenient to work with when analyzing data. The tab file gives all the information for all the different phases of the different solids, minerals, and gasses. The pickup file is capable of being used as the input for another EQ6 run. It is convenient to be able to use the pickup file as an input file for EQ6 to understand what might occur when the temperatures change in the system being analyzed.

APPENDIX B
BETA DETECTION SYSTEM

Technetium-99 is a pure beta emitter, which decays to ^{99}Ru by the emission of a 292 keV β^- particle. This process is schematically written as

$$_{43}Tc^{99} \rightarrow {}_{44}Ru^{99} + \beta^- + \nu$$

In beta analysis, the beta spectrum is a continuum. It appears over the range of zero to the endpoint energy since the decay energy is shared between the antineutrino and the beta particle, in this case from 0 keV to 292 keV.

Liquid scintillation analysis (LSA) was chosen for determining the ^{99}Tc concentration in the samples because the sample is counted directly in the liquid scintillator. This allows for high efficiency counting of beta particles. It also eliminates the problems of self-absorption, attenuation by detector windows, and backscattering from the detector.

For LSA, the sample to be counted is dissolved in a liquid scintillation cocktail, put in a glass vial, and then placed in the counter. All the beta particles emitted from the sample must pass through the liquid scintillation cocktail where the majority of the beta particles are fully stopped. Within the cocktail, the beta particle's energy is

transferred to the scintillator, and light pulses are produced. The light pulses produced enter the photomultiplier (PM) tube and bombard the photocathode. The photocathode converts the light pulses to low-energy electrons, which are accelerated toward the first dynode, and many secondary electrons are produced for each incident photoelectron. The secondary electrons produced at the first dynode are accelerated toward a second similar dynode, and more secondary electrons are produced. This process is repeated many times, the number of electrons is substantially increased, and this amplified electric charge is collected at the anode where it serves as a detectable electrical signal that is directly proportional to the number of original photoelectrons.

Different liquid scintillation cocktails can greatly affect the efficiency of the light pulses produced and hence the efficiency of the beta analysis. Therefore, different scintillation cocktails were investigated for efficiency; Pico Flour LLT was selected for use in this work. Pico Flour LLT was chosen because the counting efficiency for ^{99}Tc/J-13 solutions were between 66-88%, well above the other scintillation cocktails.

With each series of samples counted, a background sample was included that contained the scintillation cocktail and the same solution as the samples less the ^{99}Tc. An example of the output obtained from the LSA is shown on

page 199. The plot shows that there were 3222.73 counts per minute (CPM) for region B. Region B covers energy ranges from 10-250 keV. The first region, Region A, goes from 0-10 kev. This region is not included for counting the activity for ^{99}Tc because this is the region where the background is high, mostly due to electronic noise. The background counts obtained from the background sample counted with this sample would then be subtracted.

SPECTRAGRAPH 2.29 (C) Copyright Packard Instrument Co. 1987 09-Apr-93 09:28

L o g V I E W

5000.0 Y Transform Log max Endpoint 557 keV
// Active File: TR-6-6A.100 \\ NonActive File: PF-TR-6A.100

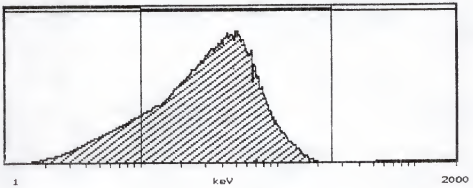

Regions of Interest

	LL	UL	CPM TR-6-6A.100	PF-TR-6A.100
A:	0.0	10.0	670.53	6.36
B:	10.0	250.	3222.73	7.57
C:	0.0	2000	3916.36	38.68
D:	0.0	0.0	0.00	0.00
E:	0.0	0.0	0.00	0.00
F:	0.0	0.0	0.00	0.00

13 APRIL 93
PAGE 67

APPENDIX C
GAMMA DETECTION SYSTEMS

Technetium-95m is a metastable radionuclide with a complex decay scheme. Its decay modes include beta-plus, electron capture, x-rays, and gamma ray emission.[56] Unlike beta analysis, in gamma analysis each gamma ray produces a photopeak at the energy of that gamma ray and, depending on the resolution and efficiency of the detector, each peak can be discriminated from the others.

The sodium iodide detector (NaI[Tl])[1] is an inorganic scintillator doped with an activator, thallium.[57] Since a gamma ray is an uncharged and highly energetic type of radiation, it does not ionize the material it passes through. To detect the gamma ray, an interaction must occur. There are only three interactions that are important relative to gamma spectroscopy: the photoelectric effect, compton scattering, and pair production. In each of these reactions, the gamma ray transfers energy to electrons. The electrons, which have a maximum energy equal to the incident gamma, will lose their energy through ionization and excitation of atoms within the absorber material. The

[1]The theory behind the detectors in this section can be found in Reference 57 or any good radiation detection book.

NaI(Tl) must therefore first convert gamma rays to fast electrons before it can detect these electrons.

When a gamma ray is incident upon the crystal lattice of a NaI(Tl), energy is absorbed from its interaction with the crystal lattice, and an electron in the crystal's valance band is excited into the conduction band. There is an activator (Tl), an impurity in the crystal, that creates interstitial states in the normally forbidden band. The positive hole left in the normally filled valance band when the electron was excited drifts to the location of an activator site and ionizes it. The migrating electron in the conduction band then drops into this ionized site and creates a neutral impurity site with its own excited energy state in the forbidden gap. The de-excitation of this excited state to the valance band will produce a photon in the visible energy range. The site in the forbidden gap is necessary because if the electron would de-excite directly from the conduction band to the valance band, the energy of the resultant photon would be too high to be in the visible region; the same holds true for the original gamma ray photon. Once the photon in the visible energy range is produced, it enters the PM tube, and the same process as described in Appendix B occurs.

The NaI(Tl) detection system was chosen for counting the ^{95m}Tc samples because it has the highest known light yield to primary and secondary electrons for gamma analysis,

and its response is close to linear with respect to the incident gamma ray energy. The resolution of the detector is not as high as that of germanium detectors. Because the ^{95m}Tc was known not to have any impurities, finer resolution to discriminate against decay of impurities was not necessary.

The NaI(Tl) was also chosen because of its high atomic number of 53, which has a significant influence as to which of the three reactions that the gamma ray would undergo to produce the electrons. Photoelectric effect is the preferred interaction for gamma spectroscopy, and its crossection is proportional to $z^{4.5}$. Technetium-95m has multiple gamma rays. The three significant ones are 204 keV (70%), 838 keV (27%), and 1.04 MeV (4%).[56] Because the 204 keV is the most abundant and also falls into the range of the photoelectric effect, this is the peak that was used for determining the technetium concentration in the analytical samples.

The specific NaI(Tl) detector used for this research has the added benefit of being a well-type detector to achieve close to a 4 π geometry, and it is a large crystal, 4 in. × 5 in., thus having a high efficiency. A sample of the output obtained by the analysis of one of the analytical samples is shown on page 204. The output shows 348 counts per second for the peak used (at energy 204.32). A background sample that was counted for the same length of

time is then subtracted from this. For this sample, the count time was only 1 h because the sample was well above background. However, for the samples from the sealed vessel experiments, 16 h counts were conducted.

VMS Peak Search Report V1.9 Generated 15-APR-1994 12:50:05

```
Configuration     : DKA200:[USER]S4273.CNF;1
Analyses by       : PEAK V16.4,ENBACK V1.5
Sample title      : Tc-95m, F7-J13, and Cu Experiment # MC
Sample date       :                        Acquisition date : 15-APR-1994 11:48:43
Sample ID         : MC-5, S4273            Sample quantity  : 5.0000 mL
Sample type       : Liquid Effluent        Sample geometry  : Tube
Detector name     : S                      Detector geometry:
Elapsed live time: 0 01:00:00.00           Elapsed real time: 0 01:00:46.78   1.3%
Start energy      :    20.00 keV           End energy       :  2560.00 keV
Sensitivity       :     5.00               Gaussian         :    10.00
Critical level    : No
```

Pk	It	Energy	Area	Bkgnd	FWHM	Channel	Left	Fw	Cts/Sec	%Err	Fit
1	0	97.84	28387	213335	14.22	9.78	8	6	7.89E+00	2.6	
2	0	204.32	1252004	577893	28.78	20.43	18	6	3.48E+02	0.1	
3	0	431.85	6550	188771	40.95	43.19	41	6	1.82E+00	10.6	
4	0	589.44	73492	215483	43.56	58.94	56	7	2.04E+01	1.1	
5	0	813.18	306707	585265	51.29	81.32	78	8	8.52E+01	0.5	
6	0	1058.36	147998	230549	55.99	105.84	102	9	4.11E+01	0.6	

Flag: "*" = Peak area was modified by background subtraction

ZS April 94
Page 75

A high-purity germanium detector (HPGE) is a semiconductor detector that is a very high-purity crystal of germanium. The general characteristics needed to understand the basic means of detecting radiation are explained in the discussion that follows.

In a crystal, there are two bands that electrons can occupy: the valance and conduction bands. The valance band contains electrons that are bound to specific lattice sites within the crystal; in germanium, the electrons are bound by a covalent bond. The conduction band contains electrons that are not bound and migrate throughout the crystal. These two bands are separated by a "forbidden" band gap. A crystal contains just enough electrons to fill the valance band, and for electrons to enter the conduction band, they must gain enough energy (on the order of several eV) to cross the gap. Thermal energy can supply a valance electron enough energy to excite it into the normally empty conduction band, leaving behind an unfilled covalent bond site (hole) in the valance band. Under the influence of an electric field, the electron migrates in the conduction band, and the hole moves in the opposite direction, parallel to the electric field applied: this motion of the pair is the conductivity of the material. The net drift of electrical charges parallel with an electric field is called the drift velocity. There is a saturation velocity in which

a further increase in electric field does not increase the drift velocity.

Although very pure, an HPGE contains a few impurities in the crystal that tend to be trivalent. These impurities are located in regions called acceptor sites. These regions are caused by defects in the germanium lattice. Since germanium normally has four covalent bonds per atom, a trivalent impurity leaves one covalent bond site unfilled (and is therefore called a p-type semiconductor). When an electron fills this site, the covalent bond is less than that of the others and actually lies in the forbidden gap, close to the valance band. Lithium, which is pentavalent, is evaporated and diffused onto one side of the germanium surface to provide a surface contact that provides an extra "donor" electron. This is called the n^+ surface contact.

The other side of the germanium crystal must contain a p^+ contact, usually a metal-to-surface barrier junction, and is called a noninjecting contact. Where the lithium contacts the germanium, an n^+-p junction exists. In the n^+ region, there are more conduction electrons than in the p region. This electron gradient causes a net diffusion of conduction electrons into the less dense p-type material, leaving behind immobile positive charges. These conduction electrons will then combine with any holes in the p-type material. The same argument holds for holes present in the p-type material diffusing into the n^+ region, leaving behind

an immobile negative charge. An electric field is created on either side of the junction because of the space charges, and further diffusion is prevented. This standing potential in the junction then causes any electrons created in or near the junction to be swept back toward the n-type material and any holes toward the p-type material. The region is thus "depleted" in that the concentration of holes and electrons is very small.

The only significant charges remaining in the depletion region are the immobile ionized donor sites and the filled acceptor sites. Because these latter charges do not contribute to the conductivity, the depletion region exhibits a very high resistivity compared with the n- and p-type materials on either side of the junction. When a positive voltage is applied to the n^+ contact with respect to the p^+ surface, the depletion region is widened. It begins at the n^+ edge of the central region and extends further into the p region with increasing voltage. This is called reverse biasing the crystal. The electric field is maximum at the n^+ side of the p region and decreases to zero at the p^+ side. Any additional increment of voltage applied raises the electric field by a constant amount throughout the detector. At very high voltage, the depletion region extends all the way from the contact to the other side of the crystal. This depletion region is the active volume of the detector. When radiation creates ionization as it

passes through this region, electron-hole pairs are created that are swept out of the region by the electric field. Their motion constitutes a basic electrical signal for detection.

The HPGE was chosen because it has the best energy resolution for detecting individual radiation peaks. The NaI(Tl), although extremely efficient, has poor resolution because there are many inefficient steps in converting the incident radiation signal into visible light and then converting it to an electrical signal. The energy needed to produce one photoelectron is approximately 1000 eV, and the number of carriers created in a typical radiation interaction is usually no more than a few thousand. The statistical fluctuation of such a small number places limitations on the energy resolution, even under ideal circumstances. To reduce this statistical limitation, the number of information carriers per pulse needs to be increased; the HPGE achieves this. Therefore, a sample containing ^{95m}Tc was analyzed using an HPGE well-type detector to confirm that ^{95m}Tc was the only radioactive constituent present since it could discriminate between very close peaks. Also, since ^{95m}Tc is a gamma emitter, its precipitation within the column was also traced using an HPGE detector with a well-shielded translation column.

APPENDIX D
CHEMICAL ASSAY DATA

CERTIFICATE OF CALIBRATION
BETA STANDARD SOLUTION

Radionuclide	Tc-99	Customer:	BATTELLE N.W. LAB.	
Half Life:	(2.13 ± 0.05) x 10^5 years	P.O.No.:	156053AKL	
Catalog No.:	7099	Reference Date:	August 1 1992	12:00 PST.
Source No.:	407-28	Contained Radioactivity:	980	µCi.
		Contained Radioactivity:	36,300	kBq

Description of Solution

a. Mass of solution:	5.0750	grams.
b. Chemical form:	NaTcO4 in water	
c. Carrier content:	None added	
d. Density:	0.9982	grams/ml @ 20°C.

Radioimpurities None detected

Radioactive Daughters

None

Radionuclide Concentration

193.2 µCi/gram.

Method of Calibration

Weighed aliquots of the solution were assayed using a liquid scintillation counter.

Uncertainty of Measurement

a. Systematic uncertainty in instrument calibration:	± 2.1%
b. Random uncertainty in assay:	± 1.3%
c. Random uncertainty in weighing(s):	± 0.0%
d. Total uncertainty at the 99% confidence level:	± 3.4%

NIST Traceability

This calibration is implicitly traceable to the National Institute of Standards and Technology.

Notes

1. Nuclear data were taken from "Table of Radioactive Isotopes", edited by Virginia S. Shirley, 1986.
2. IPL participates in an NIST measurement assurance program to establish and maintain implicit traceability for a number of nuclides, based on the blind assay(and later NIST certification) of Standard Reference Materials (As in NRC Regulatory Guide 4.15).

Ann U. Khan

QUALITY CONTROL

July 24, 1992

Date Signed

ISOTOPE PRODUCTS LABORATORIES
1800 No. Keystone Street,
Burbank, California 91504
(818) 843 - 7000

Post-it™ brand fax transmittal memo 7671	# of pages ▸ 1
To LINDA STATTER	From RON BROWN
Co. Battelle	Co. DUPONT PHARMA
Dept.	Phone # 508 671 8000
Fax # 509 376 9781	Fax #

JAN-21-1994 14:31 FROM Dupont Merck Cycle TO 15093769781 P.01
508 671 8001

NEN Products

Customer Service (617) 482-9595	NEN Products Order #	Amount
CATALOG NO.	15451860	1 mCi
W8146		

TECHNICAL DATA

NUCLIDE: TECHNETIUM-99m

CHEMICAL FORM: SODIUM PERTECHNATE IN H_2O

SPECIFIC ACTIVITY: 98.6 mCi/mg @ASSAY DATE

CONCENTRATION: 0.20 mCi/ml VOLUME: 5.00 ml

RADIONUCLIDIC PURITY: >99%

PRINCIPAL RADIOACTIVE CONTAMINANTS: NONE DETECTED @ASSAY DATE

TOTAL SOLIDS: N/A mg/ml

METHOD OF PREPARATION: $^{99m}MO(P,2n)^{99m}Tc$

ASSAY DATE: 1-17-94 LOT: 08931TC

RADIATION UNSHIELDED: 150 mr/hr

CAUTION: RXF FOR USE IN HUMANS OR CLINICAL DIAGNOSIS: This product is intended for research or manufacturing use only. It is pharmaceutically sterilized and verified for all its suitability for use in humans or as a clinical diagnostic reagent and the compliance with all federal and State laws regulating such applications is the sole responsibility of the purchaser.

LIMITED WARRANTY:

Du Pont NEN Products warrants the materials sold by it to be of merchantable quality at the time of shipment. There is no warranty, express or implied, as to the fitness of these materials for any particular purpose. The customer must notify the company, by registered mail, of any breach of warranty. Because of the inherent susceptibility to deterioration of those products containing short half-lived radionuclides, or which show a radiation decomposition rate of greater than one percent (1%) per month, notification must be made within 15 days of receipt. For all other products a 60-day period will be allowed. All claims shall be deemed waived in the event the customer fails to notify the company within the guarantee period. The maximum liability for breach of warranty shall be the invoice price for said materials and this liability shall be exclusive. Du Pont NEN Products shall not be liable for any consequential, compensatory, incidental, or special damages.

DU PONT

E-999

MCONE+

Copper Shot Assay

Arsenic (ppm)	Copper (%)	Iron (%)	Lead (%)	Antimony & Tin (%)	Manganese (%)	Phosphorus (%)	Silver (%)	Insoluble in Dilute HNO_3 (%)
5	99.5	0.005	0.005	0.01	0.001	0.001	0.002	0.020

Copper Powder Assay

Arsenic (ppm)	Copper (%)	Iron (%)	Lead (%)	Antimony & Tin (%)	Manganese (%)	Phosphorus (%)	Silver (%)	Insoluble in Dilute HNO_3 (%)
5	99.90	0.005	0.005	0.01	0.001	0.001	0.002	0.020

Tin Shot Assay

Arsenic (ppm)	Copper (%)	Iron (%)	Lead (%)	Tin (%)	Total foreign metals (as oxides)
2	0.002	0.005	0.020	99.8	0.05

Stannous Chloride Assay

Arsenic (ppm)	Iron (%)	Other Metals (as Pb)	Sulfate	Solubility in HCl	Substances not precipitated by H_2S (as Sulfates)
2	0.003	0.01	0.003	complete	0.05

Iron Powder Assay

Nitrogen Compounds (%)	Sulfide (%)	Iron (%)	Insoluble in Dilute H_2SO_4 (%)
0.003	0.02	99	0.50(%)

REFERENCES

1. J. Vida, *The Chemical Behavior of Technetium During the Treatment of High-Level Radioactive Waste*. Institute for Hot Chemistry, Karlsruhe Nuclear Research Center, KFK 4642, Translated from German by JR Jewett, Westinghouse Hanford Company, Richland, Washington PNL-TR-497 (1994).

2. J.A. Rard, *Critical Review of the Chemistry and Thermodynamics of Technetium and Some of Its Inorganic Compounds and Aqueous Species*, UCRL 53440, Lawrence Livermore National Laboratory, Livermore, California (1983).

3. F.W. Walker, J.R. Parrington, and F. Feiner, *Nuclides and Isotopes*, Fourteenth Edition, General Electric Company, Nuclear Energy Operations, San Jose, California (1989).

4. P. Cohen, *Water Coolant Technology of Power Reactors*, Westinghouse Electric Corporation, ISBN: 0-89448-020-0, American Nuclear Society (1980).

5. J. Weisman, *Elements of Nuclear Reactor Design*, Robert E. Krieger Publishing Company, Malabar, Florida (1983).

6. U.S. DOE *The Nuclear Waste Policy Act of 1982*, 42 U.S.C. 10101 (This act consists of the Act of January, 7, 1983 (Public Law 97-425 Stat. 2201), as amended by P.L. 100-203 (December 22, 1987) and P.L. 102-486 (The Energy Act of 1992, October 24, 1992).

7. C.N. Wilson and W.J. Gray, "Measurement of Soluble Nuclide Dissolution Rates from Spent Fuel", *Scientific Basis for Nuclear Waste Management XIV*, Virginia M. Oversby and Paul W. Brown, Editors., Materials Research Symposium Proceedings, Materials Research Society, Pittsburgh, Pennsylvania, Volume 176, pp. 489-498 (1990).

8. C.N. Wilson, *Results from NNWSI Series 3 Spent Fuel Dissolution Tests*, PNL-7170, Pacific Northwest Laboratory, Richland, Washington (1990).

9. M. Benedict, T.H. Pigford, and H.W. Levi, *Nuclear Chemical Engineering*, Second Edition, ISBN 0-07-004531-3 McGraw-Hill Book Company, New York (1981)

10. C.N. Wilson, *Results from Cycles 1 and 2 NNWSI Series 2 Spent Fuel Dissolution Tests*, HEDL-TME 85-22 UC-70, Hanford Engineering Development Laboratory, Richland, Washington (1987).

11. C.N. Wilson, "Summary of Results from the Series 2 and Series 3 NNWSI Bare Fuel Dissolution Tests," *Scientific Basis for Nuclear Waste Management XI*, M.J. Apted and R.E. Westerman, Editors., Materials Research Symposium Proceedings, Materials Research Society, Pittsburgh, PA, Volume 112, pp. 473-483 (1987).

12. C.N. Wilson and H.F. Shaw, "Experimental Study of the Dissolution of Spent Fuel at 85°C in Natural Ground Water," *Scientific Basis for Nuclear Waste Management X*, J.K. Bates and W.B. Seefeldt, Editors., Materials Research Symposium Proceedings 84, Materials Research Society, Pittsburgh, Pennsylvania, pp. 123-130 (1986).

13. C.N. Wilson and C.J. Bruton, "Studies on Spent Fuel Dissolution Behavior Under Yucca Mountain Repository Conditions," *Nuclear Waste Management III*, G.B. Mellinger, Ed., Ceramic Transactions, American Ceramic Society, Westerville, Ohio, Volume 9, pp. 423-441 (1990).

14. V.M. Oversby and H.F. Shaw, *Spent Fuel Performance Data: An Analysis of Data Relevant to the NNWSI Project*, UCID 20926, Lawrence Livermore National Laboratory, Livermore, California (1987).

15. Office of Civilian Radioactive Waste Management, *Nuclear Waste Policy Act (Section 113), Site Characterization Plan, Yucca Mountain Site, Nevada Research and Development Area, Nevada*, DOE/RW-0199, U.S. Department of Energy (1988).

16. V.M. Oversby, *Important Radionuclides in High Level Waste Disposal: Determination Using a Comparison of the EPA and NRC Regulations*, UCRL-94222, Lawrence Livermore National Laboratory, Livermore, California (1986).

17. P.W. Atkins, *Physical Chemistry*, Third Edition, ISBN Number 0-7167-1749-2, W.H. Freeman and Company, New York (1986).

18. D.C. Harris, *Quantitative Chemical Analysis*, Second Edition, ISBN Number 0-716-71817-0, W.H. Freeman and Company, New York (1987).

19. P.H. Sisler, R.D. Dresdner, and W.T. Mooney, *Chemistry, A SYSTEMATIC APPROACH*, ISBN Number 0-19-502630-6, Oxford University Press, Oxford, New York (1980).

20. R.E. Meyer, W.D. Arnold and F.I. Case, *Valance Effects on Solubility and Sorption: The Solubility of Tc(IV) Oxides*, NUREG/CR-4309 ORNL 6199, Oak Ridge National Laboratory, Martin Marietta Energy Systems, Oak Ridge, Tennessee (1985).

21. R.E. Meyer, W.D. Arnold and F.I. Case, *Valence Effects on the Sorption of Nuclides on Rocks and Minerals*, NUREG/CR-3389/ORNL 5978, Oak Ridge National Laboratory, Martin Marietta Energy Systems, Oak Ridge, Tennessee (1983).

22. V. Statler, University of Florida, P. Cloke, Science Application International Corporation, and J. Tulenko University of Florida, "Determination of a Method to Inhibit Technetium Migration at the Proposed Federal High Level Waste Repository at Yucca Mountain, Nevada," *1990 American Nuclear Society Annual Winter Meeting*, Nashville, Tennessee (1990).

23. V. Statler, University of Florida, *Investigation of the Effects of Iron, Tin, Stannous Chloride, Copper, Manganese and Vanadium on the Retardation of Technetium in J-13 Well Water*, Master's Thesis (1989).

24. V. Statler and W. Ellis, University of Florida, "Determination of a Method to Inhibit Technetium Migration at a Geologic Repository," *Third International High Level Waste Management Symposium*, Las Vegas, Nevada (1992).

25. T.J. Wolery, *EQ3NR: A Computer Program for Geochemical Aqueous Speciation-Solubility Calculations: User's Guide and Documentation*, UCRL 53414, Lawrence Livermore National Laboratory, Livermore, California (1983).

26. T.J. Wolery, *EQ3NR, A Computer Program for Geochemical Aqueous Speciation-Solubility Calculations: Theoretical Manual, User's Guide, and Related Documentation (Version 7.0)*, UCRL-MA-110662 PT III, Lawrence Livermore National Laboratory, Livermore, California (1992).

27. T.J. Wolery and S.A. Daveler, *EQ6, A Computer Program for Reaction Path Modeling of Aqueous Geochemical Systems: Theoretical Manual, User's Guide, and Related Documentation (Version 7.0)*, UCRL-MA-110662 PT IV, Lawrence Livermore National Laboratory, Livermore, California (1992).

28. J.M. Delany, I Puigdomenech and T.J. Wolery, *Precipitation Kinetics Option for the EQ6 Geochemical Reaction Path Code*, UCRL 53642, Lawrence Livermore National Laboratory, Livermore, California (1986).

29. T.J. Wolery, *EQ3/6, A Software Package for Geochemical Modeling of Aqueous Systems: Package Overview and Installation Guide (Version 7.0)*, UCRL-MA-110662 PT I, Lawrence Livermore National Laboratory, Livermore, California (1992).

30. B.P. McGrail and W.J. Gray, conversation, Pacific Northwest National Laboratory, Richland, Washington (2/95).

31. *FT-4C Operators Manual, Test Materials, Certifications*, Cortest Systems, Inc., Mountain View, California, (1987).

32. W.P. Freeborn and W.B. White, "The role of Eh in Nuclear Waste Form Dissolution," *Scientific Basis for Nuclear Waste Management VII*, G.L. McVay, Ed., Materials Research Symposium Proceedings Volume 26, Elsevier Science Publishing Company, Inc., New York, New York, pp. 719-726 (1983).

33. C.M. Jantzen, "Methods of Simulating Low Redox Potential (Eh) for a Basalt Repository," *Scientific Basis for Nuclear Waste Management VII*, G.L. McVay, Ed., Materials Research Symposium Proceedings Volume 26, Elsevier Science Publishing Company, Inc., New York, New York, pp. 613-621 (1983).

34. *Handbook of Chemistry and Physics*, Thirtieth Edition, Chemical Rubber Publishing Company (1947).

35. R.M. Guppy and A. Atkinson, *Experimental Investigation of Factors Affecting the Control of Redox Conditions Within a Radwaste Repository*, DOE/HMIP/RR/91/043, Department of the Environment: HMIP-Commissioned Research, Harwell Laboratory, Didcot, Oxfordshire, U.K. (1991).

36. B. Gu and R.K. Schulz, *Anion Retention in Soil: Possible Application to Reduce Migration of Buried Technetium and Iodine*, NUREG/CR 5464 Department of Soil Science, University of California, Berkeley, California (1991).

37. Dr. Dhanpat Rai, Scientist, Biochemistry Resources department at Pacific Northwest National Laboratory, Richland, Washington. Conversation, January 1996.

38. D. Rai and J.L. Ryan, "Neptunium (IV) Hydrous Oxide Solubility under Reducing and Carbonate Conditions," *Inorganic Chemistry*, 1985, American Chemical Society, Volume 24, pp. 247-251 (1985).

39. Dr. Walter Gray, Pacific Northwest National Laboratory, Richland, Washington. Conversation, January 1996.

40. L.J. Korb, D.L. Olson, Co-chairmen, *Metals Handbook® Ninth Edition, Volume 13, Corrosion*, ASM International, Metals Park, Ohio (1987).

41. D. Isherwood, *Application of the Ruthenium and Technetium Thermodynamic Data Bases Used in the EQ3/6 Geochemical Codes*, UCRL 53594, Lawrence Livermore National Laboratory, Livermore, California (1985)

42. G.H. Cartledge, "The Mechanisms of the Inhabitation of Corrosion by the Pertechnetate Ion. I. The Origin and Nature of Reaction Products", *Journal of Physics and Chemistry*, Volume 59, pp 979-984 (1955)

43. G.H. Cartledge, "Free Energies of Formation of Hydrous Oxides of Technetium in Its Lower Valencies", in *Journal of Electrochemical Society*, Volume 118 Number 2, pages 231-236 (1971)

44. G.H. Cartledge, "The Electrochemical Behavior of Technetium and Iron Containing Technetium", in *Journal of Electrochemical Society*, Volume 118 Number 11, pages 1752-1758 (1971)

45. R.E. Meyer, W.D. Arnold, F.I. Case and G.D. O'Kelley, *Thermodynamic Properties of Tc(IV) Oxides: Solubilities and the Electrode Potential of the Tc(VII)/Tc(IV) Oxide Couple*, NUREG/CR 5108 ORNL 6480, Oak Ridge National Laboratory, Oak Ridge, Tennessee (1988)

46. R.E. Meyer, W.D. Arnold, F.I. Case and G.D. O'Kelley, *Thermodynamics of Technetium Related to Nuclear Waste Disposal. Solubilities of Tc(IV) and the Electrode Potential of Tc(VII)/Tc(IV) Oxide Couple*, NUREG/CR 5235 ORNL 6503, Oak Ridge National Laboratory, Oak Ridge, Tennessee (1989)

47. R.C. Weast, *CRC Handbook of Chemistry and Physics*, Sixty-fourth Edition, CRC Press Incorporated, Boca Raton, Florida (1984).

48. N.N. Greenwood and A. Earnshaw, *Chemistry of the Elements*, Department of Inorganic and Structural Chemistry, University of Leeds, U.K., Pergamon Press (1984)

49. C.M. Jantzen, "Effects of Eh (oxidation potential) on borosilicate waste glass durability," in *Advances in Ceramics, Nuclear Waste Management*, G.G. Wicks and W.A. Ross, Editors, American Ceramic Society, Inc., Columbus, Ohio, Volume 8 (1984).

50. R.C. Weast, *CRC Handbook of Chemistry and Physics*, Sixty-fourth Edition, CRC Press Incorporated, Boca Raton, Florida (1984).

51. C.N. Wilson and C.J. Bruton, "Studies on Spent Fuel Dissolution Behavior Under Yucca Mountain Repository Conditions", *Nuclear Waste Management III*, G.B. Mellinger, Ed., Ceramic Transactions, American Ceramic Society, Westerville, Ohio, Volume 9, pp. 423-441 (1990)

52. *Chart of the Nuclides*, General Electric Company, Nuclear Energy Operations, San Jose, California, (1984).

53. M.D. Williams, V.R. Vermeul, M. Oostrom, J.C. Evans, J.S Fruchter, J.D. Istok, M.D. Humphrey, D.C. Lanigan, J.E. Szecsody, M.D. White, T.W. Wistma, and C.R. Cole, *Anoxic Plume Attenuation in a Fluctuating Water Table System: Impact of 100-D Area In Situ Redox Manipulation on Downgradient Dissolved Oxygen Concentrations*, PNNL-12192, UC-2000, Pacific Northwest National Laboratory, Richland, Washington (1999)

54. *Technetium Attenuation in the Vadose Zone: Role of Mineral Interactions*, Investigator N. J. Hess, Collaborator S.D. Conradson, LALP-99-194, Los Alamos National Laboratory, Los Alamos, New Mexico

55. Steven C. Chapra and Raymond P. Canale, *Numerical Methods for Engineers with Personal Computer Applications*, ISBN 0-07-010664-9 McGraw Hill Book Company, New York (1985).

56. *Radiological Health Handbook*, Compiled and edited by the bureau of Radiological Health, U.S. Department of Health, Education, and Welfare, Public Health Service, Food and Drug Administration, Bureau of Radiological Health, Rockville, Maryland, Revised Edition (1970)

57. G.F. Knoll, *Radiation Detection and Measurement*, ISBN Number 0-471-49545-X, John Wiley and Sons, New York, New York, (1979)

BIOGRAPHICAL SKETCH

VirLynda DeMartino was born in New York, New York. She knew by the age of nine that she wanted to be a nuclear engineer and, therefore, went to Saunders Trades and Technical High School where she obtained a Regents High School Diploma and graduated with honors in Chemical Technology. She obtained her Bachelor of Science in Engineering degree from the University of Florida's Department of Nuclear Engineering Sciences in May 1988, and in December 1989 she obtained her Master of Engineering degree from the same department.

Mrs. DeMartino has worked in the Neutron Activation Analysis laboratory, became Qualified Second Person Reactor Operator for the University of Florida Training Reactor, and interned at Science Application International Corporation in Las Vegas, Nevada, and Pacific Northwest National Laboratory in Richland, Washington. She is experienced in the following: general and radioanalytical laboratory conduct of operations, R&D of radioactive waste management investigations, assembly and use of radiation detection systems and flow-through experimentation systems, DOS and Macintosh operating systems and programs, and Windows programs. She is familiar with Fortran programming, and

OS2, UNIX, and VAX operating systems. She has authored/co-authored five publications under the surnames Statler and DeMartino.

She has received the following Honors: Associated Western Universities, Inc., Northwest Division Fellowship; Northwest College and University Association for Science Fellowship; U.S. Department of Energy High Level Waste Management Fellowship; Innovative Nuclear Power Operations Scholarship; American Nuclear Society (ANS) State Section Scholarship (2); Who's Who Among Students in American Universities and Colleges (2); University of Florida's President Award (2); College of Engineering Outstanding Leadership Award; College of Engineering Outstanding Service Award; ANS National Outstanding Service Award; ANS Student Branch Outstanding Service Award; Benton Engineering Council (BEC) Outstanding Officer Award; Outstanding Service to the Engineers' Fair (2); and the Columbia Scholastic Medal for Outstanding Service. She was on the University of Florida's Dean's List. She also has been a member of the following societies: ANS, BEC, Epsilon Lambda Chi, Florida Engineering Society, Omicron Delta Kappa, and the Society of Women Engineers.

Mrs. DeMartino has held the following University of Florida extracurricular activity positions: 1990 Engineers' Fair Chairman; 1989 Engineers' Fair Design Contest Coordinator; BEC Programs Director (in charge of the

College of Engineering's Homecoming Float, Holiday Cheer from a Gator Engineer, the College of Engineering's Pre-Engineering Colloquium, and High School Outreach); BEC Interim President; ANS 1991 Eastern Regional Student Conference (ERSC) Co-Chairman; ANS Student Branch President; ANS Student Branch Public Relations Chairman; ANS 1985 ERSC Housing Coordinator; contributed many papers at ANS related meetings; Epsilon Lambda Chi fraternity secretary; and Omicron Delta Kappa fraternity tapping committee.

I certify that I have read this study and that in my opinion it conforms to acceptable standards of scholarly presentation and is fully adequate, in scope and quality, as a dissertation for the degree of Doctor of Philosophy.

Samim Anghaie, Chairman
Professor of Nuclear and
Radiological Engineering

I certify that I have read this study and that in my opinion it conforms to acceptable standards of scholarly presentation and is fully adequate, in scope and quality, as a dissertation for the degree of Doctor of Philosophy.

Walter J. Gray, Co-Chairman
Senior Scientist, Pacific
Northwest National Laboratory

I certify that I have read this study and that in my opinion it conforms to acceptable standards of scholarly presentation and is fully adequate, in scope and quality, as a dissertation for the degree of Doctor of Philosophy.

James S. Tulenko
Professor of Nuclear
and Radiological Engineering

I certify that I have read this study and that in my opinion it conforms to acceptable standards of scholarly presentation and is fully adequate, in scope and quality, as a dissertation for the degree of Doctor of Philosophy.

Glen J. Schoessow
Professor Emeritus of Nuclear
and Radiological Engineering

I certify that I have read this study and that in my opinion it conforms to acceptable standards of scholarly presentation and is fully adequate, in scope and quality, as a dissertation for the degree of Doctor of Philosophy.

Robert J. Hanrahan
Professor of Chemistry

This dissertation was submitted to the Graduate Faculty of the College of Engineering and to the Graduate School and was accepted as partial fulfillment of the requirements for the degree of Doctor of Philosophy.

December 2000

Jack Ohanian
Dean, College of Engineering

Winfred M. Philips
Dean, Graduate School

LD
1780
20 00
.D27857
UNIVERSITY OF FLORIDA
3 1262 08555 1686